

CRAHCN-O: A Consistent Reduced Atmospheric Hybrid Chemical Network Oxygen Extension for Hydrogen Cyanide and Formaldehyde Chemistry in CO₂-, N₂-, H₂O-, CH₄-, and H₂-Dominated Atmospheres

Ben K. D. Pearce,^{1,*} Paul W. Ayers,² and Ralph E. Pudritz¹

¹Origins Institute and Department of Physics and Astronomy, McMaster University, ABB 241, 1280 Main St, Hamilton, ON, L8S 4M1, Canada

²Origins Institute and Department of Chemistry and Chemical Biology, McMaster University, ABB 156, 1280 Main St, Hamilton, ON, L8S 4M1, Canada

(Accepted to JPCA September 22, 2020)

Abstract: Hydrogen cyanide (HCN) and formaldehyde (H₂CO) are key precursors to biomolecules such as nucleobases and amino acids in planetary atmospheres; However, many reactions which produce and destroy these species in atmospheres containing CO₂ and H₂O are still missing from the literature. We use a quantum chemistry approach to find these missing reactions and calculate their rate coefficients using canonical variational transition state theory and Rice–Ramsperger–Kassel–Marcus/master equation theory at the BHHandHLYP/aug-cc-pVDZ level of theory. We calculate the rate coefficients for 126 total reactions, and validate our calculations by comparing with experimental data in the 39% of available cases. Our calculated rate coefficients are most frequently within a factor of 2 of experimental values, and generally always within an order of magnitude of these values. We discover 45 previously unknown reactions, and identify 6 from this list that are most likely to dominate H₂CO and HCN production and destruction in planetary atmospheres. We highlight ¹O + CH₃ → H₂CO + H as a new key source, and H₂CO + ¹O → HCO + OH as a new key sink, for H₂CO in upper planetary atmospheres. In this effort, we develop an oxygen extension to our consistent reduced atmospheric hybrid chemical network (CRAHCN-O), building off our previously developed network for HCN production in N₂-, CH₄- and H₂-dominated atmospheres (CRAHCN). This extension can be used to simulate both HCN and H₂CO production in atmospheres dominated by any of CO₂, N₂, H₂O, CH₄, and H₂.

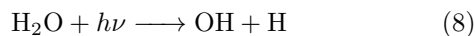
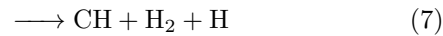
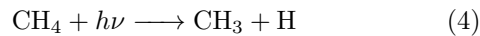
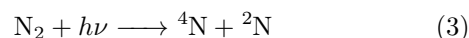
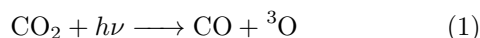
INTRODUCTION

Hydrogen cyanide (HCN) and formaldehyde (H₂CO) are key precursors to various biomolecules required for the origin of life. The four nucleobases in RNA, i.e., adenine, guanine, cytosine and uracil, form in aqueous solutions containing one or both of these reactants^{1–3}. Ribose, which pairs with phosphate to make up the backbone of RNA, forms from the oligomerization of H₂CO^{4,5}. Amino acids form via Strecker synthesis, which includes both HCN and an aldehyde (H₂CO for glycine) as reactants^{6,7}.

Given their substantial role in producing biomolecules, HCN and H₂CO may be distinguishing atmospheric features of what we call *biogenic worlds*. These are worlds capable of producing key biomolecules rather than requiring they be delivered (e.g., by meteorites). It is presently unknown whether the early Earth was biogenic.

The redox state of the oldest minerals on the planet suggests the early Earth atmosphere was composed of “weakly reducing” gases, i.e., CO₂, N₂, and H₂O, with relatively smaller amounts of CH₄, CO, and H₂^{8,9}. These atmospheric species are broken up into reactive radicals by UV radiation, lightning, and/or galactic cosmic rays (GCRs), which allows disequilibrium chemistry and the production of HCN and H₂CO to occur^{8,10}. The follow-

ing pathways are possible from the dissociation of these “weakly reducing” species^{11–15}:



* Corresponding author:pearcbe@mcmaster.ca

where the superscripts, ¹, ², ³, and ⁴ refer to the singlet, doublet, triplet and quartet electronic spin states.

One way to better understand the biogenicity of the early Earth, is to use chemical kinetic models to simulate the production of HCN and H₂CO in plausible early Earth atmospheres. Atmospheric simulations of these species for primitive Earth conditions have been performed in the past^{10,16,17}, which make use of collections of reaction rate coefficients typically gathered from various sources the literature (e.g. experiment, theoretical simulations, thermodynamics, similar reactions).

The literature, however, is still missing several reactions between the radicals produced in CO₂-⁻, N₂-⁻, H₂O-, CH₄-⁻, and H₂-dominated atmospheres, and these reactions may be crucial to understanding HCN and H₂CO chemistry in early Earth and other terrestrial environments. The largest gap in rate coefficient data is for reactions involving electronically excited species, e.g. ¹O, ²N, and ¹CH₂, which are directly produced from the dissociation of CO₂, N₂, and CH₄, respectively.

In Pearce et al.^[18] and Pearce et al.^[19], we developed an accurate and feasible method making use of computational quantum chemistry coupled with canonical variational transition state theory (CVT)²⁰ and Rice–Ramsperger–Kassel–Marcus/master equation (RRKM/ME) theory²¹ to calculate a large network of reaction rate coefficients for one-, two- and three-body reactions. We first used this method to explore the entire field of possible reactions for a list of primary species in N₂-⁻, CH₄-⁻, and H₂-dominated atmospheres, and uncovered 48 previously unknown reactions; many of which were based on excited species such as ²N and ¹CH₂. We then built an initial reduced network of 104 reactions based on this exploratory study, and used it to simulate HCN production in Titan's atmosphere¹⁸. This approach provided us with a more complete picture of HCN chemistry on Titan, as one of our newly discovered reactions was found to be one of the four dominant channels to HCN production on Titan¹⁸.

In this work, we use the same theoretical approach to expand upon our initial network, by exploring and calculating all the potential reactions between three key oxygen species present on the early Earth (CO₂, H₂O, H₂CO), their dissociation radicals (CO, ³O, ¹O, OH, and HCO), and all the non-oxygen primary species in our network (see Table 1 for the list of primary species). In this effort, we discover 45 brand new reactions, which are mainly based on HCO, H₂CN, ¹O, ²N, ¹CH₂, and CH. We calculate the rate coefficients for a total of 126 reactions, and validate our calculations by comparing with experimental data in the 39% of available cases.

Finally, we build the consistent reduced atmospheric hybrid chemical network oxygen extension (CRAHCN-O), composed of experimental rate coefficients when available, and our calculated values otherwise. CRAHCN-O is the amalgamation of the network developed in Pearce et al.^[18], and the oxygen reactions explored in this work. This network can be used to ac-

curately simulate HCN and H₂CO production in CO₂-⁻, N₂-⁻, H₂O-⁻, CH₄-⁻, and H₂-dominated atmospheres.

The paper is outlined as follows: In the Methods section, we detail the theoretical and computational approach we use to explore reactions and calculate their rate coefficients. In the Results section, we describe the results of our rate coefficient calculations, including their agreement with any available experiments. We also discuss the limitations of our theoretical approach. In the Discussion section, we highlight 6 new reactions from this work which are potentially key production and destruction pathways to H₂CO and HCN in planetary atmospheres. We also summarize CRAHCN-O and describe how it can be used for other atmospheric models. Finally, in the Conclusions section, we summarize the main conclusions from this work.

The Supporting Information (SI) contains two tables summarizing the new CRAHCN-O rate coefficient data (the non-oxygen reaction data can be found in Pearce et al.^[18]), any experimental rate coefficient data for reactions calculated in this work, the Lennard-Jones parameters used for three-body reaction rate coefficient calculations, a breakdown of some of the non-standard reaction calculations, and the quantum chemistry data used in our calculations.

METHODS

There are four phases to this work: First we explore all the potential reactions between eight oxygen species (CO₂, CO, ³O, ¹O, H₂O, OH, H₂CO, and HCO) and the primary species in Table 1. These species are the dominant sources of oxygen in the early Earth atmosphere (CO₂ and H₂O), a key biomolecule precursor (H₂CO) and their dissociation radicals. In this process, we characterize 81 known reactions and discover 45 previously unknown reactions. Second, we calculate the rate coefficients for every reaction that we find at 298 K, and validate the calculations by comparing to experimental data when available (in 39% of cases). Third, we calculate the temperature dependencies for the reactions that have no experimental measurements and have barriers (i.e. strong temperature dependencies from 50–400 K). Last, we gather the experimental and theoretical rate coefficients into the consistent reduced atmospheric hybrid chemical network oxygen extension (CRAHCN-O), which contains experimental values when available, and our calculated rate coefficients otherwise.

TABLE 1. List of primary molecular species involved in this study and their spin states. Reactions strictly between non-oxygen species (below center line) were explored in Pearce et al.^[18] and Pearce et al.^[19]. Reactions involving the oxygen species (above center line) are new to this study.

Species	Spin state	Ground/Excited state
CO ₂	singlet	ground
H ₂ CO	singlet	ground
HCO	doublet	ground
CO	singlet	ground
H ₂ O	singlet	ground
OH	doublet	ground
³ O	triplet	ground
¹ O	singlet	excited
<hr/>		
H ₂ CN	doublet	ground
HCN	singlet	ground
CN	doublet	ground
N ₂	singlet	ground
NH	triplet	ground
² N	doublet	excited
⁴ N	quartet	ground
CH ₄	singlet	ground
CH ₃	doublet	ground
¹ CH ₂	singlet	excited
³ CH ₂	triplet	ground
CH	doublet	ground
H ₂	singlet	ground
H	doublet	ground

Computational Quantum Method and Basis Set

All exploration and rate coefficient calculations are performed with the Becke-Half-and-Half-Lee-Yang-Parr¹ (BHandHLYP) density functional and the augmented correlation-consistent polarized valence double- ζ (aug-cc-pVDZ) basis set^{22–26}.

We have four key reasons for choosing this level of theory to perform our calculations:

1) We have benchmarked BHandHLYP/aug-cc-pVDZ rate coefficient calculations by comparing with experimental values in the past, and this method most frequently provides the best accuracy with respect to agreement with experimental values in comparison with other widely used, computationally cost effective methods.

In Pearce et al.^[18], we compared the accuracy of 3 methods for calculating 12 reaction rate coefficients. We found BHandHLYP/aug-cc-pVDZ rate coefficient calculations give the best, or equal to the best agreement with experiment in 8 out of 12 cases. This is compared to ω B97XD/aug-cc-pVDZ and CCSD/aug-cc-pVTZ, which gave the best, or equal to the best agreement with experiment in 7 out of 12 and 6 out of 12 cases, respectively¹⁸.

In another method-comparison study on a single reaction between BHandHLYP, CCSD, CAM-B3LYP, M06-2x, B3LYP and HF, all with the aug-cc-pVDZ basis set, we found that only BHandHLYP and CAM-B3LYP provide rate coefficients within the experimental range¹⁹.

2) BHandHLYP/aug-cc-pVDZ calculations paired with CVT and RRKM/ME theory typically compute rate coefficients within a factor of two of experimental values, and all calculations generally fall within an order of magnitude of experimental values. This accuracy is consistent with typical uncertainties assigned in large-scale experimental data evaluations^{27,28}.

For examples in our network, Baulch et al.^[27] assign uncertainties of 2–3 to HCO + HCO \longrightarrow H₂CO + CO and ³O + CH \longrightarrow CO + H and order-of-magnitude uncertainties to CO₂ + CH \longrightarrow products, H₂O + CH \longrightarrow products, and H₂CO + CH \longrightarrow products.

3) BHandHLYP/aug-cc-pVDZ calculations are computationally cost effective, and therefore feasible for a large scale exploratory study such as ours.

We have also shown in previous work for 12 rate coefficients, that increasing the basis set to the more computationally expensive aug-cc-pVTZ level does not increase the accuracy of our calculations with respect to agreement with experimental values¹⁸.

4) Finally, using the BHandHLYP/aug-cc-pVDZ level of theory for all the calculations in this oxygen extension allows us to maintain consistency with the calculations in the original network (CRAHCN¹⁸).

¹This hybrid functional uses 50% Hartree-Fock (HF) and 50% density functional theory (DFT) for the exchange energy calculation, offering a compromise between HF, which tends to overestimate energy barriers, and DFT, which tends to underestimate energy barriers.

Reaction Exploration

Using the Gaussian 09 software package²⁹, we perform a thorough search for reactions between eight oxygen species (CO_2 , CO , ^3O , ^1O , H_2O , OH , H_2CO , and HCO) and the 22 primary species in this study (see Table 1). The procedure below is carried out for $8 \times 22 = 176$ pairs of species.

Using the Avogadro molecular visualization software^{30,31}, we placed each species at a handful of different distances and orientations from its reaction partner. We use a bit of chemical intuition when determining the distance between the species, e.g., abstraction reactions in our network tend to occur at short separations ($1\text{--}2 \text{\AA}$), whereas addition reactions tend to be longer range ($2\text{--}6 \text{\AA}$).

We then copy the geometries into Gaussian input files, and use the ‘opt=modredundant’ option to freeze the bond distances between one atom of each species. We run the Gaussian simulations with vibrational analyses to allow us to identify whether points along the MEP were found. A point along a MEP is identified by a single negative frequency that oscillates in the direction of the reaction. We run multiple simulations to look for possible abstraction, addition, and bond insertion reactions. For reactions that form a single product, we continue the exploration of that product by searching for efficient decay and/or isomerization pathways. In many cases, we find the product efficiently decays into other products, sometimes after one or more isomerizations.

For cases where our above approach fails to find a MEP, we have developed a Python program that can be used to perform a more thorough scan of the potential energy surface. This program takes two species geometries as input, selects, e.g., 10 random separations and orientations for those species, and runs those Gaussian simulations in parallel. This program is especially useful for MEPs that turn out to be not strictly intuitive (e.g. $\text{OH} + ^1\text{CH}_2$).

Once we find a point along a MEP, we then characterize the reaction path by doing a coarse-grain scan backwards and forwards from the identified point in intervals of 0.1\AA . We then plot the Gibbs free energies of these optimized points along the reaction path, and analyze the points using Avogadro to find the rough location(s) of the transition state(s). In several cases we find more than one transition state along a reaction path, with one or more stable structures between the reactants and the products.

Rate coefficient calculations

One- and Two-body Reactions

We calculate one- and two-body reaction rate coefficients using canonical variational transition state theory (CVT). This is a statistical mechanics approach which

makes use of the canonical ensemble. This method can be used to calculate rate coefficients for reactions with and without energy barriers²⁰.

CVT can be explained as follows. There is a point that is far enough along the minimum energy reaction path (MEP), that the reactants that cross over this point are unlikely to cross back. This point is defined as the location where the generalized transition state (GT) rate coefficient is at its smallest value, therefore providing best dynamical bottleneck²⁰. This is expressed as:³²

$$k_{\text{CVT}}(T, s) = \min_s \{k_{\text{GT}}(T, s)\}. \quad (10)$$

where $k_{\text{GT}}(T, s)$ is the generalized transition state theory rate coefficient, T is the temperature, and s is a point along the MEP (e.g. bond distance).

To find the location along the MEP where the rate coefficient is at a minimum, we use the maximum Gibbs free energy criterion^{32,33}. It can be seen from the quasi-thermodynamic equation of transition-state theory that the maximum value for $\Delta G_{\text{GT}}(T, s)$ corresponds to a minimum value for $k_{\text{GT}}(T, s)$.

$$k_{\text{GT}}(T, s) = \frac{k_B T}{h} K^0 e^{-\Delta G_{\text{GT}}(T, s)/RT}, \quad (11)$$

where K^0 is the reaction quotient under standard state conditions (i.e. 1 cm^3 for second-order reactions, 1 cm^6 for third-order reactions), and $\Delta G_{\text{GT}}(T, s)$ is the difference in the Gibbs free energy between transition state and reactants (kJ mol^{-1}).

This method offers a compromise of energetic and entropic effects, as ΔG contains both enthalpy and entropy^{32,33}. To obtain a similar accuracy for all calculations, we refine our coarse grain scans near the Gibbs maxima to a precision of 0.01\AA .

The generalized transition state theory rate coefficient, neglecting effects due to tunneling, can be calculated with the equation^{32,34}

$$k_{\text{GT}}(T, s) = \sigma \frac{k_B T}{h} \frac{Q^\ddagger(T, s)}{\prod_{i=1}^N Q_i^{n_i}(T)} e^{-E_0(s)/RT}. \quad (12)$$

where σ is the reaction path multiplicity, k_B is the Boltzmann constant ($1.38 \times 10^{-23} \text{ J K}^{-1}$), T is temperature (K), h is the Planck constant ($6.63 \times 10^{-34} \text{ J}\cdot\text{s}$), Q^\ddagger is the partition function of the transition state per unit volume (cm^{-3}), with its zero of energy at the saddle point, Q_i is the partition function of species i per unit volume, with its zero of energy at the equilibrium position of species i , n_i is the stoichiometric coefficient of species i , N is the number of reactant species, E_0 is the difference in zero-point energies between the generalized transition state and the reactants (kJ mol^{-1}) (0 for barrierless reactions), and R is the gas constant ($8.314 \times 10^{-3} \text{ kJ K}^{-1} \text{ mol}^{-1}$).

The partition functions per unit volume have four components and are gathered from the Gaussian output files,

$$Q = \frac{q_t}{V} q_e q_v q_r. \quad (13)$$

where V is the volume (cm^{-3}) and the t , e , v , and r subscripts stand for translational, electronic, vibrational, and rotational, respectively.

In some cases, there are multiple steps (i.e. transition states) to a single reaction, and we must use mechanistic modeling in order to determine the steady-state solution of the overall rate equation. We place an example of a mechanistic model in Case Study 9 in the SI.

Three-body reactions

In the cases where two reactants form a single product, a colliding third body is required to remove excess vibrational energy from the product to prevent it from dissociating³⁵. This is expressed as,



The rate coefficient for these three-body reactions is expressed as³⁶:

$$k([M]) = \frac{k_0[M]/k_\infty}{1 + k_0[M]/k_\infty} k_\infty \quad (16)$$

where k_0 is the third-order low-pressure limit rate coefficient (cm^6s^{-1}), $[M]$ is the number density of the colliding third body, and k_∞ is the second-order high-pressure limit rate coefficient (cm^3s^{-1}).

The high-pressure limit rate coefficients are equivalent to the two-body reaction rate coefficients (i.e., $\text{A} + \text{B} \longrightarrow \text{C}$), and can be calculated using CVT as above. We make use of the ktools code of the Multiwell Program Suite for the high pressure limit rate coefficient calculations^{37–39}.

The low-pressure limit rate coefficients, on the other hand, require information about the collisional third body for their calculation. To calculate these values, we use the Multiwell Master Equation (ME) code, which employs RRKM theory. The ME contains the probabilities that the vibrationally excited product will be stabilized by a colliding third body⁴⁰. Multiwell employs Monte Carlo sampling of the ME to build up a statistical average for the two outcomes of the reaction (i.e., destabilize back into reactants, or stabilize the product).

With the output from these stochastic trials, we calculate the low-pressure limit rate coefficient with the following equation^{38,41}:

$$k_0([M]) = \frac{k_\infty f_{prod}}{[M]} \quad (17)$$

where k_∞ is the high-pressure limit rate coefficient, f_{prod} is the fractional yield of the collisionally stabilized product, and $[M]$ is the simulation number density (cm^{-3}), which we lower until k_0 converges.

We simulate three-body reactions using three different colliding bodies, corresponding to potential dominant species in the early Earth atmosphere (N_2 , CO_2 , and H_2). The energy transfer was treated with a standard exponential-down model with $\langle \Delta E \rangle_{down} = 0.8 \text{ T K}^{-1} \text{ cm}^{-1}$ ^{42,43}. The Lennard-Jones parameters for the bath gases and all the products were taken from the literature^{44–46} and can be found in Table S4.

In some cases, when two reactants come together to form a single product, the vibrationally excited product preferably decays along a different channel into something other than the original reactants (e.g. ${}^1\text{O} + \text{H}_2 \longrightarrow \text{H}_2\text{O}_{(\nu)} \cdot \longrightarrow \text{OH} + \text{H}$). In these cases, we also include the second-order reactions to these favourable decay pathways in our network. We verify the preferred decay pathways of vibrationally excited molecules by looking at previous experimental studies.

Temperature dependencies

For the one- and two-body reactions in this study with barriers, and no experimental measurements, we calculate temperature dependencies for the rate coefficients in the 50–400 K range. Barrierless reaction rate coefficients do not typically vary by more than a factor of ~ 3 between 50 and 400 K^{47–51}. To obtain temperature dependencies, we calculate the rate coefficients at 50, 100, 200, 298.15, and 400 K and fit the results to the modified Arrhenius expression

$$k(T) = \alpha \left(\frac{T}{300} \right)^\beta e^{-\gamma/T}, \quad (18)$$

where $k(T)$ is the temperature-dependent second-order rate coefficient (cm^3s^{-1}), α , β , and γ are fit parameters, and T is temperature (in K).

RESULTS

Comparison with Experiments

In Table 2 we display the three-body high- and low-pressure limit calculated rate coefficients at 298 K. Out of these 31 reactions, 12 have experimentally measured high-pressure limit rate coefficients. For the low-pressure limit rate coefficients, 9 of the 31 reactions have experimental measurements; However, the bath gases used in the low-pressure experiments often differ from the colliding third bodies in our calculations (i.e. N_2 , CO_2 , and H_2). When using several different bath gases, low-pressure limit rate coefficients tend to range by \sim an order of magnitude^{27,52–54}.

TABLE 2: Lindemann coefficients for the three body reactions in this paper, calculated at 298 K, and valid within the 50–400 K temperature range. k_∞ and k_0 are the third-order rate coefficients in the high and low pressure limits, with units cm^3s^{-1} and cm^6s^{-1} , respectively. These values are for usage in the pressure-dependent rate coefficient equation $k = \frac{k_0[M]/k_\infty}{1+k_0[M]/k_\infty} k_\infty$. Calculations are performed at the BHandHLYP/aug-cc-pVDZ level of theory. Low-pressure limit rate coefficients are calculated for three different bath gases (N_2 , CO_2 , and H_2). Reactions with rate coefficients slower than $k_\infty = 10^{-13} \text{ cm}^3\text{s}^{-1}$ are not included in this network. The error factor is the multiplicative or divisional factor from the nearest experimental or suggested value.

No.	Reaction equation	$k_\infty(298)$ calc.	$k_\infty(298)$ exp.	Error_∞	$k_0(298)$ calc.	$k_0(298)$ exp.	Error_0
*1.	$\text{CO}_2 + {}^1\text{O} + \text{M} \longrightarrow \text{CO}_3 + \text{M}$	3.8×10^{-11}	$0.1\text{--}23 \times 10^{-11}$	1	($\text{M}=\text{N}_2$) 3.0×10^{-29} (CO_2) 3.1×10^{-29} (H_2) 6.7×10^{-29}		
*2.	$\text{HCO} + {}^2\text{N} + \text{M} \longrightarrow$ $\text{HCNO} \cdot + \text{M} \cdot \longrightarrow \text{HCNO} + \text{M}$	2.0×10^{-11}			(N_2) 5.0×10^{-30} (CO_2) 5.6×10^{-30} (H_2) 9.7×10^{-30}		
*3.	$\text{HCO} + \text{CH}_3 + \text{M} \longrightarrow \text{CH}_3\text{CHO} + \text{M}$	5.7×10^{-12}	$6.3\text{--}44 \times 10^{-12}$	1	(N_2) 5.3×10^{-27} (CO_2) 6.4×10^{-27} (H_2) 1.2×10^{-27}		
4.	$\text{HCO} + \text{H} + \text{M} \longrightarrow \text{H}_2\text{CO} + \text{M}$	4.9×10^{-11}			(N_2) 7.4×10^{-30} (CO_2) 9.5×10^{-30} (H_2) 1.4×10^{-29}		
*5.	$\text{CO} + \text{CN} + \text{M} \longrightarrow \text{NCCO} + \text{M}$	6.0×10^{-12}			(N_2) 6.2×10^{-31} (CO_2) 6.8×10^{-31} (H_2) 1.3×10^{-30}		
6.	$\text{CO} + {}^1\text{O} + \text{M} \longrightarrow \text{CO}_2 + \text{M}$	2.8×10^{-11}	$0.3\text{--}7 \times 10^{-11}$	1	(N_2) 2.8×10^{-30} (CO_2) 3.0×10^{-30} (H_2) 5.9×10^{-30}	(CO_2) 2.8×10^{-29} " " " " "	10 9 5
*7.	$\text{CO} + {}^1\text{CH}_2 + \text{M} \longrightarrow \text{CH}_2\text{CO} + \text{M}$	1.3×10^{-11}			(N_2) 1.7×10^{-28} (CO_2) 1.9×10^{-28} (H_2) 3.3×10^{-28}		
8.	$\text{CO} + \text{CH} + \text{M} \longrightarrow \text{HCCO} + \text{M}$	4.6×10^{-11}	$0.5\text{--}17 \times 10^{-11}$	1	(N_2) 1.2×10^{-29} (CO_2) 1.3×10^{-29} (H_2) 2.4×10^{-29}	(Ar,He) $2.4\text{--}4.1 \times 10^{-30}$ " " " " "	3 3 6
9.	$\text{CO} + \text{H} + \text{M} \longrightarrow \text{HCO} + \text{M}$	2.7×10^{-12}			(N_2) 1.8×10^{-33} (CO_2) 2.1×10^{-33} (H_2) 3.4×10^{-33}	(Ne, H_2) $0.5\text{--}3.3 \times 10^{-34}$ (CO, H_2) $0.8\text{--}3.3 \times 10^{-34}$ (H_2) $0.8\text{--}3.3 \times 10^{-34}$	5 6 10
*10.	$\text{OH} + \text{H}_2\text{CN} + \text{M} \longrightarrow \text{H}_2\text{CNOH} + \text{M}$	6.9×10^{-12}	6.0×10^{-12}	1	(N_2) 6.5×10^{-30} (CO_2) 7.4×10^{-30} (H_2) 1.3×10^{-29}		
*11.	$\text{OH} + \text{CN} + \text{M} \longrightarrow \text{HOCH} + \text{M}$	1.0×10^{-12}			(N_2) 2.7×10^{-30} (CO_2) 2.9×10^{-30} (H_2) 5.1×10^{-30}		
12.	$\text{OH} + \text{OH} + \text{M} \longrightarrow \text{H}_2\text{O}_2 + \text{M}$	2.3×10^{-11}	$1.5\text{--}6.5 \times 10^{-11}$	1	(N_2) 4.9×10^{-32} (CO_2) 5.5×10^{-32} (H_2) 9.9×10^{-32}	(N_2) $5.1\text{--}330 \times 10^{-32}$ (CO_2) $6.4\text{--}420 \times 10^{-32}$ (He, H_2O) $1.3\text{--}1800 \times 10^{-32}$	1 1 1
*13.	$\text{OH} + {}^3\text{O} + \text{M} \longrightarrow \text{HO}_2 + \text{M}$	7.4×10^{-11}			(N_2) 8.5×10^{-32} (CO_2) 9.4×10^{-32} (H_2) 1.8×10^{-31}		
*14.	$\text{OH} + {}^1\text{O} + \text{M} \longrightarrow \text{HO}_2 + \text{M}$	1.0×10^{-9}			(N_2) 4.1×10^{-30}		

			(CO ₂) 4.5×10 ⁻³⁰ (H ₂) 8.3×10 ⁻³⁰
15.	OH + NH + M → OH· · NH· · + M· → trans-HNOH + M	7.0×10 ⁻¹²	(N ₂) 8.5×10 ⁻³¹ (CO ₂) 9.2×10 ⁻³¹ (H ₂) 1.7×10 ⁻³⁰
16.	OH + CH ₃ + M → OH· · CH ₃ · · + M· → CH ₃ OH + M	2.0×10 ⁻¹¹ 9.3–17×10 ⁻¹¹ 5	(N ₂) 2.1×10 ⁻²⁷ (CO ₂) 2.3×10 ⁻²⁷ (H ₂) 3.8×10 ⁻²⁷
17.	OH + H + M → H ₂ O + M	2.4×10 ⁻¹⁰	(N ₂) 3.0×10 ⁻³¹ (CO ₂) 3.7×10 ⁻³¹ (H ₂) 5.1×10 ⁻³¹
*18.	³ O + CN + M → NCO + M	7.1×10 ⁻¹² 9.4–16×10 ⁻¹² 1	(N ₂) 1.3×10 ⁻³⁰ (CO ₂) 1.5×10 ⁻³⁰ (H ₂) 2.6×10 ⁻³⁰
19.	³ O + ³ O + M → O ₂ + M	1.8×10 ⁻¹¹	(N ₂) 3.0×10 ⁻³⁴ (CO ₂) 3.2×10 ⁻³⁴ (H ₂) 6.1×10 ⁻³⁴
20.	³ O + ⁴ N + M → NO + M	6.6×10 ⁻¹¹	(N ₂) 1.6×10 ⁻³³ (CO ₂) 1.8×10 ⁻³³ (H ₂) 3.3×10 ⁻³³
*21.	³ O + ³ CH ₂ + M → H ₂ CO + M	6.7×10 ⁻¹¹ 1.9–20×10 ⁻¹¹ 1	(N ₂) 9.2×10 ⁻²⁹ (CO ₂) 1.1×10 ⁻²⁸ (H ₂) 1.7×10 ⁻²⁸
*22.	³ O + CH + M → HCO + M	1.1×10 ⁻¹⁰ 6.6–9.5×10 ⁻¹¹ 1	(N ₂) 5.2×10 ⁻³⁰ (CO ₂) 6.2×10 ⁻³⁰ (H ₂) 9.9×10 ⁻³⁰
23.	³ O + H + M → OH + M	3.5×10 ⁻¹⁰	(N ₂) 2.6×10 ⁻³³ (CO ₂) 2.9×10 ⁻³³ (H ₂) 4.6×10 ⁻³³
*24.	¹ O + HCN + M → HCNO + M	3.3×10 ⁻¹¹	(N ₂) 4.0×10 ⁻²⁹ (CO ₂) 4.6×10 ⁻²⁹ (H ₂) 8.0×10 ⁻²⁹
*25.	¹ O + CN + M → NCO + M	8.9×10 ⁻¹¹	(N ₂) 1.9×10 ⁻²⁹ (CO ₂) 2.1×10 ⁻²⁹ (H ₂) 3.6×10 ⁻²⁹
*26.	¹ O + ¹ O + M → O ₂ + M	2.3×10 ⁻¹⁰	(N ₂) 8.8×10 ⁻³³ (CO ₂) 9.6×10 ⁻³³ (H ₂) 1.8×10 ⁻³²
*27.	¹ O + CH ₄ + M → CH ₃ OH + M	5.8×10 ⁻⁹ 1.4–4.0×10 ⁻¹⁰ 15	(N ₂) 3.6×10 ⁻²³ (CO ₂) 3.9×10 ⁻²³ (H ₂) 6.3×10 ⁻²³
*28.	¹ O + ¹ CH ₂ + M → H ₂ CO + M	3.3×10 ⁻¹⁰	(N ₂) 6.6×10 ⁻²⁷ (CO ₂) 7.7×10 ⁻²⁷ (H ₂) 1.2×10 ⁻²⁶
*29.	¹ O + CH + M → HCO + M	9.2×10 ⁻¹¹	(N ₂) 4.9×10 ⁻²⁹ (CO ₂) 5.8×10 ⁻²⁹ (H ₂) 9.1×10 ⁻²⁹

*30. $^1\text{O} + \text{H}_2 + \text{M} \longrightarrow \text{H}_2\text{O} + \text{M}$	7.1×10^{-10}	$1.1 - 3.0 \times 10^{-10}$	2	(N ₂) 1.2×10^{-29} (CO ₂) 1.4×10^{-29} (H ₂) 2.0×10^{-29}
*31. $^1\text{O} + \text{H} + \text{M} \longrightarrow \text{OH} + \text{M}$	1.1×10^{-9}			(N ₂) 1.4×10^{-32} (CO ₂) 1.5×10^{-32} (H ₂) 2.3×10^{-32}

* Reactions with no previously known rate coefficients.

Our calculated high-pressure rate coefficients are within the range of experimental values in 9 out of 12 cases. The other three rate coefficients are factors of 2, 5, and 15 from the nearest experimental values. Typical uncertainties for rate coefficients—as assigned in large experimental data evaluations—range from factors of 2–10^{27,28}; Therefore, this calculated accuracy is consistent with the levels of uncertainty typically found in the literature.

Each low-pressure limit rate coefficient was calculated for three bath gases (N₂, CO₂, and H₂) and compared to experiments performed with matching bath gases when possible, and any bath gases otherwise. Nine of the reactions had experimentally measured low-pressure limit rate coefficients for one or more bath gases. All of our calculated rate coefficients for these reactions landed within an order of magnitude of the experimental range for the matching bath gas when possible, or another bath gas otherwise. Most commonly (67% of the time), our rate coefficients were within a factor of 3 from the nearest experimental measurement. Larger deviations tended to

occur for cases that only have a single experimental measurement for comparison.

In Table 3, we display the 95 one- and two-body reaction rate coefficients calculated at 298K with any experimental or suggested values. 47 of these reactions have experimental or suggested values, and our calculations are within approximately one order of magnitude of these values in all but one case. In 60% of cases our calculated rate coefficients are within a factor of 2 of experimental values, and in 83% of cases our calculated rate coefficients are within a factor of 6 of experimental values.

In one case, OH + CH₄ \longrightarrow H₂O + CH₃, our calculated rate coefficient has a slightly higher than an order of magnitude deviation from experiment (factor of 54). We attribute this error to the lack of a quantum tunneling correction in our calculations. Bravo-Pérez et al.^[55] performed transition state theory calculations for this reaction at the BHandHLYP/6-311G(d,p) level of theory, and calculated a tunneling factor of 30.56 at 298 K using an Eckart model. If we applied this factor to our calculation, our rate coefficient would be within a factor of two of the experimental range.

TABLE 3: Calculated reaction rate coefficients at 298 K for the one- and two-body reactions in this paper. Calculations are performed at the BHandHLYP/aug-cc-pVDZ level of theory. Reactions with rate coefficients slower than $k = 10^{-21}$ are not included in this network. The presence or absence of an energy barrier in the rate-limiting step (or the only step) of the reaction is specified. The error factor is the multiplicative or divisional factor from the nearest experimental or suggested value; the error factor is 1 if the calculated value is within the range of experimental or suggested values. First-order rate coefficients have units s⁻¹. Second-order rate coefficients have units cm³s⁻¹.

No.	Reaction equation	Forw./Rev.	Barrier?	k(298) calculated	k(298) experimental	Error factor
*32.	NCCO \longrightarrow CO + CN	F	Y	9.4×10^{-12}		
33.	CO ₂ + ¹ O \longrightarrow ¹ CO ₃ · \longrightarrow ³ CO ₃ · \longrightarrow	F	N	3.8×10^{-11}	$0.1 - 23 \times 10^{-11}$	1
	CO ₂ + ³ O					
34.	CO ₂ + ² N \longrightarrow NCO ₂ · \longrightarrow OCNO · \longrightarrow	F	^a Y	3.2×10^{-14}	$1.8 - 6.8 \times 10^{-13}$	6
	CO + NO					
35.	CO ₂ + ¹ CH ₂ \longrightarrow ¹ CH ₂ CO ₂ · \longrightarrow	F	N	8.0×10^{-13}		
	H ₂ CO + CO					
36.	CO ₂ + CH \longrightarrow CHCO ₂ · \longrightarrow HCOCO · \longrightarrow	F	^b N	3.1×10^{-12}	$1.8 - 2.1 \times 10^{-12}$	1
	HCO + CO					
37.	H ₂ O ₂ \longrightarrow OH + OH	F	Y	5.1×10^{-9}		
38.	H ₂ CO + CN \longrightarrow HCN + HCO	F	N	1.7×10^{-11}	1.7×10^{-11}	1
39.	H ₂ CO + OH \longrightarrow r, l-H ₂ COHO · \longrightarrow	F	Y	7.1×10^{-17}		
	trans-HCOHO · + H · \longrightarrow H ₂ O + CO + H					
40.	H ₂ CO + OH \longrightarrow H ₂ CO · HO · \longrightarrow H ₂ O + HCO	F	Y	1.1×10^{-12}	$6.1 - 15 \times 10^{-12}$	6
41.	H ₂ CO + ³ O \longrightarrow HCO + OH	F	Y	6.8×10^{-14}	$1.5 - 1.9 \times 10^{-13}$	2
*42.	H ₂ CO + ¹ O \longrightarrow H ₂ CO ₂ · \longrightarrow HCO ₂ H · \longrightarrow	F	N	4.6×10^{-10}		
	HCO + OH					
43.	H ₂ CO + CH ₄ \longrightarrow HCO + CH ₄	F	Y	1.9×10^{-19}	$2.2 - 4.2 \times 10^{-18}$	12
44.	H ₂ CO + ³ CH ₂ \longrightarrow HCO + CH ₃	F	Y	1.1×10^{-14}	$< 1.0 \times 10^{-14}$	1
45.	H ₂ CO + ¹ CH ₂ \longrightarrow HCO + CH ₃	F	N	1.5×10^{-12}	2.0×10^{-12}	1

46.	$\text{H}_2\text{CO} + \text{CH} \longrightarrow \text{H}_2\text{COCH}_a \cdot \longrightarrow$ $\text{H}_2\text{COCH}_b \cdot \longrightarrow \text{CH}_2\text{HCO} \cdot \longrightarrow$ $\text{CH}_3\text{CO} \cdot \longrightarrow \text{CO} + \text{CH}_3$	F	N	3.1×10^{-11}	3.8×10^{-10}	12
47.	$\text{H}_2\text{CO} + \text{CH} \longrightarrow \text{H}_2\text{COCH}_c \cdot \longrightarrow$ $\text{HCO} + {}^3\text{CH}_2$	F	N	1.1×10^{-12}		
48.	$\text{H}_2\text{CO} + \text{H} \longrightarrow \text{HCO} + \text{H}_2$	F	Y	1.8×10^{-13}	$3.9-6.7 \times 10^{-14}$	3
*49.	$\text{HCO} + \text{H}_2\text{CN} \longrightarrow \text{H}_2\text{CO} + \text{HCN}$	F	Y	7.0×10^{-15}		
50.	$\text{HCO} + \text{HCO} \longrightarrow \text{trans-}\text{C}_2\text{H}_2\text{O}_2 \cdot \longrightarrow$ $\text{anti-}\text{HCOH} \cdot + \text{CO} \cdot \longrightarrow \text{H}_2\text{CO} + \text{CO}$	F	Y	1.2×10^{-13}	$2.8-750 \times 10^{-13}$	2
51.	$\text{HCO} + \text{HCO} \longrightarrow \text{cis-}\text{C}_2\text{H}_2\text{O}_2 \cdot \longrightarrow$ $\text{CO} + \text{CO} + \text{H}_2$	F	N	7.4×10^{-11}	3.6×10^{-11}	2
52.	$\text{HCO} + \text{CN} \longrightarrow \text{HCOCN} \cdot \longrightarrow \text{CO} + \text{HCN}$	F	N	5.4×10^{-12}		
53.	$\text{HCO} + \text{OH} \longrightarrow \text{trans-}\text{HCOHO} \cdot \longrightarrow \text{CO} + \text{H}_2\text{O}$	F	N	7.0×10^{-12}	$5-18 \times 10^{-11}$	7
54.	$\text{HCO} + {}^3\text{O} \longrightarrow \text{HCO}_2 \cdot \longrightarrow \text{CO}_2 + \text{H}$	F	N	2.6×10^{-11}	5.0×10^{-11}	2
55.	$\text{HCO} + {}^3\text{O} \longrightarrow \text{CO} + \text{OH}$	F	N	3.4×10^{-11}	5.0×10^{-11}	1
*56.	$\text{HCO} + {}^1\text{O} \longrightarrow \text{HCO}_2 \cdot \longrightarrow \text{CO}_2 + \text{H}$	F	N	1.5×10^{-10}		
*57.	$\text{HCO} + \text{NH} \longrightarrow \text{H}_2\text{CO} + {}^4\text{N}$	F	Y	3.6×10^{-20}		
*58.	$\text{HCO} + \text{NH} \longrightarrow \text{CO} + \text{NH}_2$ and $\text{HCO} + \text{NH} \longrightarrow \text{HNHCO} \cdot \longrightarrow \text{H}_2\text{NCO} \cdot \longrightarrow$ $\text{CO} + \text{NH}_2$	F	N	1.4×10^{-11}		
59.	$\text{HCO} + {}^4\text{N} \longrightarrow {}^3\text{NCOH} \cdot \longrightarrow \text{NCO} + \text{H}$	F	N	2.8×10^{-11}		
60.	$\text{HCO} + {}^4\text{N} \longrightarrow \text{CO} + \text{NH}$	F	N	2.2×10^{-11}		
*61.	$\text{HCO} + {}^2\text{N} \longrightarrow {}^3\text{NCOH} \cdot \longrightarrow \text{NCO} + \text{H}$	F	N	6.6×10^{-11}		
*62.	$\text{HCO} + {}^2\text{N} \longrightarrow \text{CO} + \text{NH}$	F	N	4.8×10^{-11}		
63.	$\text{HCO} + \text{CH}_3 \longrightarrow \text{CO} + \text{CH}_4$	F	N	1.0×10^{-11}	$3.6 \times 10^{-11}-2.0 \times 10^{-10}$	4
64.	$\text{HCO} + {}^3\text{CH}_2 \longrightarrow \text{CH}_3 + \text{CO}$ and $\text{HCO} + {}^3\text{CH}_2 \longrightarrow \text{CH}_2\text{HCO} \cdot \longrightarrow$ $\text{CH}_3\text{CO} \cdot \longrightarrow \text{CH}_3 + \text{CO}$	F	N	2.1×10^{-11}	3.0×10^{-11}	1
65.	$\text{HCO} + {}^1\text{CH}_2 \longrightarrow \text{CH}_2\text{HCO} \cdot \longrightarrow$ $\text{CH}_3\text{CO} \cdot \longrightarrow \text{CH}_3 + \text{CO}$	F	N	1.2×10^{-11}	3.0×10^{-11}	3
66.	$\text{HCO} + \text{CH} \longrightarrow \text{CO} + {}^3\text{CH}_2$	F	N	1.5×10^{-11}		
*67.	$\text{HCO} + \text{CH} \longrightarrow \text{CO} + {}^1\text{CH}_2$	F	N	4.6×10^{-12}		
68.	$\text{HCO} + \text{H} \longrightarrow \text{CO} + \text{H}_2$ and $\text{HCO} + \text{H} \longrightarrow \text{H}_2\text{CO}_{(\nu)} \cdot \longrightarrow \text{CO} + \text{H}_2$	F	N	6.9×10^{-11}	$1.1-5.5 \times 10^{-10}$	2
69.	$\text{HCO} + \text{H} \longrightarrow \text{H}_2\text{CO}_{(\nu)} \cdot \longrightarrow \text{CO} + \text{H} + \text{H}$	F	N	2.4×10^{-11}		
70.	$\text{HCO} \longrightarrow \text{CO} + \text{H}$	F	Y	2.2×10^{-2}		
71.	$\text{CO} + \text{OH} \longrightarrow \text{OH} \cdots \text{CO} \cdot \longrightarrow \text{cis-}\text{HOCO} \cdot \longrightarrow$ $\text{CO}_2 + \text{H}$	F	Y	${}^c 2.9 \times 10^{-12}$	$0.9-9.7 \times 10^{-13}$	3
72.	$\text{H}_2\text{O} + {}^1\text{O} \longrightarrow \text{H}_2\text{OO} \cdot \longrightarrow \text{H}_2\text{O}_2 \cdot \longrightarrow$ $\text{OH} + \text{OH}$	F	N	4.8×10^{-10}	$1.8-3.7 \times 10^{-10}$	1
73.	$\text{H}_2\text{O} + \text{CN} \longrightarrow \text{H}_2\text{OCN} \cdot \longrightarrow \text{OH} + \text{HCN}$	F	Y	6.6×10^{-15}		
74.	$\text{H}_2\text{O} + {}^2\text{N} \longrightarrow \text{H}_2\text{ON} \cdot \longrightarrow \text{trans-}\text{HNOH} \cdot \longrightarrow$ $\text{HNO} + \text{H}$ and $\text{H}_2\text{O} + {}^2\text{N} \longrightarrow \text{H}_2\text{ON} \cdot \longrightarrow \text{trans-}\text{HNOH} \cdot \longrightarrow$ $\text{H}_2\text{NO} \cdot \longrightarrow \text{HNO} + \text{H}$	F	N	1.9×10^{-10}		
75.	$\text{H}_2\text{O} + \text{CH} \longrightarrow \text{H}_2\text{O} \cdots \text{CH} \cdot \longrightarrow \text{H}_2\text{OCH} \cdot \longrightarrow$ $\text{H}_2\text{COH} \cdot \longrightarrow \text{H}_2\text{CO} + \text{H}$	F	^d N	2.0×10^{-10}	$1.3-4.5 \times 10^{-11}$	4
*76.	$\text{H}_2\text{O} + \text{CH} \longrightarrow \text{OH} + {}^3\text{CH}_2$	F	Y	3.9×10^{-16}		
77.	$\text{OH} + \text{HCN} \longrightarrow \text{NCHOH} \cdot \longrightarrow \text{HOCN} + \text{H}$	F	Y	1.2×10^{-15}	$0.1-31 \times 10^{-15}$	1
78.	$\text{OH} + \text{CN} \longrightarrow \text{HO} \cdots \text{CN} \longrightarrow {}^3\text{HOCH}_1 \cdot \longrightarrow$ ${}^3\text{HOCH}_2 \longrightarrow \text{NCO} + \text{H}$	F	Y	1.1×10^{-12}		
79.	$\text{OH} + \text{CN} \longrightarrow \text{HCN} + {}^3\text{O}$	F	Y	4.5×10^{-13}		
*80.	$\text{OH} + \text{CN} \longrightarrow \text{HNC} + {}^3\text{O}$	F	Y	2.3×10^{-17}		
81.	$\text{OH} + \text{OH} \longrightarrow \text{trans-}\text{H}_2\text{O}_2 \cdot \longrightarrow \text{H}_2\text{O} + {}^3\text{O}$	F	N	${}^e 2.5 \times 10^{-11}$	$0.8-2.6 \times 10^{-12}$	10
82.	$\text{OH} + {}^3\text{O} \longrightarrow \text{HO}_{2(\nu)} \cdot \longrightarrow \text{O}_2 + \text{H}$	F	N	7.4×10^{-11}	$2.8-4.2 \times 10^{-11}$	2
*83.	$\text{OH} + {}^1\text{O} \longrightarrow \text{HO}_{2(\nu)} \cdot \longrightarrow \text{O}_2 + \text{H}$	F	N	1.0×10^{-9}		
84.	$\text{OH} + \text{NH} \longrightarrow \text{OH} \cdots \text{NH} \cdot \longrightarrow \text{trans-}\text{HNOH} \cdot \longrightarrow$ $\text{HNO} + \text{H}$ and $\text{OH} + \text{NH} \longrightarrow \text{OH} \cdots \text{NH} \cdot \longrightarrow \text{trans-}\text{HNOH} \cdot \longrightarrow$ $\text{H}_2\text{NO} \cdot \longrightarrow \text{HNO} + \text{H}$	F	^f N	7.0×10^{-12}	3.3×10^{-11}	5
85.	$\text{OH} + \text{NH} \longrightarrow \text{H}_2\text{O} + {}^4\text{N}$	F	Y	6.8×10^{-13}	3.1×10^{-12}	5
86.	$\text{OH} + {}^4\text{N} \longrightarrow {}^3\text{OH} \cdots \text{N} \longrightarrow {}^3\text{NOH} \cdot \longrightarrow$	F	Y	1.0×10^{-10}	$4.2-5.3 \times 10^{-11}$	2

NO + H						
*87. OH + ² N → ³ OH · · N → ³ NOH · →	F	N	1.5 × 10 ⁻¹⁰			
NO + H						
88. OH + CH ₄ → H ₂ O + CH ₃	F	Y	1.1 × 10 ⁻¹⁶	5.9–11 × 10 ⁻¹⁵		54
89. OH + CH ₃ → ³ O + CH ₄	F	Y	1.1 × 10 ⁻¹⁸	1.8 × 10 ⁻¹⁷		16
90. OH + CH ₃ → H ₂ O + ³ CH ₂	F	Y	3.5 × 10 ⁻¹⁸			
91. OH + ³ CH ₂ → OH · · CH ₂ · → H ₂ COH · →	F	N	4.6 × 10 ⁻¹¹	3.0 × 10 ⁻¹¹		2
H ₂ CO + H						
92. OH + ³ CH ₂ → H ₂ O + CH	F	N	7.6 × 10 ⁻¹³			
93. OH + ¹ CH ₂ → OH · · CH ₂ · → H ₂ COH · →	F	N	4.6 × 10 ⁻¹¹	5.0 × 10 ⁻¹¹		1
H ₂ CO + H						
94. OH + CH → ³ OH · · CH · → ³ HCOH · →	F	N	3.2 × 10 ⁻¹¹			
³ H ₂ CO · → HCO + H						
95. OH + CH → anti-HCOH _(v) · →	F	N	^a 6.3 × 10 ⁻¹²			
H ₂ CO _(v) · → CO + H ₂						
96. OH + CH → anti-HCOH _(v) · →	F	N	^a 6.3 × 10 ⁻¹²			
H ₂ CO _(v) · → CO + H + H						
97. OH + H ₂ → H ₂ O + H	F	Y	1.5 × 10 ⁻¹⁵	5.3–8.5 × 10 ⁻¹⁵		4
98. OH + H → ³ O + H ₂	F	Y	6.5 × 10 ⁻¹⁶	9.9 × 10 ⁻¹⁷ –5.6 × 10 ⁻¹⁶		1
*99. ³ O + H ₂ CN → CH ₂ NO · →	F	Y	4.0 × 10 ⁻¹⁴			
HCNO + H						
*100. ³ O + H ₂ CN ← CH ₂ NO · ←	R	N	9.8 × 10 ⁻¹¹			
HCNO + H						
101. ³ O + H ₂ CN → CH ₂ NO · →	F	Y	8.3 × 10 ⁻¹⁵			
HCNOH · → OH + HCN						
102. ³ O + HCN → ³ NCOH → NCO + H	F	Y	1.5 × 10 ⁻¹⁸			
103. ³ O + HCN ← ³ NCOH ← NCO + H	R	Y	2.5 × 10 ⁻²⁰			
104. ³ O + CN → ⁴ NCO → CO + ⁴ N	F	N	1.5 × 10 ⁻¹¹	2.7 × 10 ⁻¹² –3.7 × 10 ⁻¹¹		1
105. ³ O + CN → NCO _(v) → CO + ² N	F	N	7.1 × 10 ⁻¹²	9.4 × 10 ⁻¹² –1.6 × 10 ⁻¹¹		1
106. ³ O + NH → HNO · → NO + H	F	N	3.1 × 10 ⁻¹¹	5.0 × 10 ⁻¹¹		2
107. ³ O + NH → OH + ⁴ N	F	Y	2.2 × 10 ⁻¹⁴	<1.7 × 10 ⁻¹³ –5.0 × 10 ⁻¹²		1
108. ³ O + CH ₄ → OH + CH ₃	F	Y	1.1 × 10 ⁻¹⁹	6.6 × 10 ⁻¹⁹ –6.6 × 10 ⁻¹⁶		6
109. ³ O + CH ₃ → CH ₃ O · → H ₂ CO + H	F	N	9.4 × 10 ⁻¹¹	>3.0 × 10 ⁻¹¹ –1.9 × 10 ⁻¹⁰		1
110. ³ O + ³ CH ₂ → H ₂ CO _(v) → CO + H + H	F	N	3.4 × 10 ⁻¹¹	^b 1.0 × 10 ⁻¹¹ –1.0 × 10 ⁻¹⁰		1
111. ³ O + ³ CH ₂ → H ₂ CO _(v) → CO + H ₂	F	N	3.4 × 10 ⁻¹¹	^b 1.0 × 10 ⁻¹¹ –1.0 × 10 ⁻¹⁰		1
*112. ³ O + ¹ CH ₂ → ³ H ₂ CO · → HCO + H	F	N	2.1 × 10 ⁻¹⁰			
113. ³ O + CH → HCO _(v) → CO + H	F	N	1.1 × 10 ⁻¹⁰	6.6 × 10 ⁻¹¹		2
114. ³ O + CH → ⁴ HCO · → ⁴ COH · →	F	N	2.5 × 10 ⁻¹⁰			
OH + C						
115. ³ O + H ₂ → OH + H	F	Y	7.2 × 10 ⁻¹⁹	7.0 × 10 ⁻¹⁸ –1.1 × 10 ⁻¹⁷		10
*116. ¹ O + H ₂ CN → CH ₂ NO · →	F	Y	4.5 × 10 ⁻¹⁰			
³ O + H ₂ CN						
*117. ¹ O + H ₂ CN → CH ₂ NO · →	F	Y	6.0 × 10 ⁻¹³			
HCNO + H						
*118. ¹ O + H ₂ CN → CH ₂ NO · →	F	Y	1.2 × 10 ⁻¹³			
HCNOH · → HCN + OH						
*119. ¹ O + CN → NCO _(v) → CO + ² N	F	N	8.9 × 10 ⁻¹¹			
120. ¹ O + CH ₄ → CH ₃ OH _(v) → OH + CH ₃	F	N	5.8 × 10 ⁻⁹	1.4–4.0 × 10 ⁻¹⁰		15
*121. ¹ O + CH ₃ → CH ₃ O · → H ₂ CO + H	F	N	4.3 × 10 ⁻¹⁰			
*122. ¹ O + ³ CH ₂ → ³ H ₂ CO · → HCO + H	F	N	7.0 × 10 ⁻¹⁰			
*123. ¹ O + ¹ CH ₂ → H ₂ CO _(v) →	F	N	1.7 × 10 ⁻¹⁰			
CO + H + H						
*124. ¹ O + ¹ CH ₂ → H ₂ CO _(v) → CO + H ₂	F	N	1.7 × 10 ⁻¹⁰			
*125. ¹ O + CH → HCO _(v) → CO + H	F	N	9.2 × 10 ⁻¹¹			
126. ¹ O + H ₂ → H ₂ O _(v) → OH + H	F	N	7.1 × 10 ⁻¹⁰	1.1–3.0 × 10 ⁻¹⁰		2

^a We introduce a barrier of 17.15 kJ mol⁻¹ (half the HF barrier) to this calculation as no barrier is found at the BHandHLYP/aug-cc-pVDZ level of theory (see supplement for more details).

^b We remove the barrier from this calculation as experiment predicts this reaction to be barrierless below 400 K⁵⁶.

^c We remove the intermediate barriers from this reaction and reduce the barrierless first step by a factor of 3.4 to match the barrier effects at the B3LYP/aug-cc-pVDZ level of theory. Experiments predict this reaction to have little to no barrier²⁷.

^d We remove the barrier from the rate limiting third step of this calculation, as experiment predicts this reaction to be barrierless⁵⁷.

^e Simulations did not converge beyond a O-O bond distance of 2.90 Å. The rate coefficient is calculated with the variational transition state at

this location, which has the highest ΔG .

^f We remove the barrier from the rate limiting third step of this calculation, as data evaluations suggest little to no barrier for this reaction⁵⁸.

^g This rate coefficient is one half of the calculated rate coefficient for $\text{OH} + \text{CH} \longrightarrow \text{anti}-\text{HCOH}_{(\nu)} \cdot$ as both $\text{CO} + \text{H}_2$ and $\text{CO} + \text{H} + \text{H}$ are equally probable decay pathways for $\text{anti}-\text{HCOH}_{(\nu)}$ ^{27,28,59}.

^h Experimental values are for ${}^3\text{O} + {}^3\text{CH}_2 \longrightarrow$ products divided by 2. As both product channels $\text{CO} + \text{H} + \text{H}$ and $\text{CO} + \text{H}_2$ are suggested to be equally likely^{27,28,59}.

Method Limitations

Occasionally computational methods misdiagnose reaction energy barriers. In other words, a method may calculate a barrier when experiments suggest the reaction is barrierless, or a method may calculate no barrier when experiments suggest a small-to-modest-sized barrier ($\sim 1\text{--}20 \text{ kJ mol}^{-1}$) exists. We find this to be biggest limitation of applying a consistent computational quantum method to a large number of reactions. This is the main reason for taking a hybrid approach to building CRAHCN-O. Experiments are the most accurate method to calculate rate coefficients, therefore experimental values will always be used when possible. However, for the large number of reactions without experimentally measured rate coefficients, we must use a robust and feasible computational method to calculate and include these reactions in the network.

In four cases (noted in Table 3), our chosen computational method (BHandHLYP/aug-cc-pVDZ) predicts barriers at the first step or an intermediate step of reactions that are expected to be barrierless. In one other case, this method predicts a reaction had no barrier, when experiment suggests a barrier of $17.15 \text{ kJ mol}^{-1}$ ⁶⁰. For these few cases, we artificially remove the barriers from these calculations, or introduce an experimental barrier. Based on the calculations in this paper, we find this method correctly diagnoses barriers $\sim 92\%$ of the time.

Comparing the barrier diagnosis capabilities of BHandHLYP/aug-cc-pVDZ with two other widely used method in past work¹⁸, we find CCSD/aug-cc-pVTZ and ω B97XD/aug-cc-pVDZ share these limitations. For 11 chosen reactions, BHandHLYP/aug-cc-pVDZ misdiagnosed 4 barriers, CCSD/aug-cc-pVTZ misdiagnosed 5 barriers, and ω B97XD/aug-cc-pVDZ misdiagnosed 2 barriers.

A second limitation of our method is that we do not include a correction factor for quantum mechanical tunneling. This may not be a big concern at 298 K, where our rate coefficient calculations are typically within a factor of two of experimental values, and generally always within an order of magnitude of experimental values. However, tunneling is most relevant at lower temperatures⁶¹.

Given the lack of experimental low temperature ($\lesssim 230 \text{ K}$) rate coefficient data for the reactions in this study, we cannot obtain a valid statistical sense of the accuracy of our method for calculating low temperature rate coefficients. However, it is a reasonable assumption that our treatment leads to larger uncertainties at the lower end of

our temperature range (50–200 K), where tunneling plays a greater role; possibly up to two orders of magnitude.

DISCUSSION

Highlighted New Reactions

As we have already noted, we have discovered 45 previously unknown reactions and provide the first calculations of their rate coefficients. In Table 4, we highlight 6 of these reactions. These reactions are potentially key pathways for the production and destruction of HCN or H_2CO in planetary atmospheres due to their high rate coefficients at 298 K, and the reasonably high abundances of their reactants in atmospheres.

Different reactions tend to dominate in different regions of an atmosphere. In the diffuse upper atmosphere (thermosphere), incoming UV radiation breaks apart dominant atmospheric species to produce radicals. In the dense lower atmosphere (troposphere), radicals can be transported from the upper atmosphere via turbulent mixing, or produced by lightning and/or GCRs. In this lower region, there is also sufficient pressure to collisionally deexcite the vibrationally excited intermediates in three-body reactions.

One newly discovered reaction with a great potential to produce substantial amounts H_2CO in upper atmospheres is ${}^1\text{O} + \text{CH}_3 \longrightarrow \text{H}_2\text{CO} + \text{H}$. Firstly, there will likely be high concentrations of reactants ${}^1\text{O}$ and CH_3 in the upper atmospheres of planets containing CO_2 and CH_4 , as the former are the direct photodissociation fragments of the latter. Secondly, this reaction has a barrierless rate coefficient of $k(298 \text{ K}) = 4.3 \times 10^{-10} \text{ cm}^3 \text{s}^{-1}$, which is in the 94th percentile for highest two-body reaction rate coefficients in this study. For these reasons, we expect this reaction to be a dominant source of H_2CO in CO_2 -rich and CH_4 -containing atmospheres such as the early Earth. At the CCSD/aug-cc-pVDZ level of theory, we calculate this rate coefficient to be only 14% lower ($3.7 \times 10^{-10} \text{ cm}^3 \text{s}^{-1}$), suggesting this calculation is not very sensitive to the choice of computational method.

In lower planetary atmospheres, we find two new three-body reactions that may be important pathways to H_2CO . These reactions are ${}^1\text{O} + {}^1\text{CH}_2 + \text{M} \longrightarrow \text{H}_2\text{CO} + \text{M}$ and ${}^3\text{O} + {}^3\text{CH}_2 + \text{M} \longrightarrow \text{H}_2\text{CO} + \text{M}$. These reactions are most favourable at the high-pressure limit, where their rate coefficients are $k_\infty(298 \text{ K}) = 3.3 \times 10^{-10}$ and $6.7 \times 10^{-11} \text{ cm}^3 \text{s}^{-1}$, respectively. The pressures at which these reaction rate coefficients reach 90% of $k_\infty(298 \text{ K})$ in a N_2 bath gas are 0.61 bar and 7.1 bar, respectively.

TABLE 4. Highlighted newly discovered reactions in this work, listed with their calculated rate coefficients at 298 K and potential for importance in atmospheres. For simplicity, reaction intermediates are not listed here. See Tables 2 and 3 for full details of reaction intermediates. Second-order rate coefficients have units cm^3s^{-1} . Third-order rate coefficients have units cm^6s^{-1} .

Reaction	k(298) calculated	Importance
${}^1\text{O} + \text{CH}_3 \longrightarrow \text{H}_2\text{CO} + \text{H}$	4.3×10^{-10}	H_2CO production in upper atmospheres
${}^1\text{O} + {}^1\text{CH}_2 + \text{M} \longrightarrow \text{H}_2\text{CO} + \text{M}$	$k_\infty = 3.3 \times 10^{-10}$ $k_0(\text{N}_2) = 6.6 \times 10^{-27}$ $k_0(\text{CO}_2) = 7.7 \times 10^{-27}$ $k_0(\text{H}_2) = 1.2 \times 10^{-26}$	H_2CO production in lower atmospheres
${}^3\text{O} + {}^3\text{CH}_2 + \text{M} \longrightarrow \text{H}_2\text{CO} + \text{M}$	$k_\infty = 6.7 \times 10^{-11}$ $k_0(\text{N}_2) = 9.2 \times 10^{-29}$ $k_0(\text{CO}_2) = 1.1 \times 10^{-28}$ $k_0(\text{H}_2) = 1.7 \times 10^{-28}$	H_2CO production in lower atmospheres
${}^1\text{O} + \text{H}_2\text{CN} \longrightarrow \text{HCN} + \text{OH}$	1.2×10^{-13}	HCN production in upper atmospheres
$\text{H}_2\text{CO} + {}^1\text{O} \longrightarrow \text{HCO} + \text{OH}$	4.6×10^{-10}	H_2CO destruction in upper atmospheres
${}^1\text{O} + \text{HCN} + \text{M} \longrightarrow \text{HCNO} + \text{M}$	$k_\infty = 3.3 \times 10^{-11}$ $k_0(\text{N}_2) = 4.0 \times 10^{-29}$ $k_0(\text{CO}_2) = 4.6 \times 10^{-29}$ $k_0(\text{H}_2) = 8.0 \times 10^{-29}$	HCN destruction in lower atmospheres

Such pressures would have been present in the evolving early Earth atmosphere ~ 4.5 billion years ago.⁶²

For new potentially important routes to HCN, we find ${}^1\text{O} + \text{H}_2\text{CN} \longrightarrow \text{HCN} + \text{OH}$, which has a rate coefficient of $k(298 \text{ K}) = 1.2 \times 10^{-13} \text{ cm}^3\text{s}^{-1}$. This reaction has the potential to be an important source of HCN in upper atmospheres with high CO₂ mixing ratios, and low H₂ and CH₄ mixing ratios. The reason for this is that there is a direct competing reaction for HCN production from H₂CN + H \longrightarrow HCN + H₂, which has a rate coefficient of $k(298 \text{ K}) = 2.2 \times 10^{-11} \text{ cm}^3\text{s}^{-1}$. Therefore, the ¹O/H ratio in upper atmospheres will determine which of these two reactions dominates. We note also that this reaction has a complex reaction scheme, with two other favourable channels from the H₂CNO· intermediate: HCNO + H and ³O + H₂CN. Our calculations of this reaction rate coefficient using two other computational methods (ω B97XD, CCSD) suggests the channel to HCN + OH may be more favourable than our BHandHLYP calculation implies, by up to a factor of ~ 700 (see theoretical case study 9 in the SI for more details). Given these discrepancies, and the novelty of this reaction, we recommend experimental measurements be performed for the three product channels of ¹O + H₂CN.

A new reaction with a great potential to destroy H₂CO is H₂CO + ¹O \longrightarrow HCO + OH, which has a barrierless rate coefficient of $4.6 \times 10^{-10} \text{ cm}^3\text{s}^{-1}$ at 298 K. As with the main new production pathway to H₂CO, this rate coefficient is one of the highest two-body rate coefficients in this study, and likely plays a role of attenuating H₂CO in upper atmospheres. At the CCSD/aug-cc-pVDZ level

of theory, we calculate this rate coefficient to be only 50% lower ($2.3 \times 10^{-10} \text{ cm}^3\text{s}^{-1}$) than the value at the BHandHLYP/aug-cc-pVDZ level of theory.

Lastly, we highlight a new HCN destruction pathway in lower atmospheres, ${}^1\text{O} + \text{HCN} + \text{M} \longrightarrow \text{HCNO} + \text{M}$. This reaction may be particularly important in attenuating HCN abundances in the troposphere, which is the region where HCN dissolves in rain droplets and makes its way into surface water. This reaction rate coefficient reaches 90% of $k_\infty(298 \text{ K})$ in a N₂ bath gas at 3 bar.

CRAHCN-O

CRAHCN-O is a chemical reaction network that can be used to simulate the production of HCN and H₂CO in atmospheres ranging from ~ 50 –400 K dominated by any of the following gases: CO₂, N₂, H₂O, CH₄, and H₂. CRAHCN-O is the amalgamation of the CRAHCN network developed in Pearce et al.^[18] and the oxygen extension developed in this work. CRAHCN-O contains experimental rate coefficients (when available), and our consistently calculated theoretical rate coefficients from this work otherwise.

We summarize the oxygen extension in Tables S1 and S2 in the supplementary materials. In addition to the 126 reactions explored in this work, we include one experimental spin-forbidden collisionally induced intersystem crossing reaction (¹O + M \longrightarrow ³O + M), whose rate coefficient cannot be calculated using our theoretical method.

The original CRAHCN network can be found in the

appendices of Pearce et al.^[18].

CONCLUSIONS

In this work, we use a novel technique making use of computational quantum chemistry and experimental data to build a consistent reduced atmospheric hybrid chemical network oxygen extension (CRAHCN-O). This network can be used to simulate HCN and H₂CO chemistry in planetary atmospheres dominated by CO₂, N₂, H₂O, CH₄, and H₂.

The oxygen extension contains 127 reactions, and is made up of approximately 30% experimental and 70% consistently calculated theoretical rate coefficients. Below are the main conclusions of this work in bullet point.

- We discover 45 previously unknown reactions, and are the first to calculate their rate coefficients. These new reactions typically involve electronically excited species (e.g., ¹O, ¹CH₂, ²N).
- The majority (~62%) of our calculated rate coefficients are accurate to within a factor of two of experimental measurements. ~84% are accurate to within a factor of 6 of experimental values, and the rest are accurate to within about an order of magnitude of experimental values. This level of accuracy is consistent with the uncertainties assigned in large scale experimental data evaluations.
- We identify 6 potentially key new production and destruction pathways for H₂CO and HCN from these previously unknown reactions.
- The high, barrierless rate coefficient of ¹O + CH₃ → H₂CO + H ($k(298\text{ K}) = 4.3 \times 10^{-10}\text{ cm}^3\text{s}^{-1}$) likely makes it a key source of formaldehyde in upper atmospheres where ¹O and CH₃ are produced from the UV photodissociation of CO₂ and CH₄, respectively.

- Conversely, the high, barrierless rate coefficient of H₂CO + ¹O → HCO + OH ($k(298\text{ K}) = 4.6 \times 10^{-10}\text{ cm}^3\text{s}^{-1}$) likely makes it a key sink for formaldehyde in upper atmospheres.

- ¹O + H₂CN → HCN + OH is less efficient than the known HCN source, H₂CN + H → HCN + H₂; However the former may dominate HCN production in CO₂-rich upper atmospheres with high ¹O/H ratios from CO₂ photodissociation.

- In lower atmospheres (i.e. high partial pressures), H₂CO may form via new reactions between ¹O + ¹CH₂ and ³O + ³CH₂, which require a collisional third body at the high pressures present in these regions. HCN may be efficiently removed in this region via ¹O + HCN + M → HCNO + M.

Having now filled in the missing chemical data relevant to HCN and H₂CO production in CO₂- and H₂O-rich atmospheres, we intend to couple CRAHCN-O to a 1D chemical kinetic model to simulate the atmosphere of the early Earth.

SUPPORTING INFORMATION

Rate coefficient data, experimental data, Lennard-Jones parameters, theoretical case studies, and quantum chemistry data.

ACKNOWLEDGMENTS

B.K.D.P. is supported by an NSERC Alexander Graham Bell Canada Graduate Scholarship-Doctoral (CGS-D). P.W.A is supported by NSERC, the Canada Research Chairs, and Canarie. R.E.P. is supported by an NSERC Discovery Grant. We acknowledge Compute Canada for allocating the computer time required for this research.

REFERENCES

-
- [1] Oró, J. Mechanism of Synthesis of Adenine from Hydrogen Cyanide under Possible Primitive Earth Conditions. *Nature* **1961**, *191*, 1193–1194.
 - [2] Larowe, D. E.; Regnier, P. Thermodynamic Potential for the Abiotic Synthesis of Adenine, Cytosine, Guanine, Thymine, Uracil, Ribose, and Deoxyribose in Hydrothermal Systems. *Orig. Life Evol. Biosph.* **2008**, *38*, 383–397.
 - [3] Ferus, M. et al. Prebiotic synthesis initiated in formaldehyde by laser plasma simulating high-velocity impacts. *Astron. Astrophys.* **2019**, *626*, A52.
 - [4] Butlerow, A. Bildung einer zuckerartigen Substanz durch Synthese. *Ann. Chem. Pharm.* **1861**, *120*, 295–298.
 - [5] Breslow, R. On the mechanism of the formose reaction. *Tetrahedron Letts.* **1959**, *1*, 22–26.
 - [6] Strecker, A. Ueber einen neuen aus AldehydAmmoniak und Blausäure entstehenden Körper. *Liebigs Ann. Chem.* **1854**, *91*, 349–351.
 - [7] Miller, S. L.; Van Trump, J. E. In *Origin of Life*; Wolman, Y., Ed.; Reidel: Dordrecht, The Netherlands, 1981; pp 135–141.

- [8] Catling, D.; Kasting, J. F. In *Planets and life - the emerging science of astrobiology*; Sullivan, III, W. T., Baross, J. A., Eds.; Cambridge University Press: Cambridge, 2007; pp 91–116.
- [9] Trail, D.; Watson, E. B.; Tailby, N. D. The oxidation state of Hadean magmas and implications for early Earths atmosphere. *Nature* **2011**, *480*, 79–82.
- [10] Pinto, J. P.; Gladstone, G. R.; Yung, Y. L. Photochemical Production of Formaldehyde in Earth's Primitive Atmosphere. *Science* **1980**, *210*, 183–185.
- [11] Schmidt, J. A.; Johnson, M. S.; Schinke, R. Carbon dioxide photolysis from 150 to 210 nm: Singlet and triplet channel dynamics, UV-spectrum, and isotope effects. *Proc. Nat. Acad. Sci. U.S.A.* **2013**, *110*, 17691–17696.
- [12] Shi, X.; Yin, Q.-Z.; Gao, H.; Chang, Y.-C.; Jackson, W. M.; Wiens, R. C.; Ng, C.-Y. Branching Ratios in Vacuum Ultraviolet Photodissociation of CO and N₂: Implications for Oxygen and Nitrogen Isotopic Compositions of the Solar Nebula. *Astrophys. J.* **2017**, *850*, 48.
- [13] Gans, B.; Boyé-Péronne, S.; Broquier, M.; Delsaut, M.; Douin, S.; Fellows, C. E.; Halvick, P.; Loison, J.-C.; Lucchese, R. R.; Gauyacq, D. Photolysis of methane revisited at 121.6 nm and at 118.2 nm: quantum yields of the primary products, measured by mass spectrometry. *Phys. Chem. Chem. Phys.* **2011**, *13*, 8140–8152.
- [14] Engel, V.; Staemmler, V.; Vander Wal, R. L.; Crim, F. F.; Sension, R. J.; Hudson, B.; Andreson, P.; Hennig, S.; Weide, K.; Schinke, R. Photodissociation of water in the first absorption band: a prototype for dissociation on a repulsive potential energy surface. *J. Phys. Chem.* **1992**, *96*, 3201–3213.
- [15] Stecher, T. P.; Williams, D. A. Photodestruction of Hydrogen Molecules in H I Regions. *Astrophys. J. Lett.* **1967**, *149*, L29.
- [16] Zahnle, K. J. Photochemistry of Methane and the Formation of Hydrocyanic Acid (HCN) in the Earth's Early Atmosphere. *J. Geophys. Res.* **1986**, *91*, 2819–2834.
- [17] Tian, F.; Kasting, J. F.; Zahnle, K. Revisiting HCN formation in Earth's early atmosphere. *Earth Planet. Sci. Lett.* **2011**, *308*, 417–423.
- [18] Pearce, B. K. D.; Molaverdikhani, K.; Pudritz, R. E.; Henning, T.; Hébrard, E. HCN production in Titan's Atmosphere: Coupling quantum chemistry and disequilibrium atmospheric modeling. *Astrophys. J.* *in press* **2020**,
- [19] Pearce, B. K. D.; Ayers, P. W.; Pudritz, R. E. A Consistent Reduced Network for HCN Chemistry in Early Earth and Titan Atmospheres: Quantum Calculations of Reaction Rate Coefficients. *J. Phys. Chem. A* **2019**, *123*, 1861–1873.
- [20] Truhlar, D. G.; Garrett, B. C. Variational Transition State Theory. *Annu. Rev. Phys. Chem.* **1984**, *35*, 159–189.
- [21] Forst, W. *Unimolecular Reactions: A Concise Introduction*; Cambridge University Press: Cambridge, U.K., 2003.
- [22] Becke, A. D. A new mixing of Hartree-Fock and local density-functional theories. *J. Chem. Phys.* **1993**, *98*, 1372–1377.
- [23] Lee, C.; Yang, W.; Parr, R. G. Development of the Colle-Salvetti correlation-energy formula into a functional of the electron density. *Phys. Rev. B* **1988**, *37*, 785–789.
- [24] Dunning, Jr., T. H. Gaussian basis sets for use in correlated molecular calculations. I. The atoms boron through neon and hydrogen. *J. Chem. Phys.* **1989**, *90*, 1007–1023.
- [25] Kendall, R. A.; Dunning, Jr., T. H. Electron affinities of the firstrow atoms revisited. Systematic basis sets and wave functions. *J. Chem. Phys.* **1992**, *96*, 6796–6806.
- [26] Woon, D. E.; Dunning, Jr., T. H. Gaussian-basis sets for use in correlated molecular calculations. 3. The atoms aluminum through argon. *J. Chem. Phys.* **1993**, *98*, 1357–1371.
- [27] Baulch, D. L.; Cobos, C. J.; Cox, R. A.; Esser, C.; Frank, P.; Just, T.; Kerr, J. A.; Pilling, M. J.; Troe, J.; Walker, R. W.; et al., Evaluated kinetic data for combustion modelling. *J. Phys. Chem. Ref. Data* **1992**, *21*, 411–429.
- [28] Tsang, W.; Hampson, R. F. Chemical Kinetic Data Base for Combustion Chemistry. Part I. Methane and Related Compounds. *J. Phys. Chem. Ref. Data* **1986**, *15*, 1087–1279.
- [29] Frisch, M. J.; Trucks, G. W.; Schlegel, H. B.; Scuseira, G. E.; Robb, M. A.; Cheeseman, J. R.; Scalmani, G.; Barone, V.; Petersson, G. A.; Nakatsuji, H.; et al., *Gaussian 09*, Revision E.01; Gaussian, Inc.: Wallingford, CT, 2009.
- [30] Avogadro: an open-source molecular builder and visualization tool. Version 1.2.0. <http://avogadro.cc/>.
- [31] Hanwell, M. D.; Curtis, D. E.; Lonie, D. C.; Vandermeersch, T.; Zurek, E.; Hutchison, G. R. Avogadro: An advanced semantic chemical editor, visualization, and analysis platform. *J. Cheminform.* **2012**, *4*, 17.
- [32] Truhlar, D. G. In *Theory of Chemical Reaction Dynamics*; Baer, M., Ed.; CRC Press: Boca Raton, FL, 1985; pp 65–137.
- [33] Truhlar, D. G.; Garrett, B. C. Variational Transition-State Theory. *Acc. Chem. Res.* **1980**, *13*, 440–448.
- [34] Eyring, H. The Activated Complex in Chemical Reactions. *J. Chem. Phys.* **1935**, *3*, 107.
- [35] Vallance, C. *An Introduction to Chemical Kinetics*; 2053–2571; Morgan & Claypool Publishers: San Rafael, CA, 2017.
- [36] Carstensen, H.-H.; Dean, A. M. In *Comprehensive Chemical Kinetics*; Carr, R., Ed.; Elsevier: Amsterdam, 2007; Vol. 42; pp 101–184.
- [37] Barker, J. R.; Nguyen, T. L.; Stanton, J. F.; Aieta, C.; Ceotto, M.; Gabas, F.; Kumar, T. J. D.; Li, C. G. L.; Lohr, L. L.; Maranzana, A.; Ortiz, N. F.; Preses, J. M.; Simmie, J. M.; Sonk, J. A.; Stimač, P. J. *MultiWell-2019 Software Suite*; J. R. Barker: University of Michigan Ann Arbor, Michigan, USA, 2019.
- [38] Barker, J. R. MultipleWell, multiplepath unimolecular reaction systems. I. MultiWell computer program suite. *Int. J. Chem. Kinet.* **2001**, *33*, 232–245.
- [39] Barker, J. R. Energy transfer in master equation simulations: A new approach. *Int. J. Chem. Kinet.* **2009**, *41*, 748–763.
- [40] Pilling, M. J.; Robertson, S. H. Master Equation Models for Chemical Reactions of Importance in Combustion. *Annu. Rev. Phys. Chem.* **2003**, *54*, 245–275.
- [41] Akbar Ali, M.; Barker, J. R. Comparison of Three Isoelectronic Multiple-Well Reaction Systems: OH + CH₂O, OH + CH₂CH₂, and OH + CH₂NH. *J. Phys. Chem. A* **2015**, *119*, 7578–7592.

- [42] Gong, C.-M.; Ning, H.-B.; Li, Z.-R.; Li, X.-Y. Theoretical and kinetic study of reaction $C_2H + C_3H_6$ on the C_5H_7 potential energy surface. *Theor. Chem. Acc.* **2015**, *134*, 1599.
- [43] Zhao, L.; Ye, L.; Zhang, F.; Zhang, L. Thermal Decomposition of 1Pentanol and Its Isomers: A Theoretical Study. *J. Phys. Chem. A.* **2012**, *116*, 9238–9244.
- [44] Reid, R. C.; Prausnitz, J. M.; Sherwood, T. K. *The Properties of Gases and Liquids, Third Edition*; McGraw-Hill, Inc: New York, 1977; p 683.
- [45] Welty, J. R.; Wicks, C. E.; Wilson, R. E.; Rorrer, G. L. *Fundamentals of Momentum, Heat, and Mass Transfer, 5th Edition*; John Wiley & Sons, Inc.: Hoboken, NJ, 2008; p 711.
- [46] Wang, H.; Dames, E.; Sirjean, B.; Sheen, D. A.; Tango, R.; Violi, A.; Lai, J. Y. W.; Egolfopoulos, F. N.; Davidson, D. F.; Hanson, R. K.; et al., *JetSurF version 2.0*; 2010.
- [47] Clary, D. C. Fast Chemical Reactions: Theory Challenges Experiment. *Annu. Rev. Phys. Chem.* **1990**, *41*, 61–90.
- [48] Li, H.; Chen, B.-Z.; Huang, M.-B. CASPT2 investigation of ethane dissociation and methyl recombination using canonical variational transition state theory. *Int. J. Chem. Kinet.* **2008**, *40*, 161–173.
- [49] Hase, W. L.; Mondro, S. L.; Duchovic, R. J.; Hirst, D. M. Thermal Rate Constant for $H + CH_3 \rightarrow CH_4$ Recombination. 3. Comparison of Experiment and Canonical Variational Transition State Theory. *J. Am. Chem. Soc.* **1987**, *109*, 2916–2922.
- [50] Jasper, A. W.; Klippenstein, S. J.; Harding, L. B. Secondary Kinetics of Methanol Decomposition: Theoretical Rate Coefficients for $^3CH_2 + OH$, $^3CH_2 + ^3CH_2$, and $^3CH_2 + CH_3$. *J. Phys. Chem. A* **2007**, *111*, 8699–8707.
- [51] Daranlot, J.; Hu, X.; Xie, C.; Loison, J.-C.; Caubet, P.; Costes, M.; Wakelam, V.; Xie, D.; Guo, H.; Hickson, K. Low temperature rate constants for the $N(^4S) + CH(X^2\Pi_r)$ reaction. Implications for N_2 formation cycles in dense interstellar clouds. *Phys. Chem. Chem. Phys.* **2013**, *15*, 13888–13896.
- [52] Caldwell, J.; Back, R. A. Combination reactions of hydroxyl radicals in the flash photolysis of water vapour. *Trans. Faraday Soc.* **1965**, *61*, 1939–1945.
- [53] Black, G.; Porter, G. Vacuum ultra-violet flash photolysis of water vapour. *Proc. R. Soc. Lond. A Math. Phys. Sci.* **1962**, *266*, 185–197.
- [54] Zellner, R.; Erler, K.; Field, D. Kinetics of the recombination reaction $OH + H + M \rightarrow H_2O + M$ at low temperatures. Sixteenth Symposium (International) on Combustion. Seattle, 1977; pp 939–948.
- [55] Bravo-Pérez, G.; Alvarez-Idaboy, J. R.; Jiménez, A. G.; Cruz-Torres, A. Quantum chemical and conventional TST calculations of rate constants for the $OH +$ alkane reaction. *Chem. Phys.* **2005**, *310*, 213–223.
- [56] Mehlmann, C.; Frost, M. J.; Heard, D. E.; Orr, B. J.; Nelson, P. F. Rate constants for removal of $CH(D)$ ($\nu = 0$ and 1) by collisions with N_2 , CO , O_2 , NO and NO_2 at 298 K and with CO_2 at $296 \leq T/K \leq 873$. *J. Chem. Soc., Faraday Trans.* **1996**, *92*, 2335–2341.
- [57] Blitz, M. A.; Pesa, M.; Pilling, M. J.; Seakins, P. W. Reaction of CH with H_2O : Temperature Dependence and Isotope Effect. *J. Phys. Chem. A* **1999**, *103*, 5699–5704.
- [58] Cohen, N.; Westberg, K. R. Chemical Kinetic Data Sheets for High-Temperature Reactions. Part II. *J. Phys. Chem. Ref. Data* **1991**, *20*, 1211–1311.
- [59] Schaub, W. M.; Hsu, D. S. Y.; Lin, M. C. Dynamics and mechanisms of CO production from the reactions of CH_2 radicals with $O(^3P)$ and O_2 . Eighteenth Symposium (International) on Combustion. Seattle, 1981; pp 811–818.
- [60] Husain, D.; Mitra, S. K.; Young, A. N. Kinetic Study of Electronically Excited Nitrogen Atoms, $N(^2D_J, ^2P_J)$, by Attenuation of Atomic Resonance Radiation in the Vacuum Ultra-violet. *J. Chem. Soc., Faraday Trans. 2* **1974**, *70*, 1721–1731.
- [61] Meisner, J.; Kästner, J. Atom Tunneling in Chemistry. *Angew. Chem. Int. Ed. Engl.* **2016**, *55*, 5400–5413.
- [62] Zahnle, K.; Arndt, N.; Cockell, C.; Halliday, A.; Nisbet, E.; Selsis, F.; Sleep, N. H. Emergence of a Habitable Planet. *Space Sci. Rev.* **2007**, *129*, 35–78.
- [63] Clerc, M.; Barat, F. Kinetics of CO Formation Studied by Faruv Flash Photolysis of CO_2 . *J. Chem. Phys.* **1967**, *46*, 107–110.
- [64] Hochanadel, C. J.; Sworski, T. J.; Ogren, P. J. Ultraviolet spectrum and reaction kinetics of the formyl radical. *J. Phys. Chem.* **1980**, *84*, 231–235.
- [65] Nizamov, B.; Dagdigian, P. J. Spectroscopic and Kinetic Investigation of Methylene Amidogen by Cavity Ring-Down Spectroscopy. *J. Phys. Chem. A* **2003**, *107*, 2256–2263.
- [66] Campbell, I. M.; Thrush, B. A. Behaviour of carbon dioxide and nitrous oxide in active nitrogen. *Trans. Faraday Soc.* **1966**, *62*, 3366–3374.
- [67] Dunlea, E. J.; Ravishankara, A. R. Kinetic studies of the reactions of $O(^1D)$ with several atmospheric molecules. *Phys. Chem. Chem. Phys.* **2004**, *6*, 2152–2161.
- [68] Yu, T.; Yang, D. L.; Lin, M. C. Kinetics of CN radical reactions with formaldehyde and 1,3,5trioxane. *Int. J. Chem. Kinet.* **1993**, *25*, 1053–1064.
- [69] Yee Quee, M. J.; Thynne, J. C. J. The Photolysis of Organic Esters. *Ber. Bunsenges. Phys. Chem.* **1968**, *72*, 211–217.
- [70] Phillips, L. F. Rate of Reaction of OH with HCN Between 298 and 563 K. *Aust. J. Chem.* **1979**, *32*, 2571–2577.
- [71] Dunlea, E.-J.; Ravishankara, A. R. Kinetic studies of the reactions of $O(^1D)$ with several atmospheric molecules. *Phys. Chem. Chem. Phys.* **2004**, *6*, 2152–2161.
- [72] Vranckx, S.; Peeters, J.; Carl, S. Kinetics of $O(^1D) + H_2O$ and $O(^1D) + H_2$: absolute rate coefficients and $O(^3P)$ yields between 227 and 453 K. *Phys. Chem. Chem. Phys.* **2010**, *12*, 9213–9221.
- [73] Manion, J. A.; Huie, R. E.; Levin, R. D.; Burgess Jr., D. R.; Orkin, V. L.; Tsang, W.; McGivern, W. S.; Hudgens, J. W.; Knyazev, V. D.; Atkinson, D. B.; et al., *NIST Chemical Kinetics Database*; NIST Standard Reference Database Number 17, Version 7.0 (Web Version), Release 1.6.8, Data version 2015.09, National Institute of Standards and Technology: Gaithersburg, MD, <http://kinetics.nist.gov/>, (retrieved May 10, 2018).
- [74] Young, R. A.; Black, G.; Slanger, T. G. Reaction and Deactivation of $O(^1D)^*$. *J. Chem. Phys.* **1968**, *49*, 4758–4768.
- [75] Blitz, M. A.; Dillon, T. J.; Heard, D. E.; Pilling, M. J.; Trought, I. D. Laser induced fluorescence studies of the

- reactions of O(¹D₂) with N₂, O₂, N₂O, CH₄, H₂, CO₂, Ar, Kr and n-C₄H₁₀. *Phys. Chem. Chem. Phys.* **2004**, *6*, 2162–2171.
- [76] Wine, P. H.; Ravishankara, A. R. Kinetics of O(¹D) interactions with the atmospheric gases N₂, N₂O, H₂O, H₂, CO₂, and O₃. *Chem. Phys. Lett.* **1981**, *77*, 103–109.
- [77] Young, R. A.; Ung, A. Y.-M. Optical Studies of the Photolysis of CO₂ at 1470 Å. *J. Chem. Phys.* **1966**, *44*, 3038–3040.
- [78] Heidner, III, R. F.; Husain, D.; Wiesenfeld, J. R. Kinetic Investigation of Electronically Excited Oxygen Atoms, O(²D₂), by Time-resolved Attenuation of Atomic Resonance Radiation in the Vacuum Ultra-violet. *J. Chem. Soc., Faraday Trans. 2* **1973**, *69*, 927–938.
- [79] Amimoto, S. T.; Force, A. P.; Gulotty, Jr., R. G.; Wiesenfeld, J. R. Collisional deactivation of O(²D₂) by the atmospheric gases. *J. Chem. Phys.* **1979**, *71*, 3640–3647.
- [80] Davidson, J. A.; Sadowski, C. M.; Schiff, H. I.; Streit, G. E.; Howard, C. J.; Jennings, A. L., D. A. Schmeltekopf Absolute rate constant determinations for the deactivation of O(¹D) by time resolved decay of O(¹D) -> O(³P) emission. *J. Chem. Phys.* **1976**, *64*, 57–62.
- [81] Fell, B.; Rivas, I. V.; McFadden, D. L. Kinetic Study of Electronically Metastable Nitrogen Atoms, N(²D_J), by Electron Spin Resonance Absorption. *J. Phys. Chem.* **1981**, *85*, 224–228.
- [82] Black, G.; Slanger, T. G.; St. John, G. A.; Young, R. A. Vacuum-Ultraviolet Photolysis of N₂O. IV. Deactivation of N(²D). *J. Chem. Phys.* **1969**, *51*, 116–121.
- [83] Lin, C.-L.; Kaufman, F. Reactions of Metastable Nitrogen Atoms. *J. Chem. Phys.* **1971**, *55*, 3760–3770.
- [84] Piper, L. G.; Donahue, M. E.; Rawlins, W. T. Rate Coefficients for N(²D) Reactions. *J. Phys. Chem.* **1987**, *91*, 3883–3888.
- [85] Laufer, A. H.; Bass, A. M. Reaction between triplet methylene and CO₂: rate constant determination. *Chem. Phys. Lett.* **1977**, *46*, 151–155.
- [86] Butler, J. E.; Fleming, J. W.; Goss, L. P.; Lin, M. C. Kinetics of CH Radical Reactions Important to Hydrocarbon Combustion Systems. 1980.
- [87] Butler, J. E.; Fleming, J. W.; Goss, L. P.; Lin, M. C. Kinetics of CH radical reactions with selected molecules at room temperature. *Chem. Phys.* **1981**, *56*, 355–365.
- [88] Berman, M. R.; Fleming, J. W.; Harvey, A. B.; Lin, M. C. Temperature dependence of CH radical reactions with O₂, NO, CO and CO₂. 1982.
- [89] Niki, H.; Maker, P. D.; Savage, C. M.; Breitenbach, L. P. Relative rate constants for the reaction of hydroxyl radical with aldehydes. *J. Phys. Chem.* **1978**, *82*, 132–134.
- [90] Zabarnick, S.; Fleming, J. W.; Lin, M. C. Kinetics of hydroxyl radical reactions with formaldehyde and 1,3,5-trioxane between 290 and 600 K. *Int. J. Chem. Kinet.* **1988**, *20*, 117–129.
- [91] Stief, L. J.; Nava, D. F.; Payne, W. A.; Michael, J. V. Rate constant for the reaction of hydroxyl radical with formaldehyde over the temperature range 228–362 K. *J. Phys. Chem.* **1980**, *73*, 2254–2258.
- [92] Atkinson, R.; Pitts Jr., J. N. Kinetics of the reactions of the OH radical with HCHO and CH₃CHO over the temperature range 299–426K. *J. Chem. Phys.* **1978**, *68*, 3581–3584.
- [93] Niki, H.; Maker, P. D.; Savage, C. M.; Breitenbach, L. P. An Fourier transform infrared study of the kinetics and mechanism for the reaction of hydroxyl radical with formaldehyde. *J. Phys. Chem.* **1984**, *88*, 5342–5344.
- [94] Temps, F.; Wagner, H. G. Rate Constants for the Reactions of OH Radicals with CH₂O and HCO. *Ber. Bunsenges. Phys. Chem.* **1984**, *88*, 415–418.
- [95] Yetter, R. A.; Rabitz, H.; Dryer, F. L. Evaluation of the rate constant for the reaction OH + H₂CO: Application of modeling and sensitivity analysis techniques for determination of the product branching ratio. *J. Chem. Phys.* **1989**, *91*, 4088–4097.
- [96] Vandooren, J.; Van Tiggelen, P. J. Reaction mechanisms of combustion in low pressure acetylene-oxygen flames. Sixteenth Symposium (International) on Combustion. 1977; pp 1133–1144.
- [97] Chang, J. S.; Barker, J. R. Reaction rate and products for the reaction oxygen(³P) + H₂CO. *J. Phys. Chem.* **1979**, *83*, 3059–3064.
- [98] Klemm, R. B. Absolute rate parameters for the reactions of formaldehyde with O atoms and H atoms over the temperature range 250–500 K. *J. Chem. Phys.* **1979**, *71*, 1987–1993.
- [99] Klemm, R. B.; Skolnik, E. G.; Michael, J. V. Absolute rate parameters for the reaction of O(³P) with H₂CO over the temperature range 250 to 750 K. *J. Chem. Phys.* **1980**, *72*, 1256–1264.
- [100] Herron, J. T.; Penzhorn, R. D. Mass spectrometric study of the reactions of atomic oxygen with ethylene and formaldehyde. *J. Phys. Chem.* **1969**, *73*, 191–196.
- [101] Mack, G. P. R.; Thrush, B. A. Reaction of oxygen atoms with carbonyl compounds. Part 1.–Formaldehyde. *J. Chem. Soc., Faraday Trans. 1* **1973**, *69*, 208–215.
- [102] Zabarnick, S.; Fleming, J. W.; Lin, M. C. Temperature dependence of CH radical reactions with H₂O and CH₂O. 1988.
- [103] Ridley, B. A.; Davenport, J. A.; Stief, L. J.; Welge, K. H. Absolute Rate Constant for the Reaction H+H₂CO. *J. Chem. Phys.* **1972**, *57*, 520–523.
- [104] Brennen, W. R.; Gay, I. D.; Glass, G. P.; Niki, H. Reaction of atomic hydrogen with formaldehyde. *J. Chem. Phys.* **1965**, *43*, 2569–2570.
- [105] Oehlers, C.; Wagner, H. G.; Ziemer, H.; Dóbé, S. An Investigation of the D/H Addition-Elimination and H Atom Abstraction Channels in the Reaction D + H₂CO in the Temperature Range 296 K ≤ T ≤ 780 K. *J. Phys. Chem. A* **2000**, *104*, 10500–10510.
- [106] Vandooren, J.; Oldenhove de Guertechin, L.; Van Tiggelen, P. J. Kinetics in a lean formaldehyde flame. *Combust. Flame* **1986**, *64*, 127–139.
- [107] Westenberg, A. A.; DeHaas, N. Measurement of the rate constant for H + H₂CO -> H₂ + HCO at 297–652K. *J. Phys. Chem.* **1972**, *76*, 2213–2214.
- [108] Stoeckel, F.; Schuh, M. D.; Goldstein, N.; Atkinson, G. H. Time-resolved intracavity laser spectroscopy: 266 nm photodissociation of acetaldehyde vapor to form HCO. *Chem. Phys.* **1985**, *95*, 135–144.
- [109] Baggott, J. E.; Frey, H. M.; Lightfoot, P. D.; Walsh, R. The absorption cross section of the HCO radical at 614.59 nm and the rate constant for HCO+HCO -> H₂CO+CO. *Chem. Phys. Lett.* **1986**, *132*, 225–230.
- [110] Reilly, J. P.; Clark, J. H.; Moore, J. B.; Pimentel, G. C. HCO production, vibrational relaxation, chemical kinetics, and spectroscopy following laser photolysis of

- formaldehyde. *J. Chem. Phys.* **1978**, *69*, 4381–4394.
- [111] Friedrichs, G.; Herbon, J. T.; Davidson, D. F.; Hanson, R. K. Quantitative detection of HCO behind shock waves: The thermal decomposition of HCO. *Phys. Chem. Chem. Phys.* **2002**, *4*, 5778–5788.
- [112] Veyret, B.; Roussel, P.; Lesclaux, R. Absolute rate constant for the disproportionation reaction of formyl radicals from 295 to 475 K. *Chem. Phys. Lett.* **1984**, *103*, 389–392.
- [113] Vedeneev, V.; Sviridenkov, E.; Nadtocenko, V.; Ceskis, S.; Sarkisov, O. Spectroscopic study of elementary reactions involving HCO, NH₂ and HNO. *J. Chem. Phys.* **1984**, *4*, 111–120.
- [114] Mulenko, S. A. Investigation of the recombination of the hco radical in an atmosphere of argon and helium by the method of internal resonator laser spectroscopy. *J. Appl. Spectrosc.* **1980**, *33*, 688–694.
- [115] Ziemer, H.; Döbélé, S.; Wagner, H. G.; Olzman, M.; Viskolcz, B.; Temps, F. Kinetics of the reactions of HCO with H and D atoms. *Ber. Bunsenges. Phys. Chem.* **1998**, *102*, 897–905.
- [116] Forster, R.; Frost, M.; Fulle, D.; Hamann, H. F.; Hippel, H.; Schlepegrell, A.; Troe, J. High pressure range of the addition of HO to HO, NO, NO₂, and CO. I. Saturated laser induced fluorescence measurements at 298 K. *J. Chem. Phys.* **1995**, *103*, 2949–2958.
- [117] Niki, H.; Maker, P. D.; Savage, C. M.; Breitenbach, L. P. Fourier transform infrared spectroscopic study of the kinetics for the OH radical reaction of ¹³C¹⁶O and ¹²C¹⁸O. *J. Phys. Chem.* **1984**, *88*, 2116–2119.
- [118] Frost, M. J.; Sharkey, P.; Smith, I. W. M. Reaction between OH (OD) radicals and CO at temperatures down to 80 K: experiment and theory. *J. Phys. Chem.* **1993**, *97*, 12254–12259.
- [119] Bohn, B.; Zetzsch, C. Formation of HO₂ from OH and C₂H₂ in the presence of O₂. *J. Chem. Soc., Faraday Trans.* **1998**, *94*, 1203–1210.
- [120] Herron, J. T. Reaction kinetics involving ground X²Π and excited A²Σ⁺ hydroxyl radicals. Part 1.—Quenching kinetics of OH A²Σ⁺ and rate constants for reactions of OH X²Π with CH₃CCl₃ and CO. *J. Chem. Soc., Faraday Trans. 2* **1979**, *75*, 569–581.
- [121] Husain, D.; Plane, J. M. C.; Slater, N. K. H. Kinetic investigation of the reactions of OH(X²Π) with the hydrogen halides, HCl, DCl, HBr and DBr by time-resolved resonance fluorescence (A²Σ⁺-X²Π). *J. Chem. Soc., Faraday Trans. 2* **1981**, *77*, 1949–1962.
- [122] Lissianski, V.; Yang, H.; Qin, Z.; Mueller, M. R.; Shin, K. S.; Gardiner Jr., W. C. High-temperature measurements of the rate coefficient of the H + CO₂ → CO + OH reaction. *Chem. Phys. Lett.* **1995**, *240*, 57–62.
- [123] Ravishankara, A. R.; Thompson, R. L. Kinetic study of the reaction of OH with CO from 250 to 1040 K. *Chem. Phys. Lett.* **1983**, *99*, 377–381.
- [124] Frost, M. J.; Sharkey, P.; Smith, I. W. M. Energy and structure of the transition states in the reaction OH + CO → H + CO₂. *Faraday Discuss. Chem. Soc.* **1991**, *91*, 305–317.
- [125] Herron, J. T. Mass-Spectrometric Study of the Rate of the Reaction CO + OH. *J. Chem. Phys.* **1966**, *45*, 1854–1855.
- [126] Davidson, J. A.; Schiff, H. I.; Brown, T. J.; Howard, C. J. Temperature dependence of the deactivation of O(¹D) by CO from 113–333 K. *J. Chem. Phys.* **1978**, *69*, 1216–1217.
- [127] Noxon, J. F. Optical Emission from O(¹D) and O₂(b¹Σ_g) in Ultraviolet Photolysis of O₂ and CO₂. *J. Chem. Phys.* **1970**, *52*, 1852–1873.
- [128] Le Picard, S. D.; Canosa, A.; Rowe, B. R.; Brownsword, R. A.; Smith, I. W. M. Determination of the limiting low pressure rate constants of the reactions of CH with N₂ and CO: a CRESU measurement at 53 K. *J. Chem. Soc., Faraday Trans.* **1998**, *94*, 2889–2893.
- [129] Brownsword, R. A.; Herbert, L. B.; Smith, I. W. M.; Stewart, D. W. A. Pressure and temperature dependence of the rate constants for the association reactions of CH radicals with CO and N₂ between 202 and 584 K. *J. Chem. Soc., Faraday Trans.* **1996**, *92*, 1087–1094.
- [130] Fulle, D.; Hippler, H.; Striebel, F. The high-pressure range of the reaction CH(²Π)+CO+M→HCCO+M. *J. Chem. Phys.* **1998**, *108*, 6709–6716.
- [131] Taatjes, C. A. Association and isotopic exchange reactions of CH(CD)[X²Π]+CO . *J. Chem. Phys.* **1997**, *106*, 1786–1795.
- [132] Bosnali, M. W.; Perner, D. Notizen: Reaktionen von pulsradiolytisch erzeugtem CH(²Π) mit Methan und anderen Substanzen. *Z. Naturforsch.* **1971**, *26*, 1768–1769.
- [133] Bennett, J. E.; Blackmore, D. R. Rates of gas-phase hydrogen-atom recombination at room temperature in the presence of added gases. Thirteenth Symposium (International) on Combustion. Seattle, 1971; pp 51–59.
- [134] Wang, H. Y.; Eyre, J. A.; Dorfman, L. M. Activation energy for the gas phase reaction of hydrogen atoms with carbon monoxide. *J. Chem. Phys.* **1973**, *59*, 5199–5200.
- [135] Hikida, T.; Eyre, J. A.; Dorfman, L. M. Pulse Radiolysis Studies. XX. Kinetics of Some Addition Reactions of Gaseous Hydrogen Atoms by Fast Lymanα Absorption Spectrophotometry . *J. Chem. Phys.* **1971**, *54*, 3422–3428.
- [136] Ahumada, J. J.; Michael, J. V.; Osborne, D. T. Pressure Dependence and Third Body Effects on the Rate Constants for H+O₂, H+NO, and H+CO. *J. Chem. Phys.* **1972**, *57*, 3736–3745.
- [137] Gauthier, M. J. E.; Snelling, D. R. La photolyse de l'ozone à 253.7 nm: Desactivation de O(¹D) et de O₂(¹Σ) par les gaz de l'atmosphère. *J. Photochem.* **1975**, *4*, 27–50.
- [138] Lee, L. C.; Slanger, T. G. Atmospheric OH production—The O(¹D) + H₂O reaction rate. *Geophys. Res. Lett.* **1979**, *6*, 165–166.
- [139] Davidson, J. A.; Schiff, H. I.; Streit, G. E.; McAfee, J. R.; Schmeltekopf, A. L.; Howard, C. J. Temperature dependence of O(¹D) rate constants for reactions with N₂O, H₂, CH₄, HCl, and NH₃. *J. Chem. Phys.* **1977**, *67*, 5021–5025.
- [140] Streit, G. E.; Howard, C. J.; Schmeltekopf, A. L.; Davidson, J. A.; Schiff, H. I. Temperature dependence of O(¹D) rate constants for reactions with O₂, N₂, CO₂, O₃, and H₂O. *J. Chem. Phys.* **1976**, *65*, 4761–4764.
- [141] Dunlea, E.-J.; Ravishankara, A. R. Measurement of the rate coefficient for the reaction of O(¹D) with H₂O and re-evaluation of the atmospheric OH production rate. *Phys. Chem. Chem. Phys.* **2004**, *6*, 3333–3340.
- [142] Gericke, K.-H.; Comes, F. J. Energy partitioning in the reaction O(¹D) + H₂O → OH + OH.: The influence of O(¹D) translational energy on the reaction rate constant. *Chem. Phys. Lett.* **1981**, *81*, 218–222.

- [143] Fritz, B.; Lorenz, K.; Steinert, W.; Zellner, R. Laboratory Kinetic Investigations of the Tropospheric Oxidation of Selected Industrial Emissions. Physico-Chemical Behaviour of Atmospheric Pollutants. Dordrecht, 1982.
- [144] Zellner, R.; Ewig, F.; Paschke, R.; Wagner, G. Pressure and temperature dependence of the gas-phase recombination of hydroxyl radicals. *J. Phys. Chem.* **1988**, *92*, 4184–4190.
- [145] Sangwan, M.; Chesnokov, E. N.; Krasnoperov, L. N. Reaction OH + OH Studied over the 298–834 K Temperature and 1 – 100 bar Pressure Ranges. *J. Phys. Chem. A* **2012**, *116*, 6282–6294.
- [146] Trainor, D. W.; von Rosenberg Jr., C. W. Energy partitioning in the products of elementary reactions involving OH-radicals. Fifteenth Symposium (International) on Combustion. 1975; pp 755–764.
- [147] Trainor, D. W.; von Rosenberg Jr., C. W. Flash photolysis study of the gas phase recombination of hydroxyl radicals. *J. Chem. Phys.* **1974**, *61*, 1010–1015.
- [148] Greiner, N. R. Hydroxyl radical kinetics by kinetic spectroscopy. III. Reactions with hydrogen peroxide in the range 300–458 K. *J. Phys. Chem.* **1968**, *72*, 406–410.
- [149] Fulle, D.; Hamann, H. F.; Hippler, H.; Troe, J. High-pressure range of the addition of HO to HO. III. Saturated laser-induced fluorescence measurements between 200 and 700 K. *J. Chem. Phys.* **1996**, *105*, 1001–1006.
- [150] Dixon-Lewis, G.; Wilson, W. E.; Westenberg, A. A. Studies of Hydroxyl Radical Kinetics by Quantitative ESR. *J. Chem. Phys.* **1966**, *44*, 2877–2884.
- [151] Westenberg, A. A.; deHaas, N. Rate of the Reaction OH + OH → H₂O + O. *J. Chem. Phys.* **1973**, *58*, 4066–4071.
- [152] Farquharson, G. K.; Smith, R. H. Rate constants for the gaseous reactions OH + C₂H₄ and OH + OH. *Aust. J. Chem.* **1980**, *33*, 1425–1435.
- [153] Clyne, M. A. A.; Down, S. Kinetic behaviour of OH X²Π and A²σ⁺ using molecular resonance fluorescence spectrometry. *J. Chem. Soc., Faraday Trans. 2* **1974**, *70*, 253–266.
- [154] Sangwan, M.; Krasnoperov, L. N. Disproportionation Channel of Self-Reaction of Hydroxyl Radical, OH + OH → H₂O + O, Studied by Time-Resolved Oxygen Atom Trapping. *J. Phys. Chem. A* **2012**, *116*, 11817–11822.
- [155] Bedjanian, Y.; Le Bras, G.; Poulet, G. Kinetic Study of OH + OH and OD + OD Reactions. *J. Phys. Chem. A* **1999**, *103*, 7017–7025.
- [156] Wagner, G.; Zellner, R. Temperature Dependence of the Reaction OH + OH → H₂O + O. *Ber. Bunsenges. Phys. Chem.* **1981**, *85*, 1122–1128.
- [157] Breen, J. E.; Glass, G. P. Rate of Some Hydroxyl Radical Reactions. *Combust. Flame* **1970**, *52*, 1082–1086.
- [158] Smith, I. W. M.; Stewart, D. W. A. Low-temperature kinetics of reactions between neutral free radicals. Rate constants for the reactions of OH radicals with N atoms ($103 \leq T/K \leq 294$) and with O atoms ($158 \leq T/K \leq 294$). *J. Chem. Soc., Faraday Trans. 1* **1994**, *90*, 3221–3227.
- [159] Howard, M. J.; Smith, I. W. M. Direct Rate Measurements on the Reactions N + OH → NO + H and O + OH → O₂ + H from 250 to 515 K. *J. Chem. Soc., Faraday Trans. 2* **1981**, *77*, 997–1008.
- [160] Westenberg, A. A.; De Haas, N.; Roscoe, J. M. Radical reactions in an electron spin resonance cavity homogeneous reactor. *J. Phys. Chem.* **1970**, *74*, 3431–3438.
- [161] Howard, M. J.; Smith, I. W. M. Direct rate measurements on the reactions N + OH → NO + H And O + OH → O₂ + H. *Chem. Phys. Lett.* **1980**, *69*, 40–44.
- [162] Robertson, R.; Smith, G. P. Temperature Dependence of O + OH at 136–377 K Using Ozone Photolysis. *J. Phys. Chem. A* **2006**, *110*, 6673–6679.
- [163] Robertson, R.; Smith, G. P. Photolytic measurement of the O + OH rate constant at 295 K. *Chem. Phys. Lett.* **2002**, *358*, 157–162.
- [164] Brune, W. H.; Schwab, J. J.; Anderson, J. G. Laser magnetic resonance, resonance fluorescence, and resonance absorption studies of the reaction kinetics of O + OH → H + O₂, O + HO₂ → OH + O₂, N + OH → H + NO, and N + HO₂ → products at 300 K between 1 and 5 torr. *J. Phys. Chem.* **1983**, *87*, 4503–4514.
- [165] Lewis, R. S.; Watson, R. T. Temperature dependence of the reaction O(³P) + OH(²Π) → O₂ + H. *J. Phys. Chem.* **1980**, *84*, 3495–3503.
- [166] Kurzius, S. C.; Boudart, M. Kinetics of the branching step in the hydrogen-oxygen reaction. *Combust. Flame* **1968**, *12*, 477–491.
- [167] Wilson, W. E.; Westenberg, A. A. Study of the reaction of hydroxyl radical with methane by quantitative ESR. Eleventh Symposium (International) on Combustion. 1967; pp 1143–1150.
- [168] Wilson, W. E.; Westenberg, A. A. Direct measurements of the rate coefficient for the reaction OH + CH₄ → CH₃ + H₂O over 300–1500 K. Twentieth Symposium (International) on Combustion. 1984; pp 703–713.
- [169] Sharkey, P.; Smith, I. W. M. Kinetics of elementary reactions at low temperatures: rate constants for the reactions of OH with HCl (298 $\geq T/K \geq 138$), CH₄(298 $\geq T/K \geq 178$) and C₂H₆(298 $\geq T/K \geq 138$). *J. Chem. Soc., Faraday Trans.* **1993**, *89*, 631–637.
- [170] Mellouki, A.; Téton, S.; Laverdet, G.; Quiggars, A.; Le Bras, G. Kinetic studies of OH reactions with H₂O₂, C₃H₈ and CH₄ using the pulsed laser photolysis - laser induced fluorescence method. *J. Chim. Phys.* **1994**, *91*, 473–487.
- [171] Bryukov, M. G.; Knyazev, V. D.; Lomnicki, S. M.; McFerrin, C. A.; Dellinger, B. Temperature-Dependent Kinetics of the Gas-Phase Reactions of OH with Cl₂, CH₄, and C₃H₈. *J. Phys. Chem. A* **2004**, *108*, 10464–10472.
- [172] Bonard, A.; Daële, V.; Delfau, J.-L.; Vovelle, C. Kinetics of OH Radical Reactions with Methane in the Temperature Range 295–660 K and with Dimethyl Ether and Methyl-tert-butyl Ether in the Temperature Range 295–618 K. *J. Phys. Chem. A* **2002**, *106*, 4384–4389.
- [173] Gierczak, T.; Talukdar, R. K.; Herndon, S. C.; Vaghjiani, G. L.; Ravishankara, A. R. Rate Coefficients for the Reactions of Hydroxyl Radicals with Methane and Deuterated Methanes. *J. Phys. Chem. A* **1997**, *101*, 3125–3134.
- [174] Vaghjiani, G. L.; Ravishankara, A. R. New measurement of the rate coefficient for the reaction of OH with methane. *Nature* **1992**, *350*, 406–409.
- [175] Dunlop, J. R.; Tully, F. P. A kinetic study of OH radical reactions with methane and perdeuterated methane. *J. Phys. Chem.* **1993**, *97*, 11148–11150.
- [176] Finlayson-Pitts, B. J.; Ezell, M. J.; Jayaweera, T. M.; Berko, H. N.; Lai, C. C. Kinetics of the reactions of OH with methyl chloroform and methane: Implications for global tropospheric OH and the methane budget. *Geophys. Res. Lett.* **1992**, *19*, 1371–1374.

- [177] Fagerström, K.; Lund, A.; Mahmoud, G.; Jodkowski, J. T.; Ratajczak, E. Kinetics of the cross reaction between methyl and hydroxyl radicals. *Chem. Phys. Lett.* **1993**, *204*, 226–234.
- [178] Humpfer, R.; Oser, H.; Grotheer, H.-H.; Just, T. The reaction system $\text{CH}_3 + \text{OH}$ at intermediate temperatures. Appearance of a new product channel. Twenty-Fifth Symposium (International) on Combustion. 1994; pp 721–731.
- [179] Fagerström, K.; Lund, A.; Mahmoud, G.; Jodkowski, J. T.; Ratajczak, E. Pressure and temperature dependence of the gas-phase reaction between methyl and hydroxyl radicals. *Chem. Phys. Lett.* **1994**, *224*, 43–50.
- [180] Oser, H.; Stothard, N. D.; Humpfer, R.; Grotheer, H.-H. Direct measurement of the reaction $\text{CH}_3 + \text{OH}$ at ambient temperature in the pressure range 0.3–6.2 mbar. *J. Phys. Chem.* **1992**, *96*, 5359–5363.
- [181] Oser, H.; Stothard, N. D.; Humpfer, R.; Grotheer, H.-H.; Just, T. Direct measurement of the reaction $\text{CH}_3 + \text{OH}$ and its pathways between 300 and 480 K. Twenty-Fourth Symposium (International) on Combustion. 1992; pp 597–604.
- [182] Anastasi, C.; Bevertton, S.; Ellermann, T.; Pagsberg, P. Reaction of CH_3 Radicals with OH at Room Temperature and Pressure. *J. Chem. Soc., Faraday Trans.* **1991**, *87*, 2325–2329.
- [183] Sworski, T. J.; Hochanadel, C. J.; Ogren, P. J. Flash photolysis of H_2O in CH_4 . H and OH yields and rate constants for CH_3 reactions with H and OH. *J. Phys. Chem.* **1980**, *84*, 192–134.
- [184] Smith, I. W. M.; Zellner, R. Rate measurements of reactions of OH by resonance absorption. Part 3.-Reactions of OH with H_2 , D_2 and hydrogen and deuterium halides. *J. Chem. Soc., Faraday Trans. 2* **1974**, *70*, 1045–1056.
- [185] Atkinson, R.; Hansen, D. A.; Pitts Jr., J. N. Rate constants for the reaction of the OH radical with H_2 and NO ($\text{M}=\text{Ar}$ and N_2). *J. Chem. Phys.* **1975**, *62*, 3284–3288.
- [186] Atkinson, R.; Hansen, D. A.; Pitts Jr., J. N. Rate constants for the reaction of OH radicals with CHF_2Cl , CF_2Cl_2 , CFCl_3 , and H_2 over the temperature range 297–434 K. *J. Chem. Phys.* **1975**, *63*, 1703–1706.
- [187] Talukdar, R. K.; Gierczak, T.; Goldfarb, L.; Rudich, Y.; Madhava Rao, B. S.; Ravishankara, A. R. Kinetics of Hydroxyl Radical Reactions with Isotopically Labeled Hydrogen. *J. Phys. Chem.* **1996**, *100*, 3037–3043.
- [188] Orkin, V. L.; Kozlov, S. N.; Poskrebyshev, G. A.; Kurylo, M. J. Rate Constant for the Reaction of OH with H_2 between 200 and 480 K. *J. Phys. Chem. A* **2006**, *110*, 6978–6985.
- [189] Ravishankara, A. R.; Nicovich, J. M.; Thompson, R. L.; Tully, F. P. Kinetic study of the reaction of hydroxyl with hydrogen and deuterium from 250 to 1050 K. *J. Phys. Chem.* **1981**, *85*, 2498–2503.
- [190] Tully, F. P.; Ravishankara, A. R. Flash photolysis-resonance fluorescence kinetic study of the reactions $\text{OH} + \text{H}_2 \rightarrow \text{H}_2\text{O} + \text{H}$ and $\text{OH} + \text{CH}_4 \rightarrow \text{H}_2\text{O} + \text{CH}_3$ from 298 to 1020 K. *J. Phys. Chem.* **1980**, *84*, 3126–3130.
- [191] Overend, R. P.; Paraskevopoulos, G.; Cvitanović, R. J. Rates of OH Radical Reactions. I. Reactions with H_2 , CH_4 , C_2H_6 , and C_3H_8 at 295K. *Can. J. Chem.* **1975**, *53*, 3374–3382.
- [192] Trainor, D. W.; von Rosenberg Jr., C. W. Energy partitioning in the products of elementary reactions involving OH-radicals. Fifteenth Symposium (International) on Combustion. Seattle, 1975; pp 755–764.
- [193] Kaufman, F.; Del Greco, F. P. Fast reactions of OH radicals. 1963.
- [194] Cohen, N.; Westberg, K. R. Chemical Kinetic Data Sheets for High-Temperature Chemical Reactions. *J. Phys. Chem. Ref. Data* **1983**, *12*, 531–590.
- [195] Titarchuk, T. A.; Halpern, J. B. Kinetics of CN reactions with $\text{O}(\text{P}^3)$ and SO_2 . *Chem. Phys. Lett.* **1995**, *232*, 192–196.
- [196] Schacke, H.; Schmatjko, K. J.; Wolfrum, J. Reaktionen von Molekülen in definierten Schwingungszuständen (I) Die Reaktionen $\text{CN}(\text{v}')$ + O und $\text{CN}(\text{v}')$ + O_2 . *Ber. Bunsenges. Phys. Chem.* **1973**, *77*, 248–253.
- [197] Schmatjko, K. J.; Wolfrum, J. Direct determination of the product energy distribution in the reaction of O-atoms with CN radicals. Sixteenth Symposium (International) on Combustion. Seattle, 1977; pp 819–827.
- [198] Tsang, W. Chemical Kinetic Data Base for Propellant Combustion. II. Reactions Involving CN, NCO, and HNCO. *J. Phys. Chem. Ref. Data* **1992**, *21*, 753–791.
- [199] Morgan, J. E.; Elias, L.; Schiff, H. I. Recombination of Oxygen Atoms in the Absence of O_2 . *J. Chem. Phys.* **1960**, *33*, 930–931.
- [200] Tchen, H. Étude cinétique par R. P. E. des atomes d'oxygène 3p dans la post-décharge. *Rev. Phys. Appl.* **1972**, *7*, 205–212.
- [201] Campbell, I. M.; Gray, C. N. Rate constants for $\text{O}(\text{P}^3)$ recombination and association with $\text{N}(\text{S}^4)$. *Chem. Phys. Lett.* **1973**, *18*, 607–609.
- [202] Marshall, T. C. Studies of Atomic Recombination of Nitrogen, Hydrogen, and Oxygen by Paramagnetic Resonance. *Phys. Fluids* **1962**, *5*, 743–753.
- [203] Campbell, I. M.; Thrush, B. A. The association of oxygen atoms and their combination with nitrogen atoms. *Proc. R. Soc. Lond. A Math. Phys. Sci.* **1967**, *296*, 222–232.
- [204] Reeves, R. R.; Mannella, G.; Harteck, P. Rate of Recombination of Oxygen Atoms. *J. Chem. Phys.* **1960**, *32*, 632–633.
- [205] Kondratiev, V. N.; Nikitin, E. E. Rate Constants for the Process $\text{O}_2 + \text{Ar} \longleftrightarrow \text{O} + \text{O} + \text{Ar}$. *J. Chem. Phys.* **1966**, *45*, 1078–1079.
- [206] Hack, W.; Wagner, H. G.; Zasyplkin, A. Elementary reactions of $\text{NH}(\text{a}^1\Delta)$ and $\text{NH}(\text{X}^3\Sigma)$ with N, O and NO. *Ber. Bunsenges. Phys. Chem.* **1994**, *98*, 156–164.
- [207] Kretschmer, C. B.; Petersen, H. L. Kinetics of Three-Body Atom Recombination. *J. Chem. Phys.* **1963**, *39*, 1772–1778.
- [208] Mavroyannis, C.; Winkler, C. A. The reaction of nitrogen atoms with oxygen atoms in the absence of oxygen molecules. *Can. J. Chem.* **1961**, *39*, 1601–1607.
- [209] Froben, F. W. Die Reaktion von OAtomen mit Methan, Chloroform und Tetrachlorkohlenstoff. *Ber. Bunsenges. Phys. Chem.* **1968**, *72*, 996–998.
- [210] Westenberg, A. A.; de Haas, N. AtomMolecule Kinetics at High Temperature Using ESR Detection. Technique and Results for $\text{O} + \text{H}_2$, $\text{O} + \text{CH}_4$, and $\text{O} + \text{C}_2\text{H}_6$. *J. Chem. Phys.* **1967**, *46*, 490–501.
- [211] Falconer, J. W.; Hoare, D. E.; Overend, R. Photolysis of carbon dioxide and methane mixtures at 873 and 293 K with 163.3 nm light. *J. Chem. Soc., Faraday Trans.*

- 1** **1973**, **69**, 1541–1546.
- [212] Slagle, I. R.; Pruss, Jr., F. J.; Gutman, D. Kinetics into the steady state. I. study of the reaction of oxygen atoms with methyl radicals. *Int. J. Chem. Kinet.* **1974**, **6**, 111–123.
- [213] Slagle, I. R.; Sarzyński, D.; Gutman, D. Kinetics of the reaction between methyl radicals and oxygen atoms between 294 and 900 K. *J. Phys. Chem.* **1987**, **91**, 4375–4379.
- [214] Washida, N. Reaction of methyl radicals with O(³P), O₂ and NO. *J. Chem. Phys.* **1980**, **73**, 1665–1672.
- [215] Washida, N.; Bayes, K. D. The rate of reaction of methyl radicals with atomic oxygen. *Chem. Phys. Lett.* **1973**, **23**, 373–375.
- [216] Zellner, R.; Hartmann, D.; Karthäuser, J.; Rhäsa, D.; Weibring, G. A laser photolysis/LIF study of the reactions of O(³P) atoms with CH₃ and CH₃O₂ radicals. *J. Chem. Soc., Faraday Trans. 2* **1988**, **84**, 549–568.
- [217] Plumb, I. C.; Ryan, K. R. Kinetics of the reactions of CH₃ with O(³P) and O₂ at 295 K. *Int. J. Chem. Kinet.* **1982**, **14**, 861–874.
- [218] Washida, N.; Bayes, K. D. The reactions of methyl radicals with atomic and molecular oxygen. *Int. J. Chem. Kinet.* **1976**, **8**, 777–794.
- [219] Seakins, P. W.; Leone, S. R. A laser flash photolysis/time-resolved FTIR emission study of a new channel in the reaction of methyl + oxygen atom: production of carbon monoxide(v). *J. Phys. Chem.* **1992**, **96**, 4478–4485.
- [220] Morris, Jr., E. D.; Niki, H. Reaction of methyl radicals with atomic oxygen. *Chem. Phys. Lett.* **1973**, **5**, 47–53.
- [221] Niki, H.; Daby, E. E.; Weinstock, B. Mass spectrometric study of the kinetics and mechanism of the ethylene-atomic oxygen reaction by the discharge-flow technique at 300 K. 1969.
- [222] Böhland, T.; Temps, F.; Wagner, H. G. Direct Investigation of the Reaction CH₂(X³B₁) + O(³P) with the LMR. *Ber. Bunsenges. Phys. Chem.* **1984**, **88**, 1222–1228.
- [223] Vinckier, C.; Debruyn, W. Reactions of methylene in the oxidation process of acetylene with oxygen atoms at 295 K. 1979.
- [224] Messing, I.; Filseth, S. V.; Sadowski, C. M.; Carrington, D. Absolute rate constants for the reactions of CH with O and N atoms. *J. Chem. Phys.* **1981**, **74**, 3874–3881.
- [225] Messing, I.; Carrington, D.; Filseth, S. V.; Sadowski, C. M. Absolute rate constant for the CH + O reaction. *Chem. Phys. Lett.* **1980**, **74**, 56–57.
- [226] Zhu, Y.-F.; Arepalli, S.; Gordon, R. J. The rate constant for the reaction O(³P)+D₂ at low temperatures. *J. Chem. Phys.* **1989**, **90**, 183–188.
- [227] Presser, N.; Gordon, R. J. The kinetic isotope effect in the reaction of O(³P) with H₂, D₂, and HD. *J. Chem. Phys.* **1985**, **82**, 1291–1297.
- [228] Light, G. C.; Matsumoto, J. H. Experimental measurement of the rate of the reaction O(³P) + H₂(v = 0) → OH(v = 0) + H at T = 298 K. *Int. J. Chem. Kinet.* **1980**, **12**, 451–468.
- [229] Baulch, D. L.; Drysdale, D. D.; Horne, D. G.; Lloyd, A. C. *Evaluated Kinetic Data for High Temperature Reactions, Vol. 1: Homogeneous Gas Phase Reactions of the H₂-O₂ Systems*; Butterworths: London, 1972.
- [230] Matsumi, Y.; Tonokura, K.; Inagaki, Y.; Kawasaki, M. Isotopic branching ratios and translational energy release of hydrogen and deuterium atoms in reaction of oxygen (1D) atoms with alkanes and alkyl chlorides. *J. Phys. Chem.* **1993**, **97**, 6816–6821.
- [231] Vranckx, S.; Peeters, J.; Carl, S. A temperature dependence kinetic study of O(¹D) + CH₄: overall rate coefficient and product yields. *Phys. Chem. Chem. Phys.* **2008**, **10**, 5714–5722.
- [232] Dillon, T. J.; Horowitz, A.; Crowley, J. N. Absolute rate coefficients for the reactions of O(¹D) with a series of n-alkanes. *Chem. Phys. Lett.* **2007**, **443**, 12–16.
- [233] Cvetanović, R. J. Excited State Chemistry in the Stratosphere. *Can. J. Chem.* **1974**, **52**, 1452–1464.
- [234] Koppe, S.; Laurent, T.; Naik, P. D.; Volpp, H.-R.; Wolfrum, J.; Arusi-Parpar, T.; Rosenwaks, S. Absolute rate constants and reactive cross sections for the reactions of O(¹D) with molecular hydrogen and deuterium. *Chem. Phys. Lett.* **1993**, **214**, 546–552.
- [235] Stief, L. J.; Payne, W. A.; Klemm, R. B. A flash photolysis-resonance fluorescence study of the formation of O(¹D) in the photolysis of water and the reaction of O(¹D) with H₂, Ar, and He. *J. Chem. Phys.* **1975**, **62**, 4000–4008.
- [236] Talukdar, R. K.; Ravishankara, A. R. Rate coefficients for O(¹D) + H₂ D₂, HD reactions and H atom yield in O(¹D) + HD reaction. *Chem. Phys. Lett.* **1996**, **253**, 177–183.
- [237] Ogren, P. J.; Sworski, T. J.; Hochanadel, C. J.; Cassel, J.-M. Flash Photolysis of O₃ in O₂ and O₂ + H₂ Mixtures. Kinetics of O₂(¹Σ_g⁺) + O₃ and O(¹D) + H₂ Reactions. *J. Phys. Chem.* **1982**, **86**, 238–242.
- [238] Nuñez-Reyes, D.; Hickson, K. M. Kinetics of the Gas-Phase O(¹D) + CO₂ and C(¹D) + CO₂ Reactions over the 50296 K Range. *J. Phys. Chem. A* **2018**, **112**, 4002–4008.
- [239] Mebel, A. M.; Hayashi, M.; Kislov, V. V.; Lin, S. H. Theoretical Study of Oxygen Isotope Exchange and Quenching in the O(¹D) + CO₂ Reaction. *J. Phys. Chem. A* **2004**, **108**, 7983–7994.
- [240] Zhu, L.; Kreutz, T. G.; Hewitt, S. A.; Flynn, G. W. Diode laser probing of vibrational, rotational, and translational excitation of CO₂ following collisions with O(¹D). I. Inelastic scattering. *J. Chem. Phys.* **1990**, **93**, 3277–3288.
- [241] Sedlacek, A. J.; Harding, D. R.; Weston, R. E.; Kreutz, T. G.; Flynn, G. W. Probing the O(¹D)+CO₂ reaction with second-derivative modulated diode laser-spectroscopy. *J. Chem. Phys.* **1989**, **91**, 7550–7556.
- [242] Shortridge, R. G.; Lin, M. C. CO vibrational population distributions in the reactions of COS with O(³P_J) and O(¹D₂) atoms. *Chem. Phys. Lett.* **1975**, **35**, 146–150.
- [243] Tully, J. C. Reactions of O(¹D) with atmospheric molecules. *J. Chem. Phys.* **1975**, **62**, 1893–1898.
- [244] Clark, I. D.; Noxon, J. F. Optical Emission from O(¹D) and O₂(b¹Σ_g⁺) in Ultraviolet Photolysis of O₂ and CO₂. II. *J. Chem. Phys.* **1972**, **57**, 1033–1038.
- [245] Zipf, E. C. The collisional deactivation of metastable atoms and molecules in the upper atmosphere. *Can. J. Chem.* **1969**, **47**, 1863–1870.
- [246] Paraskevopoulos, G.; Cvetanovic, R. Competitive Reactions of the Excited Oxygen Atoms, O(¹D)*. *J. Am. Chem. Soc.* **1969**, **91**, 7572–7577.

- [247] Herron, J. T. Evaluated Chemical Kinetics Data for Reactions of N(²D), N(²P) and N₂(A³ Σ_u^+) in the Gas Phase. *J. Phys. Chem. Ref. Data* **1999**, *28*, 1453–1483.
- [248] Darwin, D. C.; Moore, C. B. Reaction Rate Constants (295 K) for 3CH₂ with H₂S, SO₂, and NO₂: Upper Bounds for Rate Constants with Less Reactive Partners. *J. Phys. Chem.* **1995**, *99*, 13467–13470.
- [249] Kovacs, D.; Jackson, J. E. CH₂ + CO₂ → CH₂O + CO, One-Step Oxygen Atom Abstraction or Addition/Fragmentation via α -Lactone? *J. Phys. Chem. A* **2001**, *105*, 7579–7587.
- [250] Krasnoperov, L. N.; Chesnokov, E. N.; Stark, H.; Ravishankara, A. R. Elementary reactions of formyl (HCO) radical studied by laser photolysis/transient absorption spectroscopy. *Proc. Combust. Inst.* **2005**, *30*, 935–943.
- [251] Saheb, V.; Nazari, A. Products of the Self-Reaction of HCO Radicals: Theoretical Kinetics Studies. *Phys. Chem. Res.* **2019**, *7*, 81–94.
- [252] Li, J.; Wang, Y.; Jiang, B.; Ma, J.; Dawes, R.; Xie, D.; Bowman, J. M.; Guo, H. Communication: A chemically accurate global potential energy surface for the HO + CO → H + CO₂ reaction. *J. Chem. Phys.* **2012**, *136*, 041103.
- [253] Skinner, D. E.; Germann, T. C.; Miller, W. H. Quantum Mechanical Rate Constants for O + OH = H + O₂ for Total Angular Momentum J > 0. *J. Phys. Chem. A* **1998**, *102*, 3828–3834.
- [254] Lique, F.; Jorfi, M.; Honvault, P.; Halvick, P.; Lin, S. Y.; Guo, H.; Xie, D. Q.; Dagdigian, P. J.; Kłos, J.; Alexander, M. H. O + OH → O₂ + H: A key reaction for interstellar chemistry. New theoretical results and comparison with experiment. *J. Chem. Phys.* **2009**, *131*, 221104.
- [255] Klippenstein, S. J.; Harding, L. B.; Ruscic, B.; Sivaramakrishnan, R.; Srinivasan, N. K.; Su, M.-C.; Michael, J. V. Thermal Decomposition of NH₂OH and Subsequent Reactions: Ab Initio Transition State Theory and Reflected Shock Tube Experiments. *J. Phys. Chem. A* **2009**, *113*, 10241–10259.
- [256] Tomeczek, J.; Gradoń, B. The role of N₂O and NNH in the formation of NO via HCN in hydrocarbon flames. *Combust. Flame* **2003**, *133*, 311–322.
- [257] Yu, H.-G.; Muckerman, J. T. MRCI Calculations of the Lowest Potential Energy Surface for CH₃OH and Direct ab Initio Dynamics Simulations of the O(¹D) + CH₄ Reaction. *J. Phys. Chem. A* **2004**, *108*, 8615–8623.
- [258] Chang, A. H. H.; Lin, S. H. A theoretical study of the O(¹D) + CH₄ reaction II. *Chem. Phys. Lett.* **2004**, *384*, 229–235.
- [259] Aoiz, F. J.; Bañares, L.; Herrero, V. J. Dynamics of Insertion Reactions of H₂ Molecules with Excited Atoms. *J. Phys. Chem. A* **2006**, *110*, 12546–12565.
- [260] Lin, S. Y.; Guo, H. Adiabatic and Nonadiabatic State-to-State Quantum Dynamics for O(¹D) + H₂(X¹ Σ_g^+ , $\nu_i = j_i = 0$) → OH(X² Π , ν_f , j_f) + H(²S) Reaction. *J. Phys. Chem. A* **2009**, *113*, 4285–4293.

SUPPORTING INFORMATION

CRAHCN-O

In Tables S1 and S2, we display the Lindemann and the Arrhenius coefficients for the new oxygen reactions in CRAHCN-O. These rate coefficients consist of experimental values when available, and our consistently calculated theoretical values otherwise.

TABLE S1: Lindemann coefficients for the three-body oxygen reactions in the consistent reduced atmospheric hybrid chemical network oxygen extension (CRAHCN-O), valid within the 50–400 K temperature range. Experimental values are used when available, and calculated rate coefficients from this work are used otherwise. k_∞ is the second-order rate coefficient in the high pressure limit with units cm³s⁻¹. k_0 is the third-order rate coefficient in the low pressure limit with units cm⁶s⁻¹. These values fit into the pressure-dependent rate coefficient equation $k = \frac{k_0[M]/k_\infty}{1+k_0[M]/k_\infty} k_\infty$.

No. Reaction equation	k_∞ (298)	k_0 (298)	Source(s)
1. CO ₂ + ¹ O + M → CO ₃ + M	1.6×10^{-10}	(M=N ₂) 3.0×10^{-29} (CO ₂) 3.1×10^{-29} (H ₂) 6.7×10^{-29}	Avg. of exper. vals, This work This work This work
2. HCO + ² N + M → HCON · + M · → HCNO + M	2.0×10^{-11}	(N ₂) 5.0×10^{-30} (CO ₂) 5.6×10^{-30} (H ₂) 9.7×10^{-30}	This work This work This work
3. HCO + CH ₃ + M → CH ₃ CHO + M	3.0×10^{-11}	(N ₂) 5.3×10^{-27} (CO ₂) 6.4×10^{-27} (H ₂) 1.2×10^{-27}	Tsang and Hampson ^[28] , This work This work This work
4. HCO + H + M → H ₂ CO + M	4.9×10^{-11}	(N ₂) 7.4×10^{-30} (CO ₂) 9.5×10^{-30} (H ₂) 1.4×10^{-29}	This work This work This work
5. CO + CN + M → NCCO + M	6.0×10^{-12}	(N ₂) 6.2×10^{-31} (CO ₂) 6.8×10^{-31} (H ₂) 1.3×10^{-30}	This work This work This work
6. CO + ¹ O + M → CO ₂ + M	4.6×10^{-11}	(N ₂) 2.8×10^{-29} (CO ₂) 2.8×10^{-29} (H ₂) 2.8×10^{-29}	Avg. of exper. vals, (CO ₂) Clerc and Barat ^[63] (CO ₂) Clerc and Barat ^[63] (CO ₂) Clerc and Barat ^[63]
7. CO + ¹ CH ₂ + M → CH ₂ CO + M	1.3×10^{-11}	(N ₂) 1.7×10^{-28} (CO ₂) 1.9×10^{-28} (H ₂) 3.3×10^{-28}	This work This work This work
8. CO + CH + M → HCCO + M	4.3×10^{-11}	(N ₂) 1.2×10^{-29}	This work

9. $\text{CO} + \text{H} + \text{M} \longrightarrow \text{HCO} + \text{M}$	2.7×10^{-12}	(CO ₂) 1.3×10^{-29} (H ₂) 2.4×10^{-29} (N ₂) 1.0×10^{-34} (CO ₂) 9.9×10^{-35} (H ₂) 1.0×10^{-34}	This work This work
10. $\text{OH} + \text{H}_2\text{CN} + \text{M} \longrightarrow \text{H}_2\text{CNOH} + \text{M}$	6.0×10^{-12}	(N ₂) 6.5×10^{-30} (CO ₂) 7.4×10^{-30} (H ₂) 1.3×10^{-29} (N ₂) 2.7×10^{-30} (CO ₂) 2.9×10^{-30} (H ₂) 5.1×10^{-30}	This work, Avg. of H ₂ exper. vals (CO) Hochanadel et al. ^[64] Avg. of H ₂ exper. vals
11. $\text{OH} + \text{CN} + \text{M} \longrightarrow \text{HOCl} + \text{M}$	1.0×10^{-12}	(N ₂) 8.0×10^{-31} (CO ₂) 2.1×10^{-30} (H ₂) 4.0×10^{-30} (N ₂) 8.5×10^{-32} (CO ₂) 9.4×10^{-32} (H ₂) 1.8×10^{-31}	Nizamov and Dagdigian ^[65] , This work This work
12. $\text{OH} + \text{OH} + \text{M} \longrightarrow \text{H}_2\text{O}_2 + \text{M}$	1.5×10^{-11}	(N ₂) 4.1×10^{-30} (CO ₂) 4.5×10^{-30} (H ₂) 8.3×10^{-30} (N ₂) 8.5×10^{-31} (CO ₂) 9.2×10^{-31} (H ₂) 1.7×10^{-30}	This work This work
13. $\text{OH} + {}^3\text{O} + \text{M} \longrightarrow \text{HO}_2 + \text{M}$	7.4×10^{-11}	(N ₂) 2.1×10^{-27} (CO ₂) 2.3×10^{-27} (H ₂) 3.8×10^{-27} (N ₂) 6.9×10^{-31} (CO ₂) 9.0×10^{-31} (H ₂) 4.3×10^{-30}	This work This work
14. $\text{OH} + {}^1\text{O} + \text{M} \longrightarrow \text{HO}_2 + \text{M}$	1.0×10^{-9}	(N ₂) 1.3×10^{-30} (CO ₂) 1.5×10^{-30} (H ₂) 2.6×10^{-30} (N ₂) 7.3×10^{-33} (CO ₂) 7.3×10^{-33} (H ₂) 7.3×10^{-33}	This work This work
15. $\text{OH} + \text{NH} + \text{M} \longrightarrow \text{OH}\cdots\text{NH}\cdot + \text{M}\cdot \longrightarrow \text{trans-HNOH} + \text{M}$	7.0×10^{-12}	(N ₂) 8.5×10^{-31} (CO ₂) 9.2×10^{-31} (H ₂) 1.7×10^{-30} (N ₂) 2.1×10^{-27} (CO ₂) 2.3×10^{-27} (H ₂) 3.8×10^{-27}	This work This work
16. $\text{OH} + \text{CH}_3 + \text{M} \longrightarrow \text{OH}\cdots\text{CH}_3\cdot + \text{M}\cdot \longrightarrow \text{CH}_3\text{OH} + \text{M}$	1.3×10^{-10}	(N ₂) 6.0×10^{-31} (CO ₂) 6.2×10^{-30} (H ₂) 9.9×10^{-30} (N ₂) 8.6×10^{-33} (CO ₂) 8.8×10^{-33} (H ₂) 8.6×10^{-33}	This work This work
17. $\text{OH} + \text{H} + \text{M} \longrightarrow \text{H}_2\text{O} + \text{M}$	2.4×10^{-10}	(N ₂) 9.2×10^{-29} (CO ₂) 1.1×10^{-28} (H ₂) 1.7×10^{-28} (N ₂) 5.2×10^{-30} (CO ₂) 6.2×10^{-30} (H ₂) 9.9×10^{-30}	This work, (N ₂) Baulch et al. ^[27] (CO ₂) Zellner et al. ^[54] (H ₂ O) Baulch et al. ^[27]
18. ${}^3\text{O} + \text{CN} + \text{M} \longrightarrow \text{NCO} + \text{M}$	7.1×10^{-12}	(N ₂) 4.6×10^{-33} (CO ₂) 4.8×10^{-33} (H ₂) 5.6×10^{-33} (N ₂) 1.9×10^{-29} (CO ₂) 2.1×10^{-29} (H ₂) 2.8×10^{-29}	This work This work
19. ${}^3\text{O} + {}^3\text{O} + \text{M} \longrightarrow \text{O}_2 + \text{M}$	1.8×10^{-11}	(N ₂) 7.3×10^{-33} (CO ₂) 7.3×10^{-33} (H ₂) 7.3×10^{-33} (N ₂) 8.6×10^{-33} (CO ₂) 8.8×10^{-33} (H ₂) 8.6×10^{-33}	This work, Avg. of N ₂ exper. vals Avg. of O ₂ exper. vals Avg. of N ₂ exper. vals
20. ${}^3\text{O} + {}^4\text{N} + \text{M} \longrightarrow \text{NO} + \text{M}$	6.6×10^{-11}	(N ₂) 1.8×10^{-32} (CO ₂) 1.8×10^{-32} (H ₂) 8.6×10^{-33} (N ₂) 9.2×10^{-29} (CO ₂) 1.1×10^{-28} (H ₂) 1.7×10^{-28}	This work, Avg. of N ₂ exper. vals (CO ₂) Campbell and Thrush ^[66] Avg. of N ₂ exper. vals
21. ${}^3\text{O} + {}^3\text{CH}_2 + \text{M} \longrightarrow \text{H}_2\text{CO} + \text{M}$	1.9×10^{-11}	(N ₂) 5.2×10^{-30} (CO ₂) 6.2×10^{-30} (H ₂) 9.9×10^{-30} (N ₂) 9.2×10^{-29} (CO ₂) 1.1×10^{-28} (H ₂) 1.7×10^{-28}	Tsang and Hampson ^[28] , This work This work
22. ${}^3\text{O} + \text{CH} + \text{M} \longrightarrow \text{HCO} + \text{M}$	6.6×10^{-11}	(N ₂) 2.6×10^{-33} (CO ₂) 2.9×10^{-33} (H ₂) 4.6×10^{-33} (N ₂) 5.2×10^{-30} (CO ₂) 6.2×10^{-30} (H ₂) 9.9×10^{-30}	This work This work
23. ${}^3\text{O} + \text{H} + \text{M} \longrightarrow \text{OH} + \text{M}$	3.5×10^{-10}	(N ₂) 4.0×10^{-29} (CO ₂) 4.6×10^{-29} (H ₂) 8.0×10^{-29} (N ₂) 1.9×10^{-29} (CO ₂) 2.1×10^{-29} (H ₂) 3.6×10^{-29}	This work This work
24. ${}^1\text{O} + \text{HCN} + \text{M} \longrightarrow \text{HCNO} + \text{M}$	3.3×10^{-11}	(N ₂) 8.9×10^{-11} (CO ₂) 9.6×10^{-33} (H ₂) 1.8×10^{-32} (N ₂) 8.8×10^{-33} (CO ₂) 9.6×10^{-33} (H ₂) 1.8×10^{-32}	This work This work
25. ${}^1\text{O} + \text{CN} + \text{M} \longrightarrow \text{NCO} + \text{M}$	8.9×10^{-11}	(N ₂) 3.6×10^{-23} (CO ₂) 3.9×10^{-23} (H ₂) 6.3×10^{-23} (N ₂) 6.6×10^{-27} (CO ₂) 7.7×10^{-27}	Avg. of exper. vals, This work This work
26. ${}^1\text{O} + {}^1\text{O} + \text{M} \longrightarrow \text{O}_2 + \text{M}$	2.3×10^{-10}	(N ₂) 3.6×10^{-23} (CO ₂) 3.9×10^{-23} (H ₂) 6.3×10^{-23} (N ₂) 6.6×10^{-27} (CO ₂) 7.7×10^{-27}	This work This work
27. ${}^1\text{O} + \text{CH}_4 + \text{M} \longrightarrow \text{CH}_3\text{OH} + \text{M}$	2.2×10^{-10}	(N ₂) 3.6×10^{-23} (CO ₂) 3.9×10^{-23} (H ₂) 6.3×10^{-23} (N ₂) 6.6×10^{-27} (CO ₂) 7.7×10^{-27}	This work This work
28. ${}^1\text{O} + {}^1\text{CH}_2 + \text{M} \longrightarrow \text{H}_2\text{CO} + \text{M}$	3.3×10^{-10}	(N ₂) 3.6×10^{-23} (CO ₂) 3.9×10^{-23} (H ₂) 6.3×10^{-23} (N ₂) 6.6×10^{-27} (CO ₂) 7.7×10^{-27}	This work This work

29. ${}^1\text{O} + \text{CH} + \text{M} \longrightarrow \text{HCO} + \text{M}$	9.2×10^{-11}	(H ₂) 1.2×10^{-26} (N ₂) 4.9×10^{-29} (CO ₂) 5.8×10^{-29} (H ₂) 9.1×10^{-29}	This work This work This work This work
30. ${}^1\text{O} + \text{H}_2 + \text{M} \longrightarrow \text{H}_2\text{O} + \text{M}$	2.1×10^{-10}	(N ₂) 1.2×10^{-29} (CO ₂) 1.4×10^{-29} (H ₂) 2.0×10^{-29}	Avg. of exper. vals, This work This work This work
31. ${}^1\text{O} + \text{H} + \text{M} \longrightarrow \text{OH} + \text{M}$	1.1×10^{-9}	(N ₂) 1.4×10^{-32} (CO ₂) 1.5×10^{-32} (H ₂) 2.3×10^{-32}	This work This work This work

TABLE S2: Arrhenius coefficients for the one- and two-body oxygen reactions in the consistent reduced atmospheric hybrid chemical network oxygen extension (CRAHCN-O). Experimental values are used when available, and calculated rate coefficients from this work are used otherwise. For the reactions with barriers from this work, rate coefficients are calculated at 50, 100, 200, 298, and 400 K, and are fit to the modified Arrhenius expression $k(T) = \alpha \left(\frac{T}{300}\right)^{\beta} e^{-\gamma/T}$. Barrierless reaction rate coefficients do not typically vary by more than a factor of 1–3 for temperatures between 50 and 400 K^{47–51}. Intermediate molecules are labelled with a bullet, and are included to describe the precise reaction pathway for multi-step reactions. First- and second-order reactions with rate coefficients slower than $k(298 \text{ K}) = 10^{-21}$ are not included in this network. First-order rate coefficients have units s⁻¹. Second-order rate coefficients have units cm³s⁻¹.

No.	Reaction equation	Forw./Rev.	α	β	γ	Source
32.	NCCO \longrightarrow CO + CN	F	$3.4 \times 10^{+7}$	14.33	12716	This work
33.	CO ₂ + ${}^1\text{O}$ \longrightarrow ${}^1\text{CO}_3\cdot$ \longrightarrow ${}^3\text{CO}_3\cdot$ \longrightarrow CO ₂ + ${}^3\text{O}$	F	7.4×10^{-11}	0	-133	Dunlea and Ravishankara ^[67]
34.	CO ₂ + ${}^2\text{N}$ \longrightarrow NCO ₂ · \longrightarrow OCNO · \longrightarrow CO + NO	F	4.6×10^{-13}	0	0	Avg. of exper. vals
35.	CO ₂ + ${}^1\text{CH}_2$ \longrightarrow ${}^1\text{CH}_2\text{CO}_2\cdot$ \longrightarrow H ₂ CO + CO	F	8.0×10^{-13}	0	0	This work
36.	CO ₂ + CH \longrightarrow CHCO ₂ · \longrightarrow HCOCO · \longrightarrow HCO + CO	F	5.7×10^{-12}	0	345	Baulch et al. ^[27]
37.	H ₂ O ₂ \longrightarrow OH + OH	F	$2.1 \times 10^{+8}$	13.73	11381	This work
38.	H ₂ CO + CN \longrightarrow HCN + HCO	F	1.5×10^{-12}	2.72	-718	Yu et al. ^[68]
39.	H ₂ CO + OH \longrightarrow r, l-H ₂ COHO · \longrightarrow trans-HCOHO · + H · \longrightarrow H ₂ O + CO + H	F	4.8×10^{-13}	0.82	2626	This work
40.	H ₂ CO + OH \longrightarrow H ₂ O + HCO	F	4.8×10^{-12}	1.18	-225	Baulch et al. ^[27]
41.	H ₂ CO + ${}^3\text{O}$ \longrightarrow HCO + OH	F	1.8×10^{-11}	0.57	1390	Baulch et al. ^[27]
42.	H ₂ CO + ${}^1\text{O}$ \longrightarrow H ₂ CO ₂ · \longrightarrow HCO ₂ H · \longrightarrow HCO + OH	F	4.6×10^{-10}	0	0	This work
43.	H ₂ CO + CH ₃ \longrightarrow HCO + CH ₄	F	6.8×10^{-12}	0	4450	Baulch et al. ^[27]
44.	H ₂ CO + ${}^3\text{CH}_2$ \longrightarrow HCO + CH ₃	F	3.5×10^{-13}	2.44	1024	This work
45.	H ₂ CO + ${}^1\text{CH}_2$ \longrightarrow HCO + CH ₃	F	1.5×10^{-12}	0	0	This work
46.	H ₂ CO + CH \longrightarrow H ₂ COCH _a · \longrightarrow H ₂ COCH _b · \longrightarrow CH ₂ HCO · \longrightarrow CH ₃ CO · \longrightarrow CO + CH ₃	F	1.6×10^{-10}	0	-260	Baulch et al. ^[27]
47.	H ₂ CO + CH \longrightarrow H ₂ COCH _c · \longrightarrow HCO + ${}^3\text{CH}_2$	F	1.1×10^{-12}	0	0	This work
48.	H ₂ CO + H \longrightarrow HCO + H ₂	F	1.5×10^{-11}	1.05	1650	Baulch et al. ^[27]
49.	HCO + H ₂ CN \longrightarrow H ₂ CO + HCN	F	4.6×10^{-14}	2.11	559	This work
50.	HCO + HCO \longrightarrow trans-C ₂ H ₂ O ₂ · \longrightarrow anti-HCOH · + CO · \longrightarrow H ₂ CO + CO	F	4.2×10^{-11}	0	0	Avg. of exper. vals
51.	HCO + HCO \longrightarrow cis-C ₂ H ₂ O ₂ · \longrightarrow CO + CO + H ₂	F	3.6×10^{-11}	0	0	Yee Quee and Thynne ^[69]
52.	HCO + CN \longrightarrow HCOCN · \longrightarrow CO + HCN	F	5.4×10^{-12}	0	0	This work
53.	HCO + OH \longrightarrow trans-HCOHO · \longrightarrow CO + H ₂ O	F	1.7×10^{-10}	0	0	Baulch et al. ^[27]
54.	HCO + ${}^3\text{O}$ \longrightarrow HCO ₂ · \longrightarrow CO ₂ + H	F	5.0×10^{-11}	0	0	Baulch et al. ^[27]
55.	HCO + ${}^3\text{O}$ \longrightarrow CO + OH	F	5.0×10^{-11}	0	0	Baulch et al. ^[27]
56.	HCO + ${}^1\text{O}$ \longrightarrow HCO ₂ · \longrightarrow CO ₂ + H	F	1.5×10^{-10}	0	0	This work
57.	HCO + NH \longrightarrow H ₂ CO + ${}^4\text{N}$	F	2.0×10^{-13}	1.00	4622	This work
58.	HCO + NH \longrightarrow CO + NH ₂ and HCO + NH \longrightarrow HNHCO · \longrightarrow H ₂ NCO · \longrightarrow CO + NH ₂	F	1.4×10^{-11}	0	0	This work

59.	$\text{HCO} + {}^4\text{N} \longrightarrow {}^3\text{NCOH}\cdot \longrightarrow \text{NCO} + \text{H}$	F	2.8×10^{-11}	0	0	This work
60.	$\text{HCO} + {}^4\text{N} \longrightarrow \text{CO} + \text{NH}$	F	2.2×10^{-11}	0	0	This work
61.	$\text{HCO} + {}^2\text{N} \longrightarrow {}^3\text{NCOH}\cdot \longrightarrow \text{NCO} + \text{H}$	F	6.6×10^{-11}	0	0	This work
62.	$\text{HCO} + {}^2\text{N} \longrightarrow \text{CO} + \text{NH}$	F	4.8×10^{-11}	0	0	This work
63.	$\text{HCO} + \text{CH}_3 \longrightarrow \text{CO} + \text{CH}_4$	F	2.0×10^{-10}	0	0	Tsang and Hampson ^[28]
64.	$\text{HCO} + {}^3\text{CH}_2 \longrightarrow \text{CH}_3 + \text{CO}$ and $\text{HCO} + {}^3\text{CH}_2 \longrightarrow \text{CH}_2\text{HCO}\cdot \longrightarrow \text{CH}_3\text{CO}\cdot \longrightarrow \text{CH}_3 + \text{CO}$	F	2.1×10^{-11}	0	0	This work
65.	$\text{HCO} + {}^1\text{CH}_2 \longrightarrow \text{CH}_2\text{HCO}\cdot \longrightarrow \text{CH}_3\text{CO}\cdot \longrightarrow \text{CH}_3 + \text{CO}$	F	1.2×10^{-11}	0	0	This work
66.	$\text{HCO} + \text{CH} \longrightarrow \text{CO} + {}^3\text{CH}_2$	F	1.5×10^{-11}	0	0	This work
67.	$\text{HCO} + \text{CH} \longrightarrow \text{CO} + {}^1\text{CH}_2$	F	4.6×10^{-12}	0	0	This work
68.	$\text{HCO} + \text{H} \longrightarrow \text{CO} + \text{H}_2$ and $\text{HCO} + \text{H} \longrightarrow \text{H}_2\text{CO}_{(\nu)}\cdot \longrightarrow \text{CO} + \text{H}_2$	F	1.5×10^{-10}	0	0	Baulch et al. ^[27]
69.	$\text{HCO} + \text{H} \longrightarrow \text{H}_2\text{CO}_{(\nu)}\cdot \longrightarrow \text{CO} + \text{H} + \text{H}$	F	2.4×10^{-11}	0	0	This work
70.	$\text{HCO} \longrightarrow \text{CO} + \text{H}$	F	$1.7 \times 10^{+13}$	1.14	10219	This work
71.	$\text{CO} + \text{OH} \longrightarrow \text{OH}\cdots\text{CO}\cdot \longrightarrow \text{cis-HOCO}\cdot \longrightarrow \text{CO}_2 + \text{H}$	F	5.5×10^{-12}	1.50	-250	Baulch et al. ^[27]
72.	$\text{H}_2\text{O} + {}^1\text{O} \longrightarrow \text{H}_2\text{OO}\cdot \longrightarrow \text{H}_2\text{O}_2\cdot \longrightarrow \text{OH} + \text{OH}$	F	1.6×10^{-10}	0	-65	Dunlea and Ravishankara ^[67]
73.	$\text{H}_2\text{O} + \text{CN} \longrightarrow \text{H}_2\text{OCN}\cdot \longrightarrow \text{OH} + \text{HCN}$	F	9.4×10^{-13}	1.58	1474	This work
74.	$\text{H}_2\text{O} + {}^2\text{N} \longrightarrow \text{H}_2\text{ON}\cdot \longrightarrow \text{trans-HNOH}\cdot \longrightarrow \text{HNO} + \text{H}$ $\text{H}_2\text{O} + {}^2\text{N} \longrightarrow \text{H}_2\text{ON}\cdot \longrightarrow \text{trans-HNOH}\cdot \longrightarrow \text{H}_2\text{NO}\cdot \longrightarrow \text{HNO} + \text{H}$	F	1.9×10^{-10}	0	0	This work
75.	$\text{H}_2\text{O} + \text{CH} \longrightarrow \text{H}_2\text{O}\cdots\text{CH}\cdot \longrightarrow \text{H}_2\text{OCH}\cdot \longrightarrow \text{H}_2\text{COH}\cdot \longrightarrow \text{H}_2\text{CO} + \text{H}$	F	1.6×10^{-11}	-1.42	0	Blitz et al. ^[57]
76.	$\text{H}_2\text{O} + \text{CH} \longrightarrow \text{OH} + {}^3\text{CH}_2$	F	5.8×10^{-13}	0.38	2178	This work
77.	$\text{OH} + \text{HCN} \longrightarrow \text{NCHOH}\cdot \longrightarrow \text{HOCH} + \text{H}$	F	5.3×10^{-14}	-1.00	1860	Phillips ^[70]
78.	$\text{OH} + \text{CN} \longrightarrow \text{HO}\cdots\text{CN} \longrightarrow {}^3\text{HOCH}_1\cdot \longrightarrow {}^3\text{HOCH}_2 \longrightarrow \text{NCO} + \text{H}$	F	9.9×10^{-13}	-0.34	-25	This work
79.	$\text{OH} + \text{CN} \longrightarrow \text{HCN} + {}^3\text{O}$	F	2.8×10^{-12}	1.07	545	This work
80.	$\text{OH} + \text{CN} \longrightarrow \text{HNC} + {}^3\text{O}$	F	4.4×10^{-8}	-6.93	6383	This work
81.	$\text{OH} + \text{OH} \longrightarrow \text{trans-}{}^3\text{H}_2\text{O}_2\cdot \longrightarrow \text{H}_2\text{O} + {}^3\text{O}$	F	1.7×10^{-12}	1.14	50	Baulch et al. ^[27]
82.	$\text{OH} + {}^3\text{O} \longrightarrow \text{HO}_{2(\nu)}\cdot \longrightarrow \text{O}_2 + \text{H}$	F	2.0×10^{-11}	0	-112	Baulch et al. ^[27]
83.	$\text{OH} + {}^1\text{O} \longrightarrow \text{HO}_{2(\nu)}\cdot \longrightarrow \text{O}_2 + \text{H}$	F	1.0×10^{-9}	0	0	This work
84.	$\text{OH} + \text{NH} \longrightarrow \text{OH}\cdots\text{NH}\cdot \longrightarrow \text{trans-HNOH}\cdot \longrightarrow \text{HNO} + \text{H}$ $\text{OH} + \text{NH} \longrightarrow \text{OH}\cdots\text{NH}\cdot \longrightarrow \text{trans-HNOH}\cdot \longrightarrow \text{H}_2\text{NO}\cdot \longrightarrow \text{HNO} + \text{H}$	F	7.0×10^{-12}	0	0	This work
85.	$\text{OH} + \text{NH} \longrightarrow \text{H}_2\text{O} + {}^4\text{N}$	F	2.9×10^{-12}	0.69	425	This work
86.	$\text{OH} + {}^4\text{N} \longrightarrow {}^3\text{OH}\cdots\text{N}\cdot \longrightarrow {}^3\text{NOH}\cdot \longrightarrow \text{NO} + \text{H}$	F	4.9×10^{-11}	0	0	Avg. of exper. vals
87.	$\text{OH} + {}^2\text{N} \longrightarrow {}^3\text{OH}\cdots\text{N}\cdot \longrightarrow {}^3\text{NOH}\cdot \longrightarrow \text{NO} + \text{H}$	F	1.5×10^{-10}	0	0	This work
88.	$\text{OH} + \text{CH}_4 \longrightarrow \text{H}_2\text{O} + \text{CH}_3$	F	8.8×10^{-13}	1.83	1396	Baulch et al. ^[27]
89.	$\text{OH} + \text{CH}_3 \longrightarrow {}^3\text{O} + \text{CH}_4$	F	9.5×10^{-13}	-0.29	4139	this work
90.	$\text{OH} + \text{CH}_3 \longrightarrow \text{H}_2\text{O} + {}^3\text{CH}_2$	F	2.2×10^{-12}	1.67	3972	This work
91.	$\text{OH} + {}^3\text{CH}_2 \longrightarrow \text{OH}\cdots\text{CH}_2\cdot \longrightarrow \text{H}_2\text{COH}\cdot \longrightarrow \text{H}_2\text{CO} + \text{H}$	F	4.6×10^{-11}	0	0	This work
92.	$\text{OH} + {}^3\text{CH}_2 \longrightarrow \text{H}_2\text{O} + \text{CH}$	F	7.6×10^{-13}	0	0	This work
93.	$\text{OH} + {}^1\text{CH}_2 \longrightarrow \text{OH}\cdots\text{CH}_2\cdot \longrightarrow \text{H}_2\text{COH}\cdot \longrightarrow \text{H}_2\text{CO} + \text{H}$	F	4.6×10^{-11}	0	0	This work
94.	$\text{OH} + \text{CH} \longrightarrow {}^3\text{OH}\cdots\text{CH}\cdot \longrightarrow {}^3\text{HCOH}\cdot \longrightarrow {}^3\text{H}_2\text{CO}\cdot \longrightarrow \text{HCO} + \text{H}$	F	3.2×10^{-11}	0	0	This work
95.	$\text{OH} + \text{CH} \longrightarrow \text{anti-HCOH}_{(\nu)}\cdot \longrightarrow \text{H}_2\text{CO}_{(\nu)}\cdot \longrightarrow \text{CO} + \text{H}_2$	F	6.3×10^{-12}	0	0	This work
96.	$\text{OH} + \text{CH} \longrightarrow \text{anti-HCOH}_{(\nu)}\cdot \longrightarrow \text{H}_2\text{CO}_{(\nu)}\cdot \longrightarrow \text{CO} + \text{H} + \text{H}$	F	6.3×10^{-12}	0	0	This work
97.	$\text{OH} + \text{H}_2 \longrightarrow \text{H}_2\text{O} + \text{H}$	F	9.5×10^{-13}	2.00	1490	Baulch et al. ^[27]
98.	$\text{OH} + \text{H} \longrightarrow {}^3\text{O} + \text{H}_2$	F	7.0×10^{-14}	2.80	1950	Baulch et al. ^[27]

99.	$^3\text{O} + \text{H}_2\text{CN} \longrightarrow \text{CH}_2\text{NO}\cdot \longrightarrow \text{HCNOH}\cdot \longrightarrow \text{HCNO} + \text{H}$	F	5.7×10^{-13}	1.72	788	This work
100.	$^3\text{O} + \text{H}_2\text{CN} \longleftarrow \text{CH}_2\text{NO}\cdot \longleftarrow \text{HCNO} + \text{H}$	R	9.8×10^{-11}	0	0	This work
101.	$^3\text{O} + \text{H}_2\text{CN} \longrightarrow \text{CH}_2\text{NO}\cdot \longrightarrow \text{HCNOH}\cdot \longrightarrow \text{HCN} + \text{OH}$	F	3.7×10^{-13}	0.86	1127	This work
102.	$^3\text{O} + \text{HCN} \longrightarrow {}^3\text{NCOH} \longrightarrow \text{NCO} + \text{H}$	F	1.3×10^{-11}	0.96	4040	This work
103.	$^3\text{O} + \text{HCN} \longleftarrow {}^3\text{NCOH} \longleftarrow \text{NCO} + \text{H}$	R	1.3×10^{-10}	0.20	5743	This work
104.	$^3\text{O} + \text{CN} \longrightarrow {}^4\text{NCO} \longrightarrow \text{CO} + {}^4\text{N}$	F	7.6×10^{-12}	0	0	Baulch et al. ^[27]
105.	$^3\text{O} + \text{CN} \longrightarrow \text{NCO}_{(\nu)} \longrightarrow \text{CO} + {}^2\text{N}$	F	9.4×10^{-12}	0	0	Baulch et al. ^[27]
106.	$^3\text{O} + \text{NH} \longrightarrow \text{HNO}\cdot \longrightarrow \text{NO} + \text{H}$	F	3.1×10^{-11}	0	0	This work
107.	$^3\text{O} + \text{NH} \longrightarrow \text{OH} + {}^4\text{N}$	F	4.5×10^{-12}	0.54	1589	This work
108.	$^3\text{O} + \text{CH}_4 \longrightarrow \text{OH} + \text{CH}_3$	F	1.1×10^{-11}	1.56	4270	Baulch et al. ^[27]
109.	$^3\text{O} + \text{CH}_3 \longrightarrow \text{CH}_3\text{O}\cdot \longrightarrow \text{H}_2\text{CO} + \text{H}$	F	1.4×10^{-10}	0	0	Baulch et al. ^[27]
110.	$^3\text{O} + {}^3\text{CH}_2 \longrightarrow \text{H}_2\text{CO}_{(\nu)} \longrightarrow \text{CO} + \text{H} + \text{H}$	F	1.2×10^{-10}	0	0	Baulch et al. ^[27]
111.	$^3\text{O} + {}^3\text{CH}_2 \longrightarrow \text{H}_2\text{CO}_{(\nu)} \longrightarrow \text{CO} + \text{H}_2$	F	8.0×10^{-11}	0	0	Baulch et al. ^[27]
112.	$^3\text{O} + {}^1\text{CH}_2 \longrightarrow {}^3\text{H}_2\text{CO}\cdot \longrightarrow \text{HCO} + \text{H}$	F	2.1×10^{-10}	0	0	This work
113.	$^3\text{O} + \text{CH} \longrightarrow \text{HCO}_{(\nu)} \longrightarrow \text{CO} + \text{H}$	F	6.6×10^{-11}	0	0	Baulch et al. ^[27]
114.	$^3\text{O} + \text{CH} \longrightarrow {}^4\text{HCO}\cdot \longrightarrow {}^4\text{COH}\cdot \longrightarrow \text{OH} + \text{C}$	F	2.5×10^{-10}	0	0	This work
115.	$^3\text{O} + \text{H}_2 \longrightarrow \text{OH} + \text{H}$	F	3.5×10^{-13}	2.67	3163	Baulch et al. ^[27]
116.	${}^1\text{O} + \text{H}_2\text{CN} \longrightarrow \text{CH}_2\text{NO}\cdot \longrightarrow {}^3\text{O} + \text{H}_2\text{CN}$	F	4.5×10^{-10}	0.70	-53	This work
117.	${}^1\text{O} + \text{H}_2\text{CN} \longrightarrow \text{CH}_2\text{NO}\cdot \longrightarrow \text{HCNO} + \text{H}$ (50–200 K) (200–400 K)	F		2.3×10^{-11}	-0.39	1070
				1.9×10^{-13}	5.30	-356
118.	${}^1\text{O} + \text{H}_2\text{CN} \longrightarrow \text{CH}_2\text{NO}\cdot \longrightarrow \text{HCNOH}\cdot \longrightarrow \text{HCN} + \text{OH}$ (50–200 K) (200–400 K)	F				This work
				1.5×10^{-11}	-0.81	1386
				1.1×10^{-13}	4.56	-46
119.	${}^1\text{O} + \text{CN} \longrightarrow \text{NCO}_{(\nu)} \longrightarrow \text{CO} + {}^2\text{N}$	F	8.9×10^{-11}	0	0	This work
120.	${}^1\text{O} + \text{CH}_4 \longrightarrow \text{CH}_3\text{OH}_{(\nu)} \longrightarrow \text{OH} + \text{CH}_3$	F	2.2×10^{-10}	0	0	Avg. of exper. vals
121.	${}^1\text{O} + \text{CH}_3 \longrightarrow \text{CH}_3\text{O}\cdot \longrightarrow \text{H}_2\text{CO} + \text{H}$	F	4.3×10^{-10}	0	0	This work
122.	${}^1\text{O} + {}^3\text{CH}_2 \longrightarrow {}^3\text{H}_2\text{CO}\cdot \longrightarrow \text{HCO} + \text{H}$	F	7.0×10^{-10}	0	0	This work
123.	${}^1\text{O} + {}^1\text{CH}_2 \longrightarrow \text{H}_2\text{CO}_{(\nu)} \longrightarrow \text{CO} + \text{H} + \text{H}$	F	1.7×10^{-10}	0	0	This work
124.	${}^1\text{O} + {}^1\text{CH}_2 \longrightarrow \text{H}_2\text{CO}_{(\nu)} \longrightarrow \text{CO} + \text{H}_2$	F	1.7×10^{-10}	0	0	This work
125.	${}^1\text{O} + \text{CH} \longrightarrow \text{HCO}_{(\nu)} \longrightarrow \text{CO} + \text{H}$	F	9.2×10^{-11}	0	0	This work
126.	${}^1\text{O} + \text{H}_2 \longrightarrow \text{H}_2\text{O}_{(\nu)} \longrightarrow \text{OH} + \text{H}$	F	2.1×10^{-10}	0	0	Avg. of exper. vals
127a.	${}^1\text{O} + \text{CO}_2 \longrightarrow {}^3\text{O} + \text{CO}_2$	F	7.4×10^{-11}	0	-133	Dunlea and Ravishankara ^[71]
127b.	${}^1\text{O} + \text{N}_2 \longrightarrow {}^3\text{O} + \text{N}_2$	F	2.1×10^{-11}	0	-115	Dunlea and Ravishankara ^[71]
127c.	${}^1\text{O} + \text{H}_2 \longrightarrow {}^3\text{O} + \text{H}_2$	F	1.4×10^{-10}	0	0	Vranckx et al. ^[72]

Experimental Data

Experiments and reviews have measured and suggested reaction rate coefficients for several of the reactions in

this network at or near ~ 298 K. These values are listed in Table S3.

TABLE S3: All available experimental or recommended reaction rate coefficients for the reactions in this study. For brevity, only the 10 most recent measurements of $\text{OH} + \text{CH}_4 \longrightarrow \text{H}_2\text{O} + \text{CH}_3$, $\text{OH} + \text{H}_2 \longrightarrow \text{H}_2\text{O} + \text{H}$, and ${}^3\text{O} + \text{CH}_3 \longrightarrow \text{H}_2\text{CO} + \text{H}$ are included; for a complete listing, we refer the reader to the NIST Chemical Kinetics Database^[73]. First-order rate coefficients have units s^{-1} . Second-order rate coefficients have units cm^3s^{-1} . Third-order rate coefficients have units cm^6s^{-1} .

k(298K)	Technique	Temp. (K)	Pressure (Torr)	Reference(s)
$\text{CO}_2 + {}^1\text{O} \longrightarrow \text{products}$				
2.3×10^{-10}	M	300	20	Young et al. ^[74]
1.4×10^{-10}	M	295	25–250	Blitz et al. ^[75]
1.0×10^{-10}	M	297	40	Wine and Ravishankara ^[76]
$>1.0 \times 10^{-12}$	M			Young and Ung ^[77]
$\text{CO}_2 + {}^1\text{O} \longrightarrow {}^3\text{O} + \text{CO}_2$				
2.1×10^{-10}	M	300	15–26	Heidner, III et al. ^[78]
1.3×10^{-10}	M	295	0–0.01	Amimoto et al. ^[79]

1.2×10^{-10}	M	298		Davidson et al. ^[80]
1.1×10^{-10}	M	298	5–50	Dunlea and Ravishankara ^[67]
$\text{CO}_2 + {}^2\text{N} \longrightarrow \text{CO} + \text{NO}$				
6.8×10^{-13}	M	300	6	Fell et al. ^[81]
6.0×10^{-13}	M	300	2–5	Black et al. ^[82]
5.0×10^{-13}	M	300	7–15	Lin and Kaufman ^[83]
3.5×10^{-13}	M	300	1–3	Piper et al. ^[84]
1.8×10^{-13}	M	300	26	Husain et al. ^[60]
$\text{CO}_2 + {}^3\text{CH}_2 \longrightarrow {}^3\text{H}_2\text{CO} + \text{CO}$				
3.9×10^{-14}	M	298	50–700	Laufer and Bass ^[85]
3.9×10^{-14}	S	298		Tsang and Hampson ^[28]
$\text{CO}_2 + \text{CH} \longrightarrow \text{HCO} + \text{CO}$				
2.1×10^{-12}	M	298	20	Mehlmann et al. ^[56]
1.9×10^{-12}	M	298	100	Butler et al. ^[86, 87]
1.8×10^{-12}	M	298	100	Berman et al. ^[88]
1.8×10^{-12}	S	298		Baulch et al. ^[27]
$\text{H}_2\text{CO} + \text{CN} \longrightarrow \text{HCN} + \text{HCO}$				
1.7×10^{-11}	M	298		Yu et al. ^[68]
$\text{H}_2\text{CO} + \text{OH} \longrightarrow \text{H}_2\text{O} + \text{HCO}$				
1.5×10^{-11}	M	298	700	Niki et al. ^[89]
1.2×10^{-11}	M	298	100	Zabarnick et al. ^[90]
$8.1\text{--}11 \times 10^{-12}$	M	298	20–80	Stief et al. ^[91]
9.3×10^{-12}	M	299	50	Atkinson and Pitts Jr. ^[92]
8.4×10^{-12}	M	299	700	Niki et al. ^[93]
8.1×10^{-12}	M	296	1–4	Temps and Wagner ^[94]
7.8×10^{-12}	M	298	3	Yetter et al. ^[95]
6.1×10^{-12}	M	298	40	Vandooren and Van Tiggelen ^[96]
1.0×10^{-11}	S	300		Baulch et al. ^[27]
1.0×10^{-11}	S	298		Tsang and Hampson ^[28]
$\text{H}_2\text{CO} + {}^3\text{O} \longrightarrow \text{HCO} + \text{OH}$				
1.9×10^{-13}	M	298	1.6	Chang and Barker ^[97]
1.7×10^{-13}	M	298	50–200	Klemm ^[98]
1.7×10^{-13}	M	298	1.7–4.4	Klemm et al. ^[99]
1.5×10^{-13}	M	300	2	Herron and Penzhorn ^[100]
1.5×10^{-13}	M	300	0.9–1.1	Mack and Thrush ^[101]
1.7×10^{-13}	S	298		Baulch et al. ^[27]
1.7×10^{-13}	S	298		Tsang and Hampson ^[28]
$\text{H}_2\text{CO} + \text{CH}_3 \longrightarrow \text{CH}_4 + \text{HCO}$				
4.2×10^{-18}	S	298		Tsang and Hampson ^[28]
2.2×10^{-18}	S	298		Baulch et al. ^[27]
$\text{H}_2\text{CO} + {}^3\text{CH}_2 \longrightarrow \text{CH}_3 + \text{HCO}$				Tsang and Hampson ^[28]
$<1.0 \times 10^{-14}$	S	298		
$\text{H}_2\text{CO} + {}^1\text{CH}_2 \longrightarrow \text{CH}_3 + \text{HCO}$				Tsang and Hampson ^[28]
2.0×10^{-12}	S	298		
$\text{H}_2\text{CO} + \text{CH} \longrightarrow \text{products}$				
3.8×10^{-10}	M	298	20–300	Zabarnick et al. ^[102]
3.8×10^{-10}	S	298		Baulch et al. ^[27]
$\text{H}_2\text{CO} + \text{H} \longrightarrow \text{HCO} + \text{H}_2$				
6.7×10^{-14}	M	298	100–450	Klemm ^[98]
5.4×10^{-14}	M	297	25–116	Ridley et al. ^[103]
4.4×10^{-14}	M	298	1–2	Brennen et al. ^[104]
4.2×10^{-14}	M	298	1–5	Oehlers et al. ^[105]
4.1×10^{-14}	M	298	22.5	Vandooren et al. ^[106]
3.9×10^{-14}	M	298	0.8–2.1	Westenberg and DeHaas ^[107]
5.9×10^{-14}	S	298		Baulch et al. ^[27]
5.5×10^{-14}	S	298		Tsang and Hampson ^[28]
$\text{HCO} + \text{HCO} \longrightarrow \text{C}_2\text{H}_2\text{O}_2$				
5.0×10^{-11}	M		0.1–10	Stoeckel et al. ^[108]
2.8×10^{-13}	M	298		Yee Quee and Thynne ^[69]

HCO + HCO \longrightarrow H ₂ CO + CO					
7.5×10^{-11}	M	295	10–30		Baggott et al. ^[109]
6.3×10^{-11}	M	298	10		Reilly et al. ^[110]
4.5×10^{-11}	M	298	210–1425		Friedrichs et al. ^[111]
3.4×10^{-11}	M	298	10–20		Veyret et al. ^[112]
3.0×10^{-11}	M	298			Vedeneev et al. ^[113]
HCO + HCO \longrightarrow CO + CO + H ₂					
3.6×10^{-11}	M	298			Yee Quee and Thynne ^[69]
HCO + OH \longrightarrow H ₂ O + CO					
1.8×10^{-10}	M	296	1–4		Temps and Wagner ^[94]
1.7×10^{-10}	S	300			Baulch et al. ^[27]
5.0×10^{-11}	S	300			Tsang and Hampson ^[28]
HCO + ³ O \longrightarrow CO ₂ + H					
5.0×10^{-11}	S	300–2500			Baulch et al. ^[27]
5.0×10^{-11}	S	298			Tsang and Hampson ^[28]
HCO + ³ O \longrightarrow CO + OH					
5.0×10^{-11}	S	300–2500			Baulch et al. ^[27]
5.0×10^{-11}	S	298			Tsang and Hampson ^[28]
HCO + CH ₃ \longrightarrow CH ₃ HCO					
4.4×10^{-11}	M	298	60–76		Mulenko ^[114]
6.3×10^{-12}	M	298			Yee Quee and Thynne ^[69]
3.0×10^{-11}	S	298			Tsang and Hampson ^[28]
HCO + CH ₃ \longrightarrow CO + CH ₄					
3.6×10^{-11}	M	298			Yee Quee and Thynne ^[69]
2.0×10^{-10}	S	298			Tsang and Hampson ^[28]
HCO + ³ CH ₂ \longrightarrow CO + CH ₃					
3.0×10^{-11}	S	298			Tsang and Hampson ^[28]
HCO + ¹ CH ₂ \longrightarrow CO + CH ₃					
3.0×10^{-11}	S	298			Tsang and Hampson ^[28]
HCO + H \longrightarrow CO + H ₂					
5.5×10^{-10}	M	298	251		Reilly et al. ^[110]
1.8×10^{-10}	M	298	$2–1425 \times 10^2$		Friedrichs et al. ^[111]
1.1×10^{-10}	M	298			Ziemer et al. ^[115]
2.0×10^{-10}	S	298			Tsang and Hampson ^[28]
1.5×10^{-10}	S	298			Baulch et al. ^[27]
CO + OH \longrightarrow CO ₂ + H					
9.7×10^{-13}	M	300	750–112500		Forster et al. ^[116]
2.3×10^{-13}	M	299	700		Niki et al. ^[117]
$1.3–1.9 \times 10^{-13}$	M	296–297	5–10		Frost et al. ^[118]
1.7×10^{-13}	M	298	150		Bohn and Zetzsch ^[119]
1.6×10^{-13}	M	298	2		Herron ^[120]
1.5×10^{-13}	M	300	24		Husain et al. ^[121]
1.4×10^{-13}	M	300	150		Lissianski et al. ^[122]
1.4×10^{-13}	M	298	100		Ravishankara and Thompson ^[123]
1.3×10^{-13}	M	297	5		Frost et al. ^[124]
8.5×10^{-14}	M	300	1.8		Herron ^[125]
1.3×10^{-13}	S	298			Baulch et al. ^[27]
CO + ¹ O + M \longrightarrow CO ₃ + M					
$k_0(\text{CO}_2) = 2.8 \times 10^{-29}$	M		300		Clerc and Barat ^[63]
CO + ¹ O \longrightarrow products					
7.3×10^{-11}	M	300	15–26		Heidner, III et al. ^[78]
5.8×10^{-11}	M	298			Davidson et al. ^[126]
5.0×10^{-11}	M	300	7–25		Young et al. ^[74]
$< 5.0 \times 10^{-11}$	M	300	3–17		Noxon ^[127]
3.3×10^{-12}	M		300		Clerc and Barat ^[63]
CO + CH + M \longrightarrow HCCO + M					
$k_0(\text{Ar}) = 4.2 \times 10^{-30}$	M	298	10–100		Mehlmann et al. ^[56]
$k_0(\text{Ar}) = 4.1 \times 10^{-30}$	M	298	0.4–4.5		Le Picard et al. ^[128]

$k_0(\text{Ar}) = 4.1 \times 10^{-30}$	M	298	4–400	Brownsworth et al. ^[129]
$k_0(\text{He}) = 4.1 \times 10^{-30}$	M	298	10–7500	Fulle et al. ^[130]
$k_0(\text{He}) = 3.9 \times 10^{-30}$	M	298	10–100	Mehlmann et al. ^[56]
$k_0(\text{He}) = 2.4 \times 10^{-30}$	M	293	12.5–500	Taatjes ^[131]
$\text{CO} + \text{CH} \longrightarrow \text{HCCO}$				
1.7×10^{-10}	M	298	10–7500	Fulle et al. ^[130]
5.9×10^{-11}	M	298	high-pressure limit	Mehlmann et al. ^[56]
3.0×10^{-11}	M	298	0.4–4.5	Le Picard et al. ^[128]
2.1×10^{-11}	M	298	100	Butler et al. ^[87]
8.3×10^{-12}	M	298	100	Berman et al. ^[88]
6.9×10^{-12}	M	298	100	Taatjes ^[131]
4.8×10^{-12}	M			Bosnali and Perner ^[132]
$\text{CO} + \text{H} + \text{M} \longrightarrow \text{HCO} + \text{M}$				
$k_0(\text{H}_2) < 3.3 \times 10^{-34}$	M	298	50–250	Bennett and Blackmore ^[133]
$k_0(\text{CH}_4, \text{H}_2\text{O}) = 1.6 \times 10^{-34}$	M	298	760	Hochanadel et al. ^[64]
$k_0(\text{H}_2) = 1.1 \times 10^{-34}$	M	298		Wang et al. ^[134]
$k_0(\text{H}_2) = 1.1 \times 10^{-34}$	M	298	800–1220	Hikida et al. ^[135]
$k_0(\text{H}_2) = 1.0 \times 10^{-34}$	M	298	760	Hochanadel et al. ^[64]
$k_0(\text{CO}) = 9.9 \times 10^{-35}$	M	298	760	Hochanadel et al. ^[64]
$k_0(\text{Ar}) = 7.2 \times 10^{-35}$	M	298	800–1220	Hikida et al. ^[135]
$k_0(\text{H}_2) = 8.0 \times 10^{-35}$	M	298	52–601	Ahumada et al. ^[136]
$k_0(\text{Kr}) = 6.9 \times 10^{-35}$	M	298	52–601	Ahumada et al. ^[136]
$k_0(\text{Ar}) = 6.2 \times 10^{-35}$	M	298	52–601	Ahumada et al. ^[136]
$k_0(\text{He}) = 6.0 \times 10^{-35}$	M	298	52–601	Ahumada et al. ^[136]
$k_0(\text{Ne}) = 4.8 \times 10^{-35}$	M	298	52–601	Ahumada et al. ^[136]
$\text{H}_2\text{O} + {}^1\text{O} \longrightarrow \text{OH} + \text{OH}$				
3.7×10^{-10}	M	300	11	Gauthier and Snelling ^[137]
3.0×10^{-11}	M	300	15–26	Heidner, III et al. ^[78]
2.6×10^{-10}	M	300	3–5	Lee and Slanger ^[138]
2.3×10^{-10}	M	298	10–30	Davidson et al. ^[139]
2.3×10^{-10}	M	298	1–12	Streit et al. ^[140]
$1.8\text{--}2.3 \times 10^{-10}$	M	295	20–36	Dunlea and Ravishankara ^[141]
$1.9\text{--}2.2 \times 10^{-10}$	M	298	7–47	Gericke and Comes ^[142]
2.1×10^{-10}	M	298	1–30	Davidson et al. ^[80]
$\text{H}_2\text{O} + \text{CH} \longrightarrow \text{products}$				
1.3×10^{-11}	M	293	200	Blitz et al. ^[57]
4.5×10^{-11}	M			Bosnali and Perner ^[132]
$\text{OH} + \text{H}_2\text{CN} \longrightarrow \text{H}_2\text{CNOH}$				
6.0×10^{-12}	M	298	120–200	Nizamov and Dagdigian ^[65]
$\text{OH} + \text{HCN} \longrightarrow \text{products}$				
3.1×10^{-14}	M	298	75–375	Fritz et al. ^[143]
1.0×10^{-16}	M	298	10	Phillips ^[70]
$\text{OH} + \text{OH} + \text{M} \longrightarrow \text{H}_2\text{O}_2 + \text{M}$				
$k_0(\text{H}_2\text{O}) = 1.8 \times 10^{-29}$	M	298	100	Caldwell and Back ^[52]
$k_0(\text{O}_2) = 5.1 \times 10^{-30}$	M	298	100	Caldwell and Back ^[52]
$k_0(\text{CO}_2) = 4.2 \times 10^{-30}$	M	298	100	Caldwell and Back ^[52]
$k_0(\text{H}_2\text{O}) = 4.0 \times 10^{-30}$	M	298	0.08–105	Zellner et al. ^[144]
$k_0(\text{N}_2) = 3.3 \times 10^{-30}$	M	298	100	Caldwell and Back ^[52]
$k_0(\text{Xe}) = 1.3 \times 10^{-30}$	M	298	100	Caldwell and Back ^[52]
$k_0(\text{Ar}) = 9.7 \times 10^{-31}$	M	298	100	Caldwell and Back ^[52]
$k_0(\text{He}) = 9.2 \times 10^{-31}$	M	298	750–7500	Sangwan et al. ^[145]
$k_0(\text{He}) = 8.5 \times 10^{-31}$	M	298	100	Caldwell and Back ^[52]
$k_0(\text{N}_2) = 6.9 \times 10^{-31}$	M	298	20–825	Zellner et al. ^[144]
$k_0(\text{H}_2\text{O}) = 2.8 \times 10^{-31}$	M	298	200	Black and Porter ^[53]
$k_0(\text{N}_2) = 2.5 \times 10^{-31}$	M	298	1	Trainor and von Rosenberg Jr. ^[146]
$k_0(\text{N}_2) = 2.5 \times 10^{-31}$	M	298	1	Trainor and von Rosenberg Jr. ^[147]
$k_0(\text{O}_2) = 7.9 \times 10^{-32}$	M	298	200	Black and Porter ^[53]
$k_0(\text{CO}_2) = 6.4 \times 10^{-32}$	M	298	200	Black and Porter ^[53]
$k_0(\text{N}_2) = 5.1 \times 10^{-32}$	M	298	200	Black and Porter ^[53]

$k_0(\text{Xe}) = 2.0 \times 10^{-32}$	M	298	200	Black and Porter ^[53]
$k_0(\text{Ar}) = 1.5 \times 10^{-32}$	M	298	200	Black and Porter ^[53]
$k_0(\text{He}) = 1.3 \times 10^{-32}$	M	298	200	Black and Porter ^[53]
$k_0(\text{H}_2\text{O}) = 4.0 \times 10^{-30}$	S	300		Baulch et al. ^[27]
$k_0(\text{N}_2) = 8.0 \times 10^{-31}$	S	300		Baulch et al. ^[27]
$k_0(\text{N}_2) = 6.0 \times 10^{-31}$	S	298		Tsang and Hampson ^[28]
$\text{OH} + \text{OH} \longrightarrow \text{H}_2\text{O}_2$				
6.5×10^{-11}	M	300	1	Greiner ^[148]
2.6×10^{-11}	M	298	75000	Fulle et al. ^[149]
2.4×10^{-11}	M	298	750–7500	Sangwan et al. ^[145]
2.2×10^{-11}	M	298	750–112500	Forster et al. ^[116]
1.5×10^{-11}	M	298	20–825	Zellner et al. ^[144]
1.5×10^{-11}	S	298		Baulch et al. ^[27]
$\text{OH} + \text{OH} \longrightarrow \text{H}_2\text{O} + {}^3\text{O}$				
2.6×10^{-12}	M	300	1	Dixon-Lewis et al. ^[150]
2.3×10^{-12}	M	298	1–4	Westenberg and deHaas ^[151]
2.1×10^{-12}	M	298	23–78	Trainor and von Rosenberg Jr. ^[146]
2.1×10^{-12}	M	298	1	Trainor and von Rosenberg Jr. ^[147]
1.7×10^{-12}	M	298		Farquharson and Smith ^[152]
$1.3\text{--}1.5 \times 10^{-12}$	M	298	1–2	Clyne and Down ^[153]
1.4×10^{-12}	M	298	2250–7500	Sangwan and Krasnoperov ^[154]
1.4×10^{-12}	M	298	1	Bedjanian et al. ^[155]
1.4×10^{-12}	M	298		Wagner and Zellner ^[156]
8.4×10^{-13}	M	298	1	Breen and Glass ^[157]
2.0×10^{-12}	S	298		Tsang and Hampson ^[28]
1.4×10^{-12}	S	298		Baulch et al. ^[27]
$\text{OH} + {}^3\text{O} \longrightarrow \text{O}_2 + \text{H}$				
4.3×10^{-11}	M	298	1	Breen and Glass ^[157]
4.2×10^{-11}	M	298	2.5–4	Smith and Stewart ^[158]
3.9×10^{-11}	M	298	4	Howard and Smith ^[159]
$2.3\text{--}3.8 \times 10^{-11}$	M	298	0.6–0.9	Westenberg et al. ^[160]
3.8×10^{-11}	M	298	3.75	Howard and Smith ^[161]
3.3×10^{-11}	M	298	40	Robertson and Smith ^[162]
3.2×10^{-11}	M	298	40	Robertson and Smith ^[163]
3.1×10^{-11}	M	300	1–5	Brune et al. ^[164]
2.9×10^{-11}	M	298		Lewis and Watson ^[165]
2.8×10^{-11}	M	300	2–8	Kurzius and Boudart ^[166]
3.9×10^{-15}	S	298		Tsang and Hampson ^[28]
2.9×10^{-11}	S	298		Baulch et al. ^[27]
$\text{OH} + \text{NH} \longrightarrow \text{HNO} + \text{H}$				
3.3×10^{-11}	S	298		Cohen and Westberg ^[58]
$\text{OH} + \text{NH} \longrightarrow \text{H}_2\text{O} + {}^4\text{N}$				
5.1×10^{-12}	S	298		Cohen and Westberg ^[58]
$\text{OH} + {}^4\text{N} \longrightarrow \text{NO} + \text{H}$				
5.3×10^{-11}	M	298	4	Howard and Smith ^[159]
5.2×10^{-11}	M	294	2.5–6	Smith and Stewart ^[158]
5.0×10^{-11}	M	298	3.75	Howard and Smith ^[161]
4.2×10^{-11}	M	300	1–5	Brune et al. ^[164]
$\text{OH} + \text{CH}_4 \longrightarrow \text{H}_2\text{O} + \text{CH}_3$				
1.1×10^{-14}	M	300	1	Wilson and Westenberg ^[167]
8.5×10^{-15}	M	298	99	Wilson and Westenberg ^[168]
7.6×10^{-15}	M	298	100	Sharkey and Smith ^[169]
6.9×10^{-15}	M	298	100	Mellouki et al. ^[170]
6.6×10^{-15}	M	298	151	Bryukov et al. ^[171]
6.4×10^{-15}	M	298	100	Bonard et al. ^[172]
6.4×10^{-15}	M	298	100	Gierczak et al. ^[173]
$6.2\text{--}6.3 \times 10^{-15}$	M	298	100–300	Vaghjiani and Ravishankara ^[174]
6.2×10^{-15}	M	298	400–750	Dunlop and Tully ^[175]
5.9×10^{-15}	M	298	1	Finlayson-Pitts et al. ^[176]

8.0×10^{-15}	S	298	Baulch et al. ^[27]
7.9×10^{-15}	S	298	Tsang and Hampson ^[28]
$\text{OH} + \text{CH}_3 + \text{M} \longrightarrow \text{CH}_3\text{OH} + \text{M}$			
$k_0(\text{SF}_6) = 7.2 \times 10^{-27}$	M	298	Fagerström et al. ^[177]
$k_0(\text{He}) = 2.6 \times 10^{-27}$	M	300	Humpfer et al. ^[178]
$k_0(\text{SF}_6) = 2.5 \times 10^{-27}$	M	298	Fagerström et al. ^[179]
$k_0(\text{He}) = 2.0 \times 10^{-27}$	M	300	Oser et al. ^[180]
$k_0(\text{He}) = 2.0 \times 10^{-27}$	M	300	Oser et al. ^[181]
$\text{OH} + \text{CH}_3 \longrightarrow \text{CH}_3\text{OH}$			
1.7×10^{-10}	M	300	Humpfer et al. ^[178]
1.7×10^{-10}	M	300	Oser et al. ^[181]
1.4×10^{-10}	M	298	Fagerström et al. ^[179]
1.4×10^{-10}	M	298	Fagerström et al. ^[177]
9.4×10^{-11}	M	298	Anastasi et al. ^[182]
9.3×10^{-11}	M	300	Oser et al. ^[180]
$\text{OH} + \text{CH}_3 \longrightarrow {}^3\text{O} + \text{CH}_4$			
1.8×10^{-17}	S	298	Cohen and Westberg ^[58]
$\text{OH} + {}^3\text{CH}_2 \longrightarrow \text{H}_2\text{CO} + \text{H}$			
3.0×10^{-11}	S	298	Tsang and Hampson ^[28]
$\text{OH} + {}^1\text{CH}_2 \longrightarrow \text{H}_2\text{CO} + \text{H}$			
5.0×10^{-11}	S	298	Tsang and Hampson ^[28]
$\text{OH} + \text{H}_2 \longrightarrow \text{H}_2\text{O} + \text{H}$			
8.5×10^{-15}	M	298	Sworski et al. ^[183]
7.2×10^{-15}	M	298	Smith and Zellner ^[184]
7.0×10^{-15}	M	298	Atkinson et al. ^[185]
7.0×10^{-15}	M	298	Atkinson et al. ^[186]
6.9×10^{-15}	M	298	Talukdar et al. ^[187]
6.7×10^{-15}	M	298	Orkin et al. ^[188]
6.2×10^{-15}	M	298	Ravishankara et al. ^[189]
6.1×10^{-15}	M	298	Tully and Ravishankara ^[190]
5.8×10^{-15}	M	298	Overend et al. ^[191]
5.3×10^{-15}	M	298	Trainor and von Rosenberg Jr. ^[192]
6.4×10^{-15}	S	298	Tsang and Hampson ^[28]
6.2×10^{-15}	S	300	Baulch et al. ^[27]
$\text{OH} + \text{H} + \text{M} \longrightarrow \text{H}_2\text{O} + \text{M}$			
$k_0(\text{CO}_2) = 9.0 \times 10^{-31}$	M	300	Zellner et al. ^[54]
$k_0(\text{N}_2) = 4.8 \times 10^{-31}$	M	300	Zellner et al. ^[54]
$k_0(\text{Ar}) = 2.3 \times 10^{-31}$	M	300	Zellner et al. ^[54]
$k_0(\text{He}) = 1.5 \times 10^{-31}$	M	300	Zellner et al. ^[54]
$k_0(\text{H}_2\text{O}) = 4.3 \times 10^{-30}$	S	300	Baulch et al. ^[27]
$k_0(\text{N}_2) = 6.8 \times 10^{-31}$	S	300	Baulch et al. ^[27]
$k_0(\text{Ar}) = 2.6 \times 10^{-31}$	S	300	Baulch et al. ^[27]
$k_0(\text{H}_2\text{O}) = 6.8 \times 10^{-31}$	S	300	Tsang and Hampson ^[28]
$\text{OH} + \text{H} \longrightarrow {}^3\text{O} + \text{H}_2$			
5.6×10^{-16}	S	300	Kaufman and Del Greco ^[193]
9.9×10^{-17}	S	298	Cohen and Westberg ^[194]
1.1×10^{-16}	S	300	Tsang and Hampson ^[28]
${}^3\text{O} + \text{CN} \longrightarrow \text{CO} + {}^4\text{N}$			
3.7×10^{-11}	M	298	Titarchuk and Halpern ^[195]
2.1×10^{-11}	M	298	Schacke et al. ^[196]
2.7×10^{-12}	M	298	Schmatjko and Wolfrum ^[197]
1.7×10^{-11}	S	298	Tsang ^[198]
7.6×10^{-12}	S	298	Baulch et al. ^[27]
${}^3\text{O} + \text{CN} \longrightarrow \text{CO} + {}^2\text{N}$			
1.6×10^{-11}	M	298	Schmatjko and Wolfrum ^[197]
9.4×10^{-12}	S	298	Baulch et al. ^[27]
${}^3\text{O} + {}^3\text{O} + \text{M} \longrightarrow \text{O}_2 + \text{M}$			
$k_0(\text{N}_2) = 7.2 \times 10^{-33} - 1.0 \times 10^{-32}$	M	300	Morgan et al. ^[199]
$k_0(\text{O}_2) = 1.0 \times 10^{-32}$	M	298	Tchen ^[200]

$k_0(N_2) = 4.8 \times 10^{-33}$	M	298	2–15	Campbell and Gray ^[201]
$k_0(O_2) = 4.5 \times 10^{-33}$	M	300	1–10	Marshall ^[202]
$k_0(N_2) = 3.1 \times 10^{-33}$	M	298	2–10	Campbell and Thrush ^[203]
$k_0(Ar) = 2.7 \times 10^{-33}$	M	300	1	Reeves et al. ^[204]
$k_0(Ar) = 1.7 \times 10^{-33}$	M	298	2–10	Campbell and Thrush ^[203]
$k_0(He) = 1.3 \times 10^{-33}$	M	298	2–10	Campbell and Thrush ^[203]
$k_0(Ar) = 3.9 \times 10^{-34}$	M	300		Kondratiev and Nikitin ^[205]
$k_0(Ar) = 1.1 \times 10^{-33}$	S	298		Tsang and Hampson ^[28]
${}^3O + NH \longrightarrow HNO \longrightarrow NO + H$				
5.0×10^{-11}	S	298		Cohen and Westberg ^[58]
${}^3O + NH \longrightarrow OH + {}^4N$				
5.0×10^{-12}	S	298		Cohen and Westberg ^[58]
$<1.7 \times 10^{-13}$	M	298	11–15	Hack et al. ^[206]
${}^3O + {}^4N + M \longrightarrow NO + M$				
$k_0(CO_2) = 1.8 \times 10^{-32}$	M	298	2–15	Campbell and Thrush ^[66]
$k_0(N_2O) = 1.5 \times 10^{-32}$	M	298	2–15	Campbell and Thrush ^[66]
$k_0(N_2) = 1.1 \times 10^{-32}$	M	298	2–10	Campbell and Thrush ^[203]
$k_0(N_2) = 9.2 \times 10^{-33}$	M	298	2–15	Campbell and Gray ^[201]
$k_0(N_2) = 9.1 \times 10^{-33}$	M	298	2–9	Kretschmer and Petersen ^[207]
$k_0(Ar) = 8.2 \times 10^{-33}$	M	298	2–10	Campbell and Thrush ^[203]
$k_0(N_2) = 5.0 \times 10^{-33}$	M	298	3–4	Mavroyannis and Winkler ^[208]
$k_0(He) = 3.8 \times 10^{-33}$	M	298	2–10	Campbell and Thrush ^[203]
${}^3O + CH_4 \longrightarrow OH + CH_3$				
6.6×10^{-16}	M	300		Froben ^[209]
1.2×10^{-17}	M	298	1–2	Westenberg and de Haas ^[210]
6.6×10^{-19}	M	293	10–150	Falconer et al. ^[211]
5.0×10^{-18}	S	298		Baulch et al. ^[27]
4.3×10^{-18}	S	298		Tsang and Hampson ^[28]
${}^3O + CH_3 \longrightarrow H_2CO + H$				
1.9×10^{-10}	M	298		Slagle et al. ^[212]
1.4×10^{-10}	M	298		Slagle et al. ^[213]
1.4×10^{-10}	M	298	$<2 \times 10^{-4}$	Washida ^[214]
1.2×10^{-10}	M	298	2.8	Washida and Bayes ^[215]
1.1×10^{-10}	M	298	19	Zellner et al. ^[216]
1.1×10^{-10}	M	295		Plumb and Ryan ^[217]
1.0×10^{-10}	M	298		Washida and Bayes ^[218]
9.4×10^{-11}	M	298	0.1	Seakins and Leone ^[219]
$>3.0 \times 10^{-11}$	M	298		Morris, Jr. and Niki ^[220]
$>3.0 \times 10^{-11}$	M	300	1–2	Niki et al. ^[221]
1.4×10^{-10}	S	298		Baulch et al. ^[27]
1.3×10^{-10}	S	298		Tsang and Hampson ^[28]
${}^3O + {}^3CH_2 \longrightarrow$ products				
1.3×10^{-10}	M	296		Böhland et al. ^[222]
1.3×10^{-10}	M	295		Vinckier and Debruyn ^[223]
2.0×10^{-10}	S	298		Baulch et al. ^[27]
1.9×10^{-11}	S	298		Tsang and Hampson ^[28]
${}^3O + CH \longrightarrow$ products				
9.5×10^{-11}	M	298	5–15	Messing et al. ^[224]
9.4×10^{-11}	M	298	5–10	Messing et al. ^[225]
${}^3O + CH \longrightarrow CO + H$				
6.6×10^{-11}	S	298		Baulch et al. ^[27]
${}^3O + H_2 \longrightarrow OH + H$				
1.1×10^{-17}	M	298	300	Zhu et al. ^[226]
1.0×10^{-17}	M	297	100–600	Presser and Gordon ^[227]
9.1×10^{-18}	M	298		Light and Matsumoto ^[228]
8.5×10^{-18}	S	298		Baulch et al. ^[27]
7.0×10^{-18}	S	298		Tsang and Hampson ^[28]
${}^3O + H + M \longrightarrow OH + M$				
$k_0(M) = 1.0 \times 10^{-33}–8 \times 10^{-30}$	S	298		Baulch et al. ^[229]

$k_0(M) = 4.4 \times 10^{-32}$	S	298		Tsang and Hampson ^[28]
$^1\text{O} + \text{CH}_4 \longrightarrow \text{OH} + \text{CH}_3$				
3.8×10^{-10}	M	300	11	Gauthier and Snelling ^[137]
2.2×10^{-10}	M	300	1–3	Matsumi et al. ^[230]
1.9×10^{-10}	M	298	10	Vranckx et al. ^[231]
1.7×10^{-10}	M	298	45	Dillon et al. ^[232]
1.4×10^{-10}	M	295	25–250	Blitz et al. ^[75]
4.0×10^{-10}	S	298		Cvetanović ^[233]
$^1\text{O} + \text{H}_2 \longrightarrow \text{OH} + \text{H}$				
3.0×10^{-10}	M	300	11	Gauthier and Snelling ^[137]
2.7×10^{-10}	M	298	0.1	Koppe et al. ^[234]
2.5×10^{-10}	M	298	7–21	Stief et al. ^[235]
2.2×10^{-10}	M	298	1	Matsumi et al. ^[230]
1.2×10^{-10}	M	298		Talukdar and Ravishankara ^[236]
1.1×10^{-10}	M	298	100	Ogren et al. ^[237]

M: Monitoring decay of reactants and/or production of products.

S: Suggested value based on experiments and/or evaluations at a range of temperatures.

Lennard-Jones Parameters

TABLE S4: Lennard-Jones force constants used in this study. Values are obtained from viscosity data when possible.

Molecule	σ (\AA)	ϵ/k_b (K)	Source
CO_3	^a 3.996	^a 190	Welty et al. ^[45]
NCCO	^b 4.38	^b 339	Welty et al. ^[45]
CO_2	3.996	190	Welty et al. ^[45]
CH_3CHO	3.97	436	Wang et al. ^[46]
H_2CNOH	^e 3.585	^e 507	Welty et al. ^[45]
CH_3OH	3.585	507	Welty et al. ^[45]
CH_2CO	3.97	436	Wang et al. ^[46]
HCON	^c 3.59	^c 498	Wang et al. ^[46]
HO CN	^c 3.59	^c 498	Wang et al. ^[46]
HCNO	^c 3.59	^c 498	Wang et al. ^[46]
H_2CO	3.59	498	Wang et al. ^[46]
HCCO	^d 4.221	^d 185	Welty et al. ^[45]
NCO	^g 3.63	^g 569.1	Reid et al. ^[44]
H_2O_2	4.196	289.3	Reid et al. ^[44]
trans-HNOH	^f 3.47	^f 119	Welty et al. ^[45]
HCO	3.59	498	Wang et al. ^[46]
HO_2	3.458	107.4	Wang et al. ^[46]
N_2	3.681	91.5	Welty et al. ^[45]
H_2O	2.649	356	Welty et al. ^[45]
O_2	3.433	113	Welty et al. ^[45]
NO	3.47	119	Welty et al. ^[45]
OH	2.75	80	Wang et al. ^[46]
H_2	2.968	33.3	Welty et al. ^[45]

^a L-J parameters based on those for CO_2

^b L-J parameters based on those for NCCN

^c L-J parameters based on those for H_2CO

^d L-J parameters based on those for C_2H_2

^e L-J parameters based on those for CH_3OH

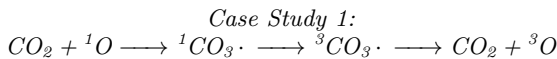
^f L-J parameters based on those for NO

^g L-J parameters based on those for HCN

Theoretical Case Studies

The following case studies provide additional details for some of the non-standard reactions in this study.

Examples include intersystem crossing reactions, reactions with vibrational intermediates or complex pathways, and reactions where BHandHLYP/aug-cc-pVDZ misdiagnosed the barrier.



The deexcitation of ${}^1\text{O}$ by CO_2 has been studied considerably both experimentally and theoretically^{74,78,79,238–246}.

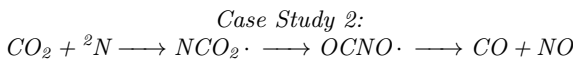
Experiments confirm that the dominant quenching pathway leads to ground state oxygen atoms (${}^3\text{O}$)^{74,80,242,245,246}. RRKM and statistical models have been used to explore the quenching mechanism^{239,243}, the dominant of which is to react ${}^1\text{O}$ by CO_2 to form singlet CO_3 , which then undergoes intersystem crossing to the triplet CO_3 potential energy surface before decaying into ${}^3\text{O} + \text{CO}_2$.

An experiment by Sedlacek et al.^[241] measures the singlet PES quenching pathway, $\text{CO}_2 + {}^1\text{O} \longrightarrow {}^1\text{CO}_3 \cdot \longrightarrow \text{CO} + \text{O}_2$, to be approximately 1000 times less efficient than the dominant mechanism.

Experimentally measured rate coefficients for the overall quenching of ${}^1\text{O}$ by CO_2 in the 295–300 K range from $1.0\text{--}2.3 \times 10^{-10} \text{ cm}^3\text{s}^{-1}$ ^{167,74–76,78–80}.

In this work, we calculate the rate coefficient for $\text{CO}_2 + {}^1\text{O} \longrightarrow \text{CO}_3$ at the BHandHLYP/aug-cc-pVDZ level of theory to be $k(298 \text{ K}) = 3.8 \times 10^{-11} \text{ cm}^3\text{s}^{-1}$, and assume this to be the rate-limiting step in the quenching pathway to $\text{CO}_2 + {}^3\text{O}$. This value is only a factor of 3 lower than the nearest experimental measurement by Wine and Ravishankara^[76].

We also include the third-order reaction $\text{CO}_2 + {}^1\text{O} + \text{M} \longrightarrow \text{CO}_3 + \text{M}$ in our network for $\text{M} = \text{N}_2$, CO_2 , and H_2 .



Experimental measurements of the rate coefficient for this reaction at 300 K are between $1.8\text{--}6.8 \times 10^{-13} \text{ cm}^3\text{s}^{-1}$ ^{160,81–84}. Herron^[247] reviewed these experiments and suggested a value of $3.6 \times 10^{-13} \text{ cm}^3\text{s}^{-1}$.

There have been no theoretical studies performed on this reaction to date.

Husain et al.^[60] suggest this reaction has a small energy barrier due to its fairly slow rate coefficient for a reaction of high exothermicity.

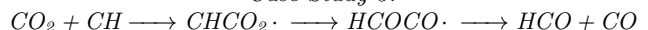
We do not find a barrier for this reaction at the BHandHLYP/aug-cc-pVDZ level of theory. We also do not find a barrier at the CCSD/aug-cc-pVDZ level of theory.

On the other hand, at the HF/aug-cc-pVDZ level of theory, we find a barrier of 34.3 kJ mol^{-1} at the transition state for a C-N bond distance of 1.89 \AA .

In a computational methods comparison study on the reaction of $\text{CH}_4 + \text{H} \longrightarrow \text{CH}_3 + \text{H}_2$, we found the variational transition state barrier at the HF/aug-cc-pVDZ level of theory to be approximately twice the size of the barrier calculated at the BHandHLYP/aug-cc-pVDZ level of theory. We insert an artificial barrier of half the

HF value ($17.15 \text{ kJ mol}^{-1}$) into the calculation for $k(298 \text{ K})$ at the BHandHLYP/aug-cc-pVDZ level of theory, and obtain a rate coefficient of $3.2 \times 10^{-14} \text{ cm}^3\text{s}^{-1}$. This value is ~ 6 times smaller than the nearest experimental value.

Case Study 3:



The rate coefficients for this reaction have been measured experimentally at 298 K and range from $1.8\text{--}2.1 \times 10^{-12} \text{ cm}^3\text{s}^{-1}$ ^{156,86–88}. Baulch et al.^[27] reviewed the earliest of these experimental results and has suggested a $k(298 \text{ K})$ value of $1.8 \times 10^{-12} \text{ cm}^3\text{s}^{-1}$. Mehlmann et al.^[56] predict this reaction to have little or no activation barrier below 400 K.

We find no theoretical studies of this reaction.

We find the first step of this reaction to be the rate-limiting step. At the BHandHLYP/aug-cc-pVDZ level of theory, the first step of this reaction has a barrier; However, at the B3LYP/aug-cc-pVDZ level of theory, this reaction step is barrierless. We remove the barrier from our calculation to match expectation from experiment⁵⁶ and obtain an overall rate coefficient of $k(298 \text{ K}) = 3.1 \times 10^{-12} \text{ cm}^3\text{s}^{-1}$ at the BHandHLYP/aug-cc-pVDZ level of theory. This is within a factor of 1.5 of the nearest experimental value.

Case Study 4: $\text{CO}_2 + {}^3\text{CH}_2 \longrightarrow \text{H}_2\text{CO} + \text{CO}$

Laufer and Bass^[85] experimentally measured the rate coefficient for this reaction at 298 K to be $3.9 \times 10^{-14} \text{ cm}^3\text{s}^{-1}$. Darwin and Moore^[248] performed upper bound experiments on this reaction and found $k(298)$ to be no greater than $1.4 \times 10^{-14} \text{ cm}^3\text{s}^{-1}$.

Kovacs and Jackson^[249] studied this reaction theoretically, and found the lowest energy path is to form the ${}^3\text{CH}_2 \cdots \text{CO}_2$ complex, followed the subsequent reaction into ${}^3\text{CH}_2\text{CO}_2$ over a $19.3 \text{ kcal mol}^{-1}$ barrier (at the G2 level of theory). They find that the lowest energy path from the ${}^3\text{CH}_2 \cdots \text{CO}_2$ complex is to fragment back into ${}^3\text{CH}_2$ and CO_2 over a $1.1 \text{ kcal mol}^{-1}$ barrier. They also suggest an intersystem crossing reaction from this complex to the singlet surface is unlikely, and that ${}^3\text{CH}_2$ would may require collisional reaction to the singlet state in order for this reaction to proceed.

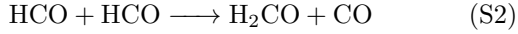
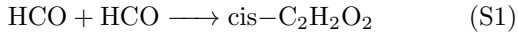
We find similar results to Kovacs and Jackson^[249] at the BHandHLYP/aug-cc-pVDZ and CCSD/aug-cc-pVDZ levels of theory. $\text{CO}_2 + {}^3\text{CH}_2$ proceeds via a barrierless reaction to form the ${}^3\text{CH}_2 \cdots \text{CO}_2$ complex with a C-C bond distance of 3.25 (3.23) \AA at the BHandHLYP/aug-cc-pVDZ (CCSD/aug-cc-pVDZ) level of theory. This reaction efficiently decays back into $\text{CO}_2 + {}^3\text{CH}_2$, and the barrier to ${}^3\text{CH}_2\text{CO}_2$ is 15.7 (19.3) kcal mol^{-1} at the BHandHLYP/aug-cc-pVDZ (CCSD/aug-cc-pVDZ) level of theory. We find the rate coefficient for the reaction $\text{CO}_2 + {}^3\text{CH}_2 \longrightarrow$

$^3\text{CH}_2 \cdots \text{CO}_2 \longrightarrow ^3\text{CH}_2\text{CO}_2$ to be $k(298 \text{ K}) = 1.8 \times 10^{-23} (2.3 \times 10^{-25}) \text{ cm}^3\text{s}^{-1}$ at the BHandHLYP/aug-cc-pVDZ (CCSD/aug-cc-pVDZ) level of theory, which is too slow to consider in our network.

Our results and those of Kovacs and Jackson^[249] suggest this reaction likely does not occur on the triplet surface. For this reason, we do not include it in our network, and instead only include the singlet surface reaction $\text{CO}_2 + ^1\text{CH}_2 \longrightarrow \text{H}_2\text{CO} + \text{CO}$. We find $\text{CO}_2 + ^1\text{CH}_2 \longrightarrow \text{H}_2\text{CO} + \text{CO}$ to have a rate coefficient of $8.0 \times 10^{-13} \text{ cm}^3\text{s}^{-1}$ at 298 K, which is only a factor of 2 larger than the experimental value for $\text{CO}_2 + ^3\text{CH}_2 \longrightarrow \text{H}_2\text{CO} + \text{CO}$. This adds some evidence to the suggestion that $^3\text{CH}_2$ must first collisionally excite to $^1\text{CH}_2$ before reacting with CO_2 to produce $\text{H}_2\text{CO} + \text{CO}$.

Case Study 5: $\text{HCO} + \text{HCO} \longrightarrow \text{products}$

Three potential product channels of the self-reaction of HCO have been reported experimentally^{69,109–112,250}.



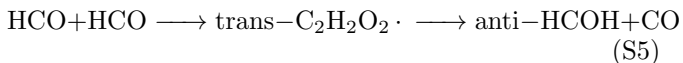
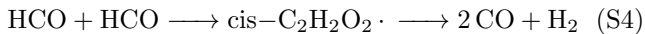
Rate coefficients for $\text{HCO} + \text{HCO} \longrightarrow \text{H}_2\text{CO} + \text{CO}$ have been experimentally measured at 295–298 K and range from $3.0\text{--}7.5 \times 10^{-11} \text{ cm}^3\text{s}^{-1}$ ^{109–113}. The lack of temperature dependence in the range of 298–475 K suggests this reaction is barrierless¹¹².

Yee Quee and Thynne^[69] performed the only experimental measurement of the rate coefficient for $\text{HCO} + \text{HCO} \longrightarrow 2 \text{CO} + \text{H}_2$ at 298 K, which they find to be $3.6 \times 10^{-11} \text{ cm}^3\text{s}^{-1}$.

Rate coefficients for $\text{HCO} + \text{HCO} \longrightarrow \text{trans}-\text{C}_2\text{H}_2\text{O}_2$ have been experimentally measured at 298 K to be in the range of $2.8\text{--}500 \times 10^{-13} \text{ cm}^3\text{s}^{-1}$ ^{169,108}.

There are no experimental measurements of the rate coefficient for $\text{HCO} + \text{HCO} \longrightarrow \text{cis}-\text{C}_2\text{H}_2\text{O}_2$.

Saheb and Nazari^[251] performed theoretical quantum computational simulations, and found the most important product channels to be:



We find no direct abstraction reaction for $\text{HCO} + \text{HCO} \longrightarrow \text{H}_2\text{CO} + \text{CO}$ on the singlet surface. We do however find an inefficient abstraction reaction for $\text{HCO} + \text{HCO} \longrightarrow \text{anti}-\text{HCOH} + \text{CO}$, with a

$k(298 \text{ K})$ rate coefficient of $3.4 \times 10^{-24} \text{ cm}^3\text{s}^{-1}$ at the BHandHLYP/aug-cc-pVDZ level of theory.

We find the reaction $\text{HCO} + \text{HCO} \longrightarrow \text{trans}-\text{C}_2\text{H}_2\text{O}_2$ to have a barrierless rate coefficient of $4.1 \times 10^{-13} \text{ cm}^3\text{s}^{-1}$ at 298 K at the BHandHLYP/aug-cc-pVDZ level of theory. At the same level of theory, we calculate the rate coefficient of the subsequent reaction $\text{trans}-\text{C}_2\text{H}_2\text{O}_2 \longrightarrow \text{anti}-\text{HCOH} + \text{CO}$ ($k(298 \text{ K}) = 7.1 \times 10^{-34} \text{ s}^{-1}$) to be slightly smaller than the decay back into $\text{HCO} + \text{HCO}$ ($k(298 \text{ K}) = 1.7 \times 10^{-33} \text{ s}^{-1}$). Finally, we find $\text{anti}-\text{HCOH}$ efficiently isomerizes into H_2CO . We calculate the overall rate coefficient at 298 K for $\text{HCO} + \text{HCO} \longrightarrow \text{trans}-\text{C}_2\text{H}_2\text{O}_2 \longrightarrow \text{anti}-\text{HCOH} + \text{CO} \longrightarrow \text{H}_2\text{CO} + \text{CO}$ to be $1.2 \times 10^{-13} \text{ s}^{-1}$, which is slightly reduced from the barrierless value due to the slight preference in the decay back to $\text{HCO} + \text{HCO}$ over $\text{anti}-\text{HCOH} + \text{CO}$. This is only a factor of 2 smaller than the nearest experimental value for $\text{HCO} + \text{HCO} \longrightarrow \text{trans}-\text{C}_2\text{H}_2\text{O}_2$ ⁶⁹.

We calculate the reaction $\text{HCO} + \text{HCO} \longrightarrow \text{cis}-\text{C}_2\text{H}_2\text{O}_2 \cdot \longrightarrow \text{CO} + \text{CO} + \text{H}_2$ to have a rate coefficient of $k(298 \text{ K}) = 7.4 \times 10^{-11} \text{ cm}^3\text{s}^{-1}$ at the BHandHLYP/aug-cc-pVDZ level of theory. This is only a factor of 2 larger than the only experimental value.

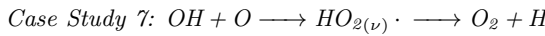
Case Study 6: $\text{CO} + \text{OH} \longrightarrow \text{intermediates} \longrightarrow \text{CO}_2 + \text{H}$

Experimental measurements of the rate coefficient for this reaction at 296–300 K range from 8.5×10^{-14} to $9.7 \times 10^{-13} \text{ cm}^3\text{s}^{-1}$ ^{1116–125}. Baulch et al.^[27] review the kinetic data from experiments and suggest a very slight temperature dependence, suggesting this reaction proceeds with little or no reaction barrier.

There are multiple reaction pathways for this reaction, but the fastest is that which proceeds through the $\text{OH} \cdots \text{CO} \cdot$ and $\text{cis}-\text{HOCO} \cdot$ intermediates²⁵².

At the BHandHLYP/aug-cc-pVDZ level of theory, we calculate $k(298 \text{ K})$ for the barrierless first step, $\text{CO} + \text{OH} \longrightarrow \text{OH} \cdots \text{CO} \cdot$, to be $9.7 \times 10^{-12} \text{ cm}^3\text{s}^{-1}$. However, we find intermediate barriers at the second and third steps of this calculation at the BHandHLYP/aug-cc-pVDZ level of theory, making the overall rate coefficient for $\text{CO} + \text{OH} \longrightarrow \text{OH} \cdots \text{CO} \cdot \longrightarrow \text{cis}-\text{HOCO} \cdot \longrightarrow \text{CO}_2 + \text{H}$, $5.7 \times 10^{-19} \text{ cm}^3\text{s}^{-1}$. This is several orders of magnitude smaller than the range of experimental values. At the B3LYP/aug-cc-pVDZ level of theory, these barriers are more comparable, resulting in only a factor of 3.4 reduction between the barrierless first step and the overall rate coefficient. *Ab initio* calculations show similar barrier heights to our the B3LYP/aug-cc-pVDZ calculations²⁵².

We reduce the calculated rate coefficient for the barrierless first step at the BHandHLYP/aug-cc-pVDZ level of theory by a factor of 3.4 to match the barrier effects at the B3LYP/aug-cc-pVDZ level of theory. This gives us a rate coefficient of $k(298) = 2.9 \times 10^{-12} \text{ cm}^3\text{s}^{-1}$, which is a factor of 3 higher than the nearest experimental value.

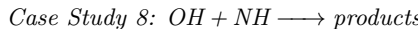


Experimental measurements for this reaction at 298–300 K range from $2.3\text{--}4.3 \times 10^{-11} \text{ cm}^3 \text{s}^{-1}$ ^{157–166}.

This reaction proceeds through HO₂, which, in its ground vibrational state has been noted to be long-lived^{253,254}. Our calculations confirm that the decay of HO₂ into O₂ + H is slow ($< 10^{-47} \text{ s}^{-1}$). This suggests this reaction proceeds through an excited vibrational state, as is to be expected when two reactants combine to form a single product³⁵.

We calculate the rate coefficient of OH + ³O → HO₂ at 298 K at the BHandHLYP/aug-cc-pVDZ level of theory to be $7.4 \times 10^{-11} \text{ cm}^3 \text{s}^{-1}$, and assume the subsequent vibrational decay into O₂ + H. Our calculated rate coefficient is within a factor of 2 of the experimental range.

There are currently no experimental measurements for the rate coefficient of OH + ¹O → O₂ + H, which we find also proceeds through HO₂. We calculate the rate coefficient of OH + ¹O → HO₂ at 298 K at the BHandHLYP/aug-cc-pVDZ level of theory to be $1.0 \times 10^{-9} \text{ cm}^3 \text{s}^{-1}$, and similarly assume the vibrational decay into O₂ + H.



No experiments have been performed to date on the reaction of OH + NH. Cohen and Westberg^[58] use analogous reactions to suggest rate coefficients of $k(298 \text{ K}) = 3.3 \times 10^{-11} \text{ cm}^3 \text{s}^{-1}$ and $5.1 \times 10^{-12} \text{ cm}^3 \text{s}^{-1}$ for OH + NH → HNO + H and OH + NH → H₂O + ⁴N, respectively. They suggest little or no barrier exists for either pathway.

²⁵⁵ performed theoretical transition state theory calculations for this reaction using a range of computational quantum methods. They calculated 298 K reaction rate coefficients of $6.8 \times 10^{-11} \text{ cm}^3 \text{s}^{-1}$ and $1.4 \times 10^{-12} \text{ cm}^3 \text{s}^{-1}$ for OH + NH → HNO + H and OH + NH → H₂O + ⁴N, respectively.

We find the OH + NH → HNO + H reaction to proceed through multiple intermediates, including OH· · · NH· ·, trans-HNOH· ·, and H₂NO· ·. We calculate the barrierless first step of this reaction OH + NH → OH· · · NH· · at 298 K at the BHandHLYP/aug-cc-pVDZ level of theory to be $7.0 \times 10^{-12} \text{ cm}^3 \text{s}^{-1}$. However, at this level of theory, we find a large forward barrier at the third reaction step (i.e., trans-HNOH· · → HNO + H), which reduces the overall rate coefficient to $2.6 \times 10^{-14} \text{ cm}^3 \text{s}^{-1}$. This is over three orders of magnitude smaller than the recommended and theoretical values. Conversely, at the B3LYP/aug-cc-pVDZ level of theory, the third forward reaction step barrier is smaller than the reverse barrier, which makes the barrierless first step the rate limiting step.

We remove the barrier at the third reaction step from our calculation to match the kinetic data and theoretical studies, and obtain an overall rate coefficient for OH +

NH → HNO + H of $k(298 \text{ K}) = 7.0 \times 10^{-12} \text{ cm}^3 \text{s}^{-1}$ at the BHandHLYP/aug-cc-pVDZ level of theory. This value is a factor of 5 smaller than the suggested value⁵⁸.

We calculate the rate coefficient for OH + NH → H₂O + ⁴N at 298 K at the BHandHLYP/aug-cc-pVDZ level of theory to be $6.8 \times 10^{-13} \text{ cm}^3 \text{s}^{-1}$. This is a factor of 5 smaller than the suggested value by Cohen and Westberg^[58].



No experiments to date have measured the rate coefficient of ³O + H₂CN → HCN + OH. Tomeczek and Gradoń^[256] suggested a temperature-independent rate of $8.3 \times 10^{-11} \text{ cm}^3 \text{s}^{-1}$ based on calculations using published chemical compositions of the flames of methane, nitrogen and oxygen at >1850 K. They note that this calculation does not include the effects of an energy barrier, and thus this value is not reliable at 298 K. Tomeczek and Gradoń^[256] also suggested this same rate coefficient for the reaction H + H₂CN → HCN + H₂.

No previous theoretical studies regarding this reaction have been performed.

Unlike H + H₂CN → HCN + H₂, which we found in previous work to proceed efficiently through a barrierless abstraction mechanism¹⁹, we find no abstraction pathway for ³O + H₂CN → HCN + OH. Instead, we find that ³O and H₂CN efficiently react to form CH₂NO· with a rate coefficient of $3.1 \times 10^{-11} \text{ cm}^3 \text{s}^{-1}$. This product most commonly decays back into the original reactants; However, there are two other favourable pathways. The mechanistic model for these reactions is shown in Figure S1.

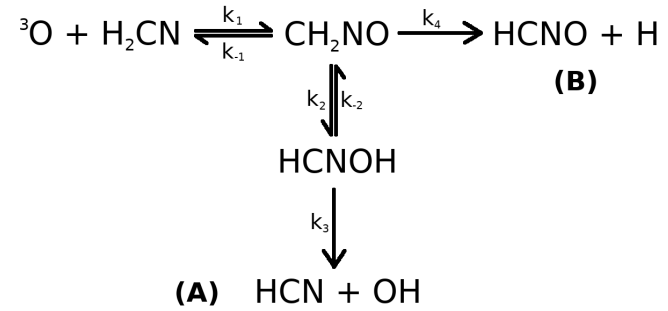


FIG. S1. Mechanistic model for the reaction of ³O + H₂CN. Two efficient product channels on the doublet surface exist: (A) HCN + OH and (B) HCNO + H.

Using the mechanistic model above, we use the steady-state solutions to the kinetic rate equations to calculate the overall rate coefficients for paths A and B. This is done by equating the kinetic rate equations for each species in the mechanistic model to zero (e.g. $d[\text{CH}_2\text{NO}]/dt = 0 = k_1[\text{³O} + \text{H}_2\text{CN}] + k_{-2}[\text{HCNOH}] - (k_1 + k_2)[\text{CH}_2\text{NO}]$), and substituting these equations

into the overall kinetic rate equations for products A and B from the initial reactants. This gives us the following rate coefficients for paths A and B:

$$k_A = \frac{k_1 k_3}{\alpha}, \quad (\text{S6})$$

$$\alpha = \frac{(k_{-1} + k_2 + k_4)(k_{-2} + k_3)}{k_2} - k_{-2}. \quad (\text{S7})$$

$$k_B = \frac{k_1 k_4}{\beta}, \quad (\text{S8})$$

$$\beta = k_{-1} + k_2 + k_4 - \frac{k_{-2} k_2}{k_{-2} + k_3}. \quad (\text{S9})$$

We calculate these rate coefficients at the BHandHLYP/aug-cc-pVDZ level of theory to be $k_A = 4.0 \times 10^{-14}$ and $k_B = 8.3 \times 10^{-15} \text{ cm}^3 \text{s}^{-1}$ at 298 K, respectively.

We propose that the suggested barrierless rate coefficient for ${}^3\text{O} + \text{H}_2\text{CN} \longrightarrow \text{HCN} + \text{OH}$ by Tomeczek and Gradoń^[256] is not an accurate estimate for this overall reaction at 298 K. In fact, the large barrier for $\text{CH}_2\text{NO}\cdot \longrightarrow \text{HCNOH}\cdot$ isomerization at 298 K plays a key role in decreasing this overall rate coefficient. We find the isomerization barrier to also have similar heights when using the B3LYP and CCSD computational methods.

We use similar mechanistic modeling to calculate the rate coefficients for the reactions of ${}^1\text{O} + \text{H}_2\text{CN} \longrightarrow \text{CH}_2\text{NO}\cdot \longrightarrow$ products; However along with the two decay pathways above, there is an additional decay pathway to ${}^3\text{O} + \text{H}_2\text{CN}$. We are the first to calculate these three ${}^1\text{O} + \text{H}_2\text{CN}$ reaction rate coefficients.

At the BHandHLYP/aug-cc-pVDZ level of theory, we calculate the rate coefficients for the reaction of ${}^1\text{O} + \text{H}_2\text{CN}$ to products (A) $\text{HCN} + \text{OH}$, (B) $\text{HCNO} + \text{H}$, and (C) ${}^3\text{O} + \text{H}_2\text{CN}$, to be 1.2×10^{-13} , 6.0×10^{-13} , and $4.5 \times 10^{-10} \text{ cm}^3 \text{s}^{-1}$, respectively.

Given the potential importance of ${}^1\text{O} + \text{H}_2\text{CN} \longrightarrow \text{HCN} + \text{OH}$ to produce HCN in atmospheres, and the similar barrier heights to the three product channels, we also calculated these rate coefficients at the $\omega\text{B97XD}/\text{aug-cc-pVDZ}$ and $\text{CCSD}/\text{aug-cc-pVDZ}$ levels of theory.

At the $\omega\text{B97XD}/\text{aug-cc-pVDZ}$ level of theory, we calculate the rate coefficients for the reaction of ${}^1\text{O} + \text{H}_2\text{CN}$ to products (A), (B), and (C), to be 5.3×10^{-11} , 2.8×10^{-10} , and $6.6 \times 10^{-23} \text{ cm}^3 \text{s}^{-1}$, respectively.

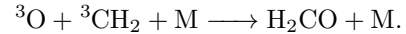
At the $\text{CCSD}/\text{aug-cc-pVDZ}$ level of theory, we calculate the rate coefficients for the reaction of ${}^1\text{O} + \text{H}_2\text{CN}$ to products (A), (B), and (C), to be 8.8×10^{-11} , 1.9×10^{-11} , and $2.2 \times 10^{-10} \text{ cm}^3 \text{s}^{-1}$.

In the case of BHandHLYP and CCSD, the dominant channel for the reaction of ${}^1\text{O} + \text{H}_2\text{CN}$ is (C). This is not the case for ωB97XD , where channel (C) is negligible,

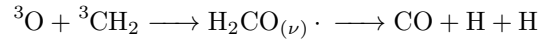
and the dominant channel is (B). The rate coefficient for the potentially important HCN source, channel (A), varies by a factor of 733 across the three levels of theory. Given these discrepancies, we recommend these reactions be followed up with an experimental study.

Case Study 10: ${}^3\text{O} + \text{CH}_2 \longrightarrow \text{products}$

${}^3\text{O} + {}^3\text{CH}_2$ combine to form a vibrationally excited H_2CO molecule⁵⁹. In high atmospheric pressures, this molecule can be collisionally deexcited in the reaction



However, in upper atmospheres, where collisions are less frequent, the vibrationally excited H_2CO will dissociate via 2 equally favourable pathways^{27,28,59}



Experimental measurements of the rate coefficient of ${}^3\text{O} + {}^3\text{CH}_2 \longrightarrow \text{products}$ at 295–296 K are $1.3 \times 10^{-10} \text{ cm}^3 \text{s}^{-1}$ ^{222,223}. Reviews of this reaction over a range of temperatures and pressures suggest a wider range of 1.9×10^{-11} – $2.0 \times 10^{-10} \text{ cm}^3 \text{s}^{-1}$ ^{27,28}.

We calculate the rate coefficient of ${}^3\text{O} + {}^3\text{CH}_2 \longrightarrow \text{H}_2\text{CO}$ at the BHandHLYP/aug-cc-pVDZ level of theory to be $k(298 \text{ K}) = 6.7 \times 10^{-11} \text{ cm}^3 \text{s}^{-1}$, which is within the range of suggested values, and only a factor of 2 lower than the two experimental measurements. We allow this reaction to proceed along the two equally favourable dissociation channels, each with a calculated rate coefficient of $3.4 \times 10^{-11} \text{ cm}^3 \text{s}^{-1}$.

Excited oxygen (${}^1\text{O}$) and methylene (${}^1\text{CH}_2$) also react to produce vibrationally excited H_2CO .

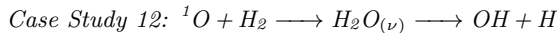
We calculate the rate coefficient of ${}^1\text{O} + {}^1\text{CH}_2 \longrightarrow \text{H}_2\text{CO}$ at the BHandHLYP/aug-cc-pVDZ level of theory to be $k(298 \text{ K}) = 3.3 \times 10^{-10} \text{ cm}^3 \text{s}^{-1}$. We assume that the two dissociation pathways for vibrationally excited H_2CO are also equally favourable for this reaction, and allow this reaction to proceed to form $\text{CO} + \text{H} + \text{H}$ and $\text{CO} + \text{H}_2$ with equal rate coefficients of $1.7 \times 10^{-10} \text{ cm}^3 \text{s}^{-1}$.

Case Study 11: ${}^1\text{O} + \text{CH}_4 \longrightarrow \text{CH}_3\text{OH}_{(\nu)} \longrightarrow \text{OH} + \text{CH}_3$

${}^1\text{O}$ and CH_4 mainly react to form vibrationally excited CH_3OH , the dominant subsequent pathway of which is to produce $\text{OH} + \text{CH}_3$ ^{75,137,230–232,257,258}.

Experimental measurements of ${}^1\text{O} + \text{CH}_4 \longrightarrow \text{OH} + \text{CH}_3$ from 295–300 K range from 1.4– 3.8×10^{-10} ^{75,137,230–233}.

We calculate the rate coefficient of $^1\text{O} + \text{CH}_4 \longrightarrow \text{CH}_3\text{OH}$ at 298 K with the BHandHLYP/aug-cc-pVDZ level of theory to be $5.8 \times 10^{-9} \text{ cm}^3\text{s}^{-1}$, and assume the vibrational decay into $\text{OH} + \text{CH}_3$ as suggested. Our calculated rate coefficient is a factor of 15 larger than the nearest experimental value.



Experimental measurements of the rate coefficient for $^1\text{O} + \text{H}_2 \longrightarrow \text{OH} + \text{H}$ at 298–300 K are between 1.1 and $3.0 \times 10^{-10} \text{ cm}^3\text{s}^{-1}$ ^{1137,230,234–237}.

TABLE S5: Quantum Chemistry Simulation Data at the BHandHLYP/aug-cc-pVDZ level of theory. Cartesian coordinates are in angstroms. Energies are in kJ mol⁻¹. E_e is the electronic energy, ZPE is the zero point energy, and q_x are the partition functions (t: translational, e: electronic, v:vibrational, r:rotational).

Reac.	Species	Geometry (Atom, X, Y, Z)	E _e + ZPE	q _t /V (m ⁻³)	q _e	q _v	q _r
1/33	CO ₂	O, 0.00000, 0.00000, 1.15274 O, 0.00000, 0.00000, -1.15274 C, 0.00000, 0.00000, 0.00000	-494917.399028	2.82E+32	1	1.07E+00	5.23E+02
	¹ O	O, 0.00000, 0.00000, 0.00000	-196788.921964	6.19E+31	1	1.00E+00	1.00E+00
	TS	O, 1.15275, 1.18505, 0.00000 O, -1.15275, 1.18630, 0.00000 C, 0.00000, 1.18425, 0.00000 O, -0.00000, -3.25954, 0.00000	-691707.204162	4.49E+32	1	1.07E+00	1.26E+05
	CO ₃	O, 0.77156, -0.80876, 0.00000 O, -0.00000, 1.42285, 0.00000 C, 0.00000, 0.25955, 0.00000 O, -0.77156, -0.80876, 0.00000	-691904.373961	4.49E+32	1	1.14E+00	2.10E+04
	HCO	C, 0.06118, 0.57927, 0.00000 O, 0.06118, -0.58725, 0.00000 H, -0.85649, 1.22238, 0.00000	-298768.200141	1.51E+32	2	1.00E+00	7.26E+02
	² N	N, 0.00000, 0.00000, 0.00000	-143024.189856	5.07E+31	2	1.00E+00	1.00E+00
	TS	C, 0.76711, 0.41879, -0.00000 O, 1.58153, -0.41503, 0.00000 H, 0.96548, 1.52043, 0.00001 N, -2.60291, -0.10184, 0.00000	-441966.317654	2.73E+32	1	8.98E+00	3.02E+04
	HCON	N, -0.86610, 0.41919, 0.00000 C, -0.11780, -0.57337, 0.00000 H, -0.15944, -1.65573, -0.00000 O, 0.86612, 0.27020, 0.00000	-442240.538001	2.73E+32	1	1.13E+00	6.70E+03
	HCO	C, 0.06118, 0.57927, 0.00000 O, 0.06118, -0.58725, 0.00000 H, -0.85649, 1.22238, 0.00000	-298768.200141	1.51E+32	2	1.00E+00	7.26E+02
3	CH ₃	C, 0.00000, -0.00018, 0.00042 H, -0.93570, -0.53955, -0.00085 H, 0.93580, -0.53939, -0.00085 H, -0.00010, 1.08002, -0.00085	-104455.380974	5.63E+31	2	1.08E+00	2.53E+02
	TS	C, 0.88372, 0.43321, -0.00001 O, 1.69253, -0.40737, 0.00000 H, 1.09010, 1.53196, 0.00003 C, -2.20157, -0.09394, 0.00000 H, -1.99765, -1.15406, -0.00023 H, -2.36283, 0.42288, -0.93450 H, -2.36272, 0.42250, 0.93473	-403228.049716	2.83E+32	1	1.10E+02	3.37E+04
	CH ₃ HCO	C, 0.23234, 0.39590, 0.00000 O, 1.22430, -0.27597, 0.00000 H, 0.31342, 1.50005, 0.00000 C, -1.16060, -0.14740, -0.00000 H, -1.14984, -1.23540, -0.00002 H, -1.69424, 0.22607, -0.87809	-403547.142484	2.83E+32	1	2.04E+00	1.18E+04

This reaction is known to proceed through vibrationally excited H₂O in its ground electronic state^{259,260}.

We calculate the rate coefficient for $^1\text{O} + \text{H}_2 \longrightarrow \text{H}_2\text{O}$ at 298 K at the BHandHLYP/aug-cc-pVDZ level of theory to be $7.1 \times 10^{-10} \text{ cm}^3\text{s}^{-1}$, and assume vibrational decay into OH + H, as suggested. This calculated value is a factor of 2 larger than the nearest experimental value.

Quantum Chemistry Data

			H, -1.69423, 0.22604, 0.87812 C, 0.06118, 0.57927, 0.00000 O, 0.06118, -0.58725, 0.00000 H, -0.85649, 1.22238, 0.00000 H, 0.00000, 0.00000, 0.00000 C, -0.28186, 0.33762, 0.00000 O, 0.67158, -0.33299, -0.00000 H, -0.28760, 1.45702, -0.00001 H, -3.39393, -0.81883, -0.00000 H ₂ CO C, 0.00000, -0.52451, 0.00000 H, 0.00000, -1.10548, -0.93804 H, 0.00000, -1.10548, 0.93804 O, 0.00000, 0.66975, 0.00000	-298768.200141	1.51E+32	2	1.00E+00	7.26E+02
4	HCO							
	H							
	TS							
5/32	CO		C, 0.00000, 0.00000, -0.64038 O, 0.00000, 0.00000, 0.48029	-297385.023729	1.43E+32	1	1.00E+00	1.06E+02
	CN		N, 0.00000, 0.00000, 0.53434 C, 0.00000, 0.00000, -0.62339	-243282.319290	1.28E+32	2	1.00E+00	1.06E+02
	TS		C, 1.13871, 0.41518, 0.00000 O, 2.04295, -0.24325, 0.00000 C, -1.16088, -0.01782, 0.00000 N, -2.31580, -0.06260, 0.00000	-540672.179190	3.84E+32	2	2.24E+01	2.35E+04
	NCCO		C, 0.37853, 0.66420, 0.00000 O, -0.21702, 1.66650, 0.00000 C, 0.00000, -0.71311, 0.00000 N, -0.07643, -1.86265, 0.00000	-540810.648060	3.84E+32	2	2.11E+00	1.29E+04
6	CO		C, 0.00000, 0.00000, -0.64038 O, 0.00000, 0.00000, 0.48029	-297385.023729	1.43E+32	1	1.00E+00	1.06E+02
	¹ O		O, 0.00000, 0.00000, 0.00000 C, 0.00000, 0.99997, 0.00000	-196788.921964	6.19E+31	1	1.00E+00	1.00E+00
	TS		O, 0.02096, 2.12000, 0.00000 O, -0.02096, -2.86997, 0.00000	-494175.802924	2.82E+32	1	5.76E+00	5.40E+02
	CO ₂		O, 0.00000, 0.00000, 1.15274 O, 0.00000, 0.00000, -1.15274	-494917.399028	2.82E+32	1	1.07E+00	5.23E+02
7	CO		C, 0.00000, 0.00000, 0.00000 C, 0.00000, 0.00000, -0.64038 O, 0.00000, 0.00000, 0.48029	-297385.023729	1.43E+32	1	1.00E+00	1.06E+02
	¹ CH ₂		C, 0.00000, 0.17399, 0.00000 H, 0.86403, -0.52196, 0.00000 H, -0.86403, -0.52196, 0.00000	-102649.483309	5.08E+31	1	1.00E+00	1.31E+02
	TS		C, 2.47339, -0.00000, -0.19261 H, 2.41166, 0.86347, 0.50078 H, 2.41166, -0.86347, 0.50078 C, -0.77250, 0.00000, 0.11035 O, -1.87858, 0.00000, -0.06351	-400037.72065	2.63E+32	1	2.15E+01	1.84E+04
	CH ₂ CO		C, 0.00000, 1.20512, 0.00000 H, 0.00000, 1.73207, -0.94080 H, 0.00000, 1.73207, 0.94080 C, 0.00000, -0.10497, 0.00000 O, 0.00000, -1.25813, 0.00000	-400388.686988	2.63E+32	1	2.15E+01	1.84E+04
8	CO		C, 0.00000, 0.00000, -0.64038 O, 0.00000, 0.00000, 0.48029	-297385.023729	1.43E+32	1	1.00E+00	1.06E+02
	CH		C, 0.00000, 0.00000, 0.16040 H, 0.00000, 0.00000, -0.96239	-100985.100094	4.54E+31	2	1.00E+00	1.44E+01
	TS		O, 1.82058, -0.05901, 0.00001 C, 0.71145, 0.09535, -0.00002 C, -2.71813, -0.17214, 0.00000 H, -2.52455, 0.93281, 0.00002	-398372.996120	2.54E+32	2	2.18E+01	1.37E+04
	HCCO		O, 1.18704, 0.00714, 0.00000 C, 0.02509, 0.03870, 0.00000 C, -1.25522, -0.13284, 0.00000 H, -2.11561, 0.50772, 0.00000	-398657.883874	2.54E+32	2	1.30E+00	2.38E+03
9/70	CO		C, 0.00000, 0.00000, -0.64038 O, 0.00000, 0.00000, 0.48029	-297385.023729	1.43E+32	1	1.00E+00	1.06E+02

	H	H, 0.00000, 0.00000, 0.00000	-1307.704984	9.79E+29	2	1.00E+00	1.00E+00
	TS	C, 0.11420, 0.54220, 0.00000	-298683.580276	1.51E+32	2	1.20E+00	1.41E+03
		O, 0.11420, -0.58284, 0.00000					
		H, -1.59873, 1.40955, 0.00000					
	HCO	C, 0.06118, 0.57927, 0.00000	-298768.200141	1.51E+32	2	1.00E+00	7.26E+02
		O, 0.06118, -0.58725, 0.00000					
		H, -0.85649, 1.22238, 0.00000					
10	OH	O, 0.00000, 0.00000, 0.10734	-198772.724511	6.78E+31	2	1.00E+00	1.09E+01
		H, 0.00000, 0.00000, -0.85876					
	H ₂ CN	C, -0.50346, 0.00000, 0.00005	-246571.579821	1.43E+32	2	1.02E+00	1.39E+03
		N, 0.73653, 0.00000, -0.00006					
		H, -1.06749, 0.93849, 0.00008					
		H, -1.06748, -0.93850, 0.00008					
	TS	C, -2.37784, 0.00002, 0.00000	-445348.754555	2.92E+32	1	8.34E+01	2.81E+04
		N, -1.13825, -0.00003, -0.00000					
		H, -2.94152, 0.93860, 0.00000					
		H, -2.94161, -0.93850, 0.00000					
		O, 3.23175, 0.00002, -0.00000					
		H, 2.26392, -0.00008, 0.00002					
	H ₂ CNOH	C, 1.12891, 0.03186, 0.00000	-445534.784357	2.92E+32	1	1.26E+00	9.21E+03
		N, 0.00000, -0.52723, 0.00000					
		H, 1.99406, -0.61679, 0.00000					
		H, 1.24226, 1.11291, 0.00000					
		O, -1.02428, 0.39277, 0.00000					
		H, -1.81556, -0.13885, 0.00000					
11	OH	O, 0.00000, 0.00000, 0.10734	-198772.724511	6.78E+31	2	1.00E+00	1.09E+01
		H, 0.00000, 0.00000, -0.85876					
	CN	N, 0.00000, 0.00000, 0.53434	-243282.319290	1.28E+32	2	1.00E+00	1.06E+02
	TS	C, 0.00000, 0.00000, -0.62339	-442062.400452	2.73E+32	1	1.94E+01	1.33E+04
		O, 2.02443, -0.06749, 0.00004					
		H, 2.25767, 0.87068, -0.00016					
		C, -0.83094, -0.23012, -0.00008					
		N, -1.92392, 0.14999, 0.00005					
	HO CN	O, -1.10707, -0.10788, 0.00000	-442526.105760	2.73E+32	1	1.20E+00	3.09E+03
		H, -1.51638, 0.75904, 0.00000					
		C, 0.17972, -0.00835, 0.00000					
		N, 1.32780, 0.02201, 0.00000					
12/37	OH	O, 0.00000, 0.00000, 0.10734	-198772.724511	6.78E+31	2	1.00E+00	1.09E+01
	TS	H, 0.00000, 0.00000, -0.85876	-397549.192985	1.92E+32	1	5.74E+00	7.66E+03
		H, 2.54691, 0.64509, 0.00001					
		O, 1.92094, -0.09102, -0.00000					
		O, -2.09755, 0.01948, -0.00001					
		H, -1.13405, -0.07280, 0.00008					
	H ₂ O ₂	H, -0.77756, 0.90318, 0.46392	-397675.0332	1.92E+32	1	1.18E+00	1.80E+03
		O, 0.00000, 0.70715, -0.05799					
		O, 0.00000, -0.70715, -0.05799					
		H, 0.77756, -0.90318, 0.46392					
13/82	OH	O, 0.00000, 0.00000, 0.10734	-198772.724511	6.78E+31	2	1.00E+00	1.09E+01
	³ O	H, 0.00000, 0.00000, -0.85876					
	TS	O, 0.00000, 0.00000, 0.00000	-197065.919094	6.19E+31	3	1.00E+00	1.00E+00
		O, 0.05549, -1.30535, 0.00000	-395840.349553	1.83E+32	2	1.99E+00	4.59E+03
		H, -0.88787, -1.51445, 0.00000					
		O, 0.05549, 1.49465, 0.00000					
	HO ₂	O, 0.05455, -0.59846, 0.00000	-396037.107149	1.83E+32	2	1.00E+00	1.01E+03
		H, -0.87278, -0.86200, 0.00000					
		O, 0.05455, 0.70621, 0.00000					
14/83	OH	O, 0.00000, 0.00000, 0.10734	-198772.724511	6.78E+31	2	1.00E+00	1.09E+01
	¹ O	H, 0.00000, 0.00000, -0.85876					
	TS	O, 0.00000, 0.00000, 0.00000	-196788.921964	6.19E+31	1	1.00E+00	1.00E+00
		O, 0.05201, -1.95355, 0.00000	-395562.986482	1.83E+32	2	3.93E+00	9.64E+03
		H, -0.83215, -2.34312, 0.00000					
		O, 0.05201, 2.24645, 0.00000					
	HO ₂	O, 0.05455, -0.59846, 0.00000	-396037.107149	1.83E+32	2	1.00E+00	1.01E+03

			H, -0.87278, -0.86200, 0.00000							
15/84	OH	O	O , 0.05455, 0.70621, 0.00000	-198772.724511	6.78E+31	2	1.00E+00	1.09E+01		
		O	O, 0.00000, 0.00000, 0.10734							
	NH	H	H, 0.00000, 0.00000, -0.85876	-144933.050538	5.63E+31	3	1.00E+00	1.24E+01		
	TS	N	N, 0.00000, 0.00000, -0.00325							
		H	H, 0.00000, 0.00000, 1.03180	-343708.426804	1.75E+32	2	5.54E+00	1.91E+03		
		O	O, -2.17408, 0.00399, 0.00000							
		H	H, -1.20704, -0.02598, 0.00000	-343946.299730	1.75E+32	2	1.03E+00	1.59E+03		
		N	N, 2.19591, -0.00793, 0.00000							
		H	H, 3.22830, 0.04955, 0.00000							
	trans-HNOH	O	O, 0.61481, 0.14770, 0.00000							
		H	H, 1.08132, -0.68683, -0.00002	-198772.724511	6.78E+31	2	1.00E+00	1.09E+01		
16	OH	N	N, -0.69487, -0.17685, 0.00000	-104455.380974	5.63E+31	2	1.08E+00	2.53E+02		
		H	H, -1.13566, 0.74315, -0.00002							
	CH ₃	C	O, 0.00000, 0.00000, 0.10734							
		H	H, 0.00000, 0.00000, -0.85876	-303228.966649	1.75E+32	1	2.25E+01	1.89E+04		
		C	C, 0.00000, -0.00018, 0.00042							
		H	H, -0.93570, -0.53955, -0.00085	-2.00791, 0.82878, 0.69215						
		H	H, 0.93580, -0.53939, -0.00085	H, -1.99100, -1.01453, 0.37303						
	TS	H	H, -0.00010, 1.08002, -0.00085	H, -2.01663, 0.18355, -1.06337						
		O	O, 2.09354, 0.00024, -0.00019	H, 1.12603, 0.00353, -0.00297						
	CH ₃ OH	C	C, -0.66089, 0.02058, -0.00000	C, -0.74192, -0.12123, -0.00000	-303559.118023	1.75E+32	1	2.25E+01	1.89E+04	
		H	H, -1.08060, -0.98379, 0.00002	H, -1.01884, 0.54531, 0.89096						
17	OH	H	H, -1.14827, 0.73955, -0.00000	H, -1.01889, 0.54529, -0.89094						
		H	O, 0.00000, 0.34111, 0.00000	O, 0.74192, -0.12123, -0.00000	-198772.724511	6.78E+31	2	1.00E+00	1.09E+01	
	TS	TS	H, 0.86325, -0.09257, 0.00000	H, 0.86325, -2.63628, 0.00000	-1307.704984	9.79E+29	2	1.00E+00	1.00E+00	
		H ₂ O	H, -0.86325, -2.63628, 0.00000	O, 0.00000, 0.00000, 0.11552	-200081.985222	7.40E+31	1	2.35E+00	6.75E+02	
		O	O, 0.00000, 0.00000, 0.11552	H, 0.00000, 0.75819, -0.46207	-200534.424509	7.40E+31	1	1.00E+00	8.42E+01	
18/105	³ O	H	H, 0.00000, 0.00000, -0.75819	H, 0.00000, -0.75819, -0.46207						
	CN	TS	O, 0.00000, 0.00000, 0.00000	O, 0.00798, 2.00597, 0.00000	-197065.919094	6.19E+31	3	1.00E+00	1.00E+00	
		TS	C, 0.00000, 0.00000, -0.62339	C, 0.00000, 0.84844, 0.00000	-243282.319290	1.28E+32	2	1.00E+00	1.06E+02	
		NCO	O, -0.00698, -2.39155, 0.00000	O, -0.00698, -2.39155, 0.00000	-440349.175060	2.63E+32	2	5.74E+00	1.92E+03	
		NCO	N, 0.00000, 0.00000, -1.25802	N, 0.00000, 0.00000, -0.03723	-440893.44121	2.63E+32	2	1.14E+00	5.23E+02	
19	³ O	O	C, 0.00000, 0.00000, 1.12869	O, 0.00000, 0.00000, 1.12869	-197065.919094	6.19E+31	3	1.00E+00	1.00E+00	
	TS	TS	O, 0.00000, 0.00000, 1.68500	O, 0.00000, 0.00000, 1.68500	-394132.721728	1.75E+32	1	1.00E+00	5.58E+02	
	O ₂	O	O, 0.00000, 0.00000, -1.68500	O, 0.00000, 0.00000, 0.59090	-394357.104834	1.75E+32	1	1.00E+00	6.87E+01	
20	³ O	O	O, 0.00000, 0.00000, 0.59090	O, 0.00000, 0.00000, -0.59090	-197065.919094	6.19E+31	3	1.00E+00	1.00E+00	
	⁴ N	N	O, 0.00000, 0.00000, 0.00000	N, 0.00000, 0.00000, 0.088167	-143303.088167	5.07E+31	4	1.00E+00	1.00E+00	
	TS	O	O, 0.00000, 0.00000, 1.73133	O, 0.00000, 0.00000, 1.73133	-340369.447179	1.59E+32	2	1.00E+00	1.26E+03	
		N	N, 0.00000, 0.00000, -1.97867	N, 0.00000, 0.00000, -1.97867						
	NO	N	N, 0.00000, 0.00000, -0.60608	N, 0.00000, 0.00000, -0.60608	-340897.750289	1.59E+32	2	1.00E+00	1.19E+02	
21/110/	³ O	O	O, 0.00000, 0.00000, 0.53032	O, 0.00000, 0.00000, 0.53032	-197065.919094	6.19E+31	3	1.00E+00	1.00E+00	
111	³ CH ₂	C	C, 0.00000, 0.00000, 0.10395	C, 0.00000, 0.00000, 0.10395	-102701.224038	5.08E+31	3	1.01E+00	8.96E+01	

			H, 0.00000, -0.99689, -0.31186					
			H, 0.00000, 0.99689, -0.31186					
		TS	C, -1.75812, 0.00000, -0.10105	-299769.148387	1.59E+32	1	7.92E+00	1.11E+04
			H, -1.88717, -0.99758, 0.29252					
			H, -1.88706, 0.99760, 0.29251					
			O, 1.79037, -0.00000, 0.00266					
		H ₂ CO	C, 0.00000, -0.52451, 0.00000	-300426.644475	1.59E+32	1	1.00E+00	1.39E+03
			H, 0.00000, -1.10548, -0.93804					
			H, 0.00000, -1.10548, 0.93804					
			O, 0.00000, 0.66975, 0.00000					
22/113		³ O	O, 0.00000, 0.00000, 0.00000	-197065.919094	6.19E+31	3	1.00E+00	1.00E+00
		CH	C, 0.00000, 0.00000, 0.16040	-100985.100094	4.54E+31	2	1.00E+00	1.44E+01
		TS	H, 0.00000, 0.00000, -0.96239					
			C, -0.07140, 1.87828, 0.00000	-298053.759583	1.59E+32	2	2.19E+00	6.85E+03
			H, 0.99963, 1.54414, 0.00000					
			O, -0.07140, -1.60172, 0.00000					
		HCO	C, 0.06118, 0.57927, 0.00000	-298768.200141	1.51E+32	2	1.00E+00	7.26E+02
			O, 0.06118, -0.58725, 0.00000					
			H, -0.85649, 1.22238, 0.00000					
23		³ O	O, 0.00000, 0.00000, 0.00000	-197065.919094	6.19E+31	3	1.00E+00	1.00E+00
		H	H, 0.00000, 0.00000, 0.00000	-1307.704984	9.79E+29	2	1.00E+00	1.00E+00
		TS	O, 0.00000, 0.00000, 0.40000	-198374.076468	6.78E+31	2	1.00E+00	1.51E+02
			H, 0.00000, 0.00000, -3.20000					
		OH	O, 0.00000, 0.00000, 0.10734	-198772.724511	6.78E+31	2	1.00E+00	1.09E+01
			H, 0.00000, 0.00000, -0.85876					
24		¹ O	O, 0.00000, 0.00000, 0.00000	-196788.921964	6.19E+31	1	1.00E+00	1.00E+00
		HCN	N, 0.00000, 0.00000, 0.64811	-245122.398339	1.36E+32	1	1.05E+00	1.38E+02
			C, 0.00000, 0.00000, -0.49567					
			H, 0.00000, 0.00000, -1.56273					
		TS	N, 0.00000, -1.06045, 0.00000	-441914.02557	2.73E+32	1	8.34E+00	8.25E+02
			C, 0.02645, -2.20367, 0.00000					
			H, 0.05117, -3.27048, 0.00000					
			O, -0.02623, 2.98946, 0.00000					
		HCNO	N, 0.02185, -0.00027, 0.00000	-442327.940896	2.73E+32	1	1.36E+00	4.47E+01
			C, 1.16967, -0.00244, 0.00000					
			H, 2.23036, 0.01076, 0.00000					
			O, -1.17517, 0.00072, 0.00000					
25/119		¹ O	O, 0.00000, 0.00000, 0.00000	-196788.921964	6.19E+31	1	1.00E+00	1.00E+00
		CN	N, 0.00000, 0.00000, 0.53434	-243282.319290	1.28E+32	2	1.00E+00	1.06E+02
		TS	C, 0.00000, 0.00000, -0.62339					
			N, 0.00966, 2.10501, 0.00000	-440073.39254	2.63E+32	2	2.09E+01	2.19E+03
			C, 0.00000, 0.94749, 0.00000					
			O, -0.00846, -2.55250, 0.00000					
		NCO	N, 0.00000, 0.00000, -1.25802	-440893.44121	2.63E+32	2	1.14E+00	5.23E+02
			C, 0.00000, 0.00000, -0.03723					
			O, 0.00000, 0.00000, 1.12869					
26		¹ O	O, 0.00000, 0.00000, 0.00000	-196788.921964	6.19E+31	1	1.00E+00	1.00E+00
		TS	O, 0.00000, 0.00000, 2.04500	-393578.707096	1.75E+32	1	1.00E+00	8.22E+02
			O, 0.00000, 0.00000, -2.04500					
		O ₂	O, 0.00000, 0.00000, 0.59090	-394357.104834	1.75E+32	1	1.00E+00	6.87E+01
			O, 0.00000, 0.00000, -0.59090					
27/120		¹ O	O, 0.00000, 0.00000, 0.00000	-196788.921964	6.19E+31	1	1.00E+00	1.00E+00
		CH ₄	C, 0.00006, -0.00000, -0.00001	-106174.920693	6.21E+31	1	1.01E+00	4.36E+02
			H, -1.07741, 0.05086, 0.15637					
			H, 0.23679, -0.86565, -0.61803					
			H, 0.33754, 0.90709, -0.50065					
			H, 0.50273, -0.09229, 0.96235					
		TS	O, -0.00883, -0.00036, 0.00001	-302964.255863	1.75E+32	1	3.99E+01	1.88E+04
			C, 0.00176, 0.00007, 4.10000					
			H, 1.08254, -0.00454, 4.23687					
			H, -0.46157, -0.63868, 4.85102					
			H, -0.37408, 1.01698, 4.20726					
			H, -0.24178, -0.37626, 3.10643					

	CH ₃ OH	C, -0.66089, 0.02058, -0.00000 H, -1.08060, -0.98379, 0.00002 H, -1.01884, 0.54531, 0.89096 H, 1.14827, 0.73955, -0.00000 H, -1.01889, 0.54529, -0.89094 O, 0.74192, -0.12123, -0.00000	-303559.118023	1.75E+32	1	2.25E+01	1.89E+04
28/123/ 124	¹ O ¹ CH ₂	O, 0.00000, 0.00000, 0.00000 C, 0.00000, 0.17399, 0.00000 H, 0.86403, -0.52196, 0.00000 H, -0.86403, -0.52196, 0.00000 TS C, -0.00000, -2.12831, 0.00000 H, 0.00001, -2.82181, -0.86541 H, 0.00001, -2.82181, 0.86541 O, -0.00000, 2.30169, 0.00000	-196788.921964 -102649.483309	6.19E+31 5.08E+31	1 1	1.00E+00 1.00E+00	1.00E+00 1.31E+02
	H ₂ CO	C, 0.00000, -0.52451, 0.00000 H, 0.00000, -1.10548, -0.93804 H, 0.00000, -1.10548, 0.93804 O, 0.00000, 0.66975, 0.00000	-300426.644475	1.59E+32	1	1.00E+00	1.39E+03
29/125	¹ O CH	O, 0.00000, 0.00000, 0.00000 C, 0.00000, 0.00000, 0.16040 H, 0.00000, 0.00000, -0.96239 TS C, 0.00040, 2.16520, 0.00000 H, -0.00558, 3.28715, 0.00000 O, 0.00040, -2.03480, 0.00000	-196788.921964 -100985.100094	6.19E+31 4.54E+31	1 2	1.00E+00 1.00E+00	1.00E+00 1.44E+01
	HCO	C, 0.06118, 0.57927, 0.00000 O, 0.06118, -0.58725, 0.00000 H, -0.85649, 1.22238, 0.00000	-298768.200141	1.51E+32	2	1.00E+00	7.26E+02
30/126	¹ O H ₂	O, 0.00000, 0.00000, 0.00000 H, 0.00000, 0.00000, 0.37683 H, 0.00000, 0.00000, -0.37683 TS O, -0.03050, 0.00000, -0.04133 H, -0.07372, 0.00000, 3.22838 H, 0.42785, 0.00000, 2.66290	-196788.921964 -3031.139750	6.19E+31 2.77E+30	1 1	1.00E+00 1.00E+00	1.00E+00 3.52E+00
	H ₂ O	O, 0.00000, 0.00000, 0.11552 H, 0.00000, 0.75819, -0.46207 H, 0.00000, -0.75819, -0.46207	-199821.299327	7.40E+31	1	1.69E+00	3.05E+02
31	¹ O H TS	O, 0.00000, 0.00000, 0.00000 H, 0.00000, 0.00000, 0.00000 O, 0.00000, 0.00000, 0.40111 H, 0.00000, 0.00000, -3.208897	-196788.921964 -1307.704984 -198097.052086	6.19E+31 9.79E+29 6.78E+31	1 2 2	1.00E+00 1.00E+00 1.00E+00	1.00E+00 1.00E+00 1.52E+02
	OH	O, 0.00000, 0.00000, 0.10734 H, 0.00000, 0.00000, -0.85876	-198772.724511	6.78E+31	2	1.00E+00	1.09E+01
34	CO ₂	O, 0.00000, 0.00000, 1.15274 O, 0.00000, 0.00000, -1.15274 C, 0.00000, 0.00000, 0.00000	-494917.399028	2.82E+32	1	1.07E+00	5.23E+02
	² N TS	N, 0.00000, 0.00000, 0.00000 O, -0.86912, -0.18695, 0.00000 O, 0.82054, 1.38960, 0.00000 C, 0.00000, 0.59496, 0.00000 N, 0.05552, -1.88442, 0.00000	-143024.189856 -637970.617821	5.07E+31 4.27E+32	2 2	1.00E+00 1.55E+00	1.00E+00 3.16E+04
35	CO ₂	O, 0.00000, 0.00000, 1.15274 O, 0.00000, 0.00000, -1.15274 C, 0.00000, 0.00000, 0.00000	-494917.399028	2.82E+32	1	1.07E+00	5.23E+02
	¹ CH ₂	C, 0.00000, 0.17399, 0.00000 H, 0.86403, -0.52196, 0.00000 H, -0.86403, -0.52196, 0.00000	-102649.483309	5.08E+31	1	1.00E+00	1.31E+02
	TS	O, -0.18028, 0.00179, 0.13798 O, 0.00273, -0.00097, 2.44510 C, 1.87376, -0.00106, 0.08413 H, 1.89316, 0.87643, -0.57756 H, 1.89070, -0.87713, -0.57949 C, 0.01552, 0.00025, 1.29877	-597572.747704	4.27E+32	1	2.26E+00	3.51E+04
36	CO ₂	O, 0.00000, 0.00000, 1.15274	-494917.399028	2.82E+32	1	1.07E+00	5.23E+02

			O, 0.00000, 0.00000, -1.15274					
		CH	C, 0.00000, 0.00000, 0.00000					
			C, 0.00000, 0.00000, 0.16040	-100985.100094	4.54E+31	2	1.00E+00	1.44E+01
		TS	H, 0.00000, 0.00000, -0.96239	-595888.681116	4.16E+32	2	2.21E+00	2.83E+04
			O, 0.08464, 0.17353, -0.00075					
			O, 0.14479, -0.08889, 2.30201					
			C, 0.30010, 0.02434, 1.16779					
			C, 1.97451, -0.06352, 0.21201					
			H, 2.20906, 0.46573, -0.72551					
38	H ₂ CO		C, 0.00000, -0.52451, 0.00000	-300426.644475	1.59E+32	1	1.00E+00	1.39E+03
			H, 0.00000, -1.10548, -0.93804					
			H, 0.00000, -1.10548, 0.93804					
		CN	O, 0.00000, 0.66975, 0.00000					
			N, 0.00000, 0.00000, 0.53434	-243282.319290	1.28E+32	2	1.00E+00	1.06E+02
		TS	C, 0.00000, 0.00000, -0.62339	-543711.303085	4.06E+32	2	1.64E+02	6.13E+04
			C, -1.59264, 0.42271, 0.00000					
			O, -2.43063, -0.41920, 0.00000					
			H, -1.82790, 1.50034, 0.00000					
			H, -0.50772, 0.16496, 0.00000					
			C, 1.79717, -0.17616, 0.00000					
			N, 2.93621, 0.02986, 0.00000					
39	H ₂ CO		C, 0.00000, -0.52451, 0.00000	-300426.644475	1.59E+32	1	1.00E+00	1.39E+03
			H, 0.00000, -1.10548, -0.93804					
			H, 0.00000, -1.10548, 0.93804					
		OH	O, 0.00000, 0.66975, 0.00000					
			O, 0.00000, 0.00000, 0.10734	-198772.724511	6.78E+31	2	1.00E+00	1.09E+01
		TS	H, 0.00000, 0.00000, -0.85876	-499174.684035	3.12E+32	2	2.07E+00	1.53E+04
			C, -0.47128, 0.58564, 0.03055					
			H, -0.39530, 1.10409, 0.99025					
			H, -0.37939, 1.19869, -0.87035					
			O, -0.98079, -0.54821, -0.03120					
			O, 1.28145, -0.06128, -0.04899					
			H, 1.19707, -0.94064, 0.33831					
40	H ₂ CO		C, 0.00000, -0.52451, 0.00000	-300426.644475	1.59E+32	1	1.00E+00	1.39E+03
			H, 0.00000, -1.10548, -0.93804					
			H, 0.00000, -1.10548, 0.93804					
		OH	O, 0.00000, 0.66975, 0.00000					
			O, 0.00000, 0.00000, 0.10734	-198772.724511	6.78E+31	2	1.00E+00	1.09E+01
		TS(H ₂ CO ··· HO)	H, 0.00000, 0.00000, -0.85876	-499203.669555	3.12E+32	2	1.58E+02	4.45E+04
			C, 2.18732, 0.23648, 0.00000					
			H, 2.20924, 1.33906, -0.00001					
			H, 3.16350, -0.27616, 0.00002					
			O, 1.15885, -0.37226, -0.00001					
			H, -2.25487, -0.16518, 0.00001					
			O, -3.18908, 0.08268, 0.00000					
	H ₂ CO ··· HO		C, 1.50833, 0.32662, 0.00000	-499213.793483	3.12E+32	2	1.98E+01	2.63E+04
			H, 1.23510, 1.39327, -0.00004					
			H, 2.58204, 0.08647, 0.00006					
			O, 0.67771, -0.53625, -0.00001					
			O, -2.13399, 0.13053, 0.00000					
			H, -1.21695, -0.19369, 0.00002					
	TS(H ₂ O + HCO)		C, 0.72110, 0.45885, 0.00000	-499195.617147	3.12E+32	2	8.89E+00	2.45E+04
			H, 1.03115, 1.52036, 0.00000					
			H, -0.42319, 0.30139, -0.00001					
			O, 1.48873, -0.44329, 0.00000					
			O, -1.88081, -0.00753, 0.00000					
			H, -1.79788, -0.96824, 0.00000					
41	H ₂ CO		C, 0.00000, -0.52451, 0.00000	-300426.644475	1.59E+32	1	1.00E+00	1.39E+03
			H, 0.00000, -1.10548, -0.93804					
			H, 0.00000, -1.10548, 0.93804					
		³ O	O, 0.00000, 0.66975, 0.00000					
		TS	O, 0.00000, 0.00000, 0.00000	-197065.919094	6.19E+31	3	1.00E+00	1.00E+00
			C, -0.59392, 0.42546, 0.00000	-497479.543088	3.02E+32	3	2.33E+00	2.04E+04
			H, -0.77716, 1.51734, 0.00000					

			H, 0.60545, 0.13501, 0.00000					
			O, -1.43123, -0.39780, 0.00000					
			O, 1.89813, -0.12784, 0.00000					
42	H ₂ CO	C, 0.00000, -0.52451, 0.00000	-300426.644475	1.59E+32	1	1.00E+00	1.39E+03	
		H, 0.00000, -1.10548, -0.93804						
		H, 0.00000, -1.10548, 0.93804						
		O, 0.00000, 0.66975, 0.00000						
	¹ O	O, 0.00000, 0.00000, 0.00000	-196788.921964	6.19E+31	1	1.00E+00	1.00E+00	
	TS	C, -1.77953, 0.34320, 0.00000	-497218.371475	3.02E+32	1	3.92E+01	4.27E+04	
		H, -1.48268, 1.40545, 0.00000						
		H, -2.86259, 0.13442, -0.00000						
		O, -0.97089, -0.53624, 0.00000						
		O, 2.84870, 0.08636, 0.00000						
43	H ₂ CO	C, 0.00000, -0.52451, 0.00000	-300426.644475	1.59E+32	1	1.00E+00	1.39E+03	
		H, 0.00000, -1.10548, -0.93804						
		H, 0.00000, -1.10548, 0.93804						
		O, 0.00000, 0.66975, 0.00000						
	CH ₃	C, 0.00000, -0.00018, 0.00042	-104455.380974	5.63E+31	2	1.08E+00	2.53E+02	
		H, -0.93570, -0.53955, -0.00085						
		H, 0.93580, -0.53939, -0.00085						
		H, -0.00010, 1.08002, -0.00085						
	TS	C, 0.78646, 0.45348, 0.00000	-404839.859919	2.92E+32	2	2.61E+01	2.82E+04	
		H, 1.07291, 1.52901, 0.00000						
		H, -0.51355, 0.21771, 0.00000						
		O, 1.57243, -0.42799, 0.00000						
		C, -1.89866, -0.09510, 0.00000						
		H, -1.90272, -1.18086, -0.00001						
		H, -2.28144, 0.35391, 0.91205						
		H, -2.28144, 0.35392, -0.91204						
44	H ₂ CO	C, 0.00000, -0.52451, 0.00000	-300426.644475	1.59E+32	1	1.00E+00	1.39E+03	
		H, 0.00000, -1.10548, -0.93804						
		H, 0.00000, -1.10548, 0.93804						
		O, 0.00000, 0.66975, 0.00000						
	³ CH ₂	C, 0.00000, 0.00000, 0.10395	-102701.224038	5.08E+31	3	1.01E+00	8.96E+01	
		H, 0.00000, -0.99689, -0.31186						
		H, 0.00000, 0.99689, -0.31186						
	TS	C, 0.14050, 0.09150, 0.05065	-403114.922172	2.83E+32	3	1.19E+01	2.48E+04	
		O, 0.06828, -0.07800, 1.21819						
		H, 0.89195, -0.40846, -0.59523						
		C, -1.56816, 1.76660, -1.21646						
		H, -0.63273, 0.85440, -0.54742						
		H, -2.29851, 2.25059, -0.58010						
		H, -1.47869, 1.90289, -2.28736						
45	H ₂ CO	C, 0.00000, -0.52451, 0.00000	-300426.644475	1.59E+32	1	1.00E+00	1.39E+03	
		H, 0.00000, -1.10548, -0.93804						
		H, 0.00000, -1.10548, 0.93804						
		O, 0.00000, 0.66975, 0.00000						
	¹ CH ₂	C, 0.00000, 0.17399, 0.00000	-102649.483309	5.08E+31	1	1.00E+00	1.31E+02	
		H, 0.86403, -0.52196, 0.00000						
		H, -0.86403, -0.52196, 0.00000						
	TS	C, -0.68910, 0.48572, -0.08639	-403080.446732	2.83E+32	1	1.22E+01	2.60E+04	
		O, -1.38273, -0.46949, 0.05703						
		H, -0.94950, 1.48003, 0.31230						
		C, 2.03635, -0.06055, -0.09460						
		H, 0.26632, 0.44354, -0.67581						
		H, 1.72584, -1.10952, 0.07940						
		H, 1.93572, 0.39090, 0.91387						
46	H ₂ CO	C, 0.00000, -0.52451, 0.00000	-300426.644475	1.59E+32	1	1.00E+00	1.39E+03	
		H, 0.00000, -1.10548, -0.93804						
		H, 0.00000, -1.10548, 0.93804						
		O, 0.00000, 0.66975, 0.00000						
	CH	C, 0.00000, 0.00000, 0.16040	-100985.100094	4.54E+31	2	1.00E+00	1.44E+01	
		H, 0.00000, 0.00000, -0.96239						

	TS	C, 1.06314, 0.52104, 0.00000 H, 1.80273, 1.34082, 0.00000 H, 0.00007, 0.80950, 0.00000 O, 1.40579, -0.62540, -0.00000 C, -2.65560, 0.06709, -0.00001 H, -3.49440, -0.67583, 0.00003	-401415.141966 2.73E+32 2 3.29E+01 4.06E+04
47	H ₂ CO	C, 0.00000, -0.52451, 0.00000 H, 0.00000, -1.10548, -0.93804 H, 0.00000, -1.10548, 0.93804 O, 0.00000, 0.66975, 0.00000	-300426.644475 1.59E+32 1 1.00E+00 1.39E+03
	CH	C, 0.00000, 0.00000, 0.16040 H, 0.00000, 0.00000, -0.96239	-100985.100094 4.54E+31 2 1.00E+00 1.44E+01
	TS	C, 1.08832, 0.24164, 0.00000 H, 2.10074, -0.17241, 0.00000 H, 0.95325, 1.32808, 0.00000 O, 0.13808, -0.50703, 0.00000 C, -1.57241, 0.05352, 0.00000 H, -1.25410, 1.12959, -0.00000	-401442.155736 2.73E+32 2 3.98E+00 1.17E+04
48	H ₂ CO	C, 0.00000, -0.52451, 0.00000 H, 0.00000, -1.10548, -0.93804 H, 0.00000, -1.10548, 0.93804 O, 0.00000, 0.66975, 0.00000	-300426.644475 1.59E+32 1 1.00E+00 1.39E+03
	H	H, 0.00000, 0.00000, 0.00000	-1307.704984 9.79E+29 2 1.00E+00 1.00E+00
	TS	C, 0.30393, 0.29916, 0.00000 H, 0.44476, 1.39878, 0.00000 H, 1.38940, -0.36012, 0.00000 O, -0.74353, -0.23991, 0.00000 H, 2.29052, -0.91436, 0.00000	-301720.745549 1.67E+32 2 1.41E+00 3.18E+03
49	HCO	C, 0.06118, 0.57927, 0.00000 O, 0.06118, -0.58725, 0.00000 H, -0.85649, 1.22238, 0.00000	-298768.200141 1.51E+32 2 1.00E+00 7.26E+02
	H ₂ CN	C, -0.50346, 0.00000, 0.00005 N, 0.73653, 0.00000, -0.00006 H, -1.06749, 0.93849, 0.00008 H, -1.06748, -0.93850, 0.00008	-246571.579821 1.43E+32 2 1.02E+00 1.39E+03
	TS	C, -1.44215, -0.44322, 0.00000 N, -2.34396, 0.37970, -0.00000 H, -1.57250, -1.52975, 0.00000 H, -0.32410, -0.09039, 0.00000 C, 1.30754, 0.42132, 0.00000 H, 1.35232, 1.53659, 0.00000 O, 2.21995, -0.30537, -0.00000	-545332.454817 4.17E+32 1 4.02E+01 5.76E+04
50	HCO	C, 0.06118, 0.57927, 0.00000 O, 0.06118, -0.58725, 0.00000 H, -0.85649, 1.22238, 0.00000	-298768.200141 1.51E+32 2 1.00E+00 7.26E+02
	TS(trans-C ₂ H ₂ O ₂)	C, 1.44538, -0.41941, -0.00002 O, 2.35078, 0.31649, 0.00001 H, 1.50835, -1.53463, 0.00001 C, -1.44538, 0.41941, 0.00001 O, -2.35078, -0.31649, 0.00000 H, -1.50835, 1.53463, -0.00003	-597543.869830 4.27E+32 1 1.20E+02 6.31E+04
	trans-C ₂ H ₂ O ₂	O, 1.70599, 0.17033, -0.00001 O, -1.70599, -0.17032, -0.00001 C, 0.65011, -0.38894, 0.00001 C, -0.65011, 0.38894, 0.00001 H, 0.54322, -1.48641, 0.00003 H, -0.54322, 1.48641, 0.00003	-597808.108026 4.27E+32 1 2.77E+00 2.48E+04
	TS(anti-HCOH + CO)	O, -1.89257, 0.11748, 0.00000 O, 1.47449, -0.48359, 0.00000 C, -0.81507, -0.24983, 0.00000 C, 1.01515, 0.66227, 0.00000 H, 0.36217, -0.99882, 0.00000 H, 1.78192, 1.45305, 0.00000	-597543.515387 4.27E+32 1 2.64E+00 3.37E+04
51	HCO	C, 0.06118, 0.57927, 0.00000	-298768.200141 1.51E+32 2 1.00E+00 7.26E+02

		O, 0.06118, -0.58725, 0.00000						
		H, -0.85649, 1.22238, 0.00000						
		C, -3.21999, 0.45642, 0.00056	-597252.486589	4.27E+32	1	5.45E+03	2.47E+05	
		O, -3.82943, -0.53056, -0.00062						
		H, -3.64889, 1.50598, 0.00221						
		C, 3.22001, 0.45642, -0.00056						
		O, 3.82941, -0.53056, 0.00061						
		H, 3.64892, 1.50597, -0.00222						
52	HCO	C, 0.06118, 0.57927, 0.00000	-298768.200141	1.51E+32	2	1.00E+00	7.26E+02	
		O, 0.06118, -0.58725, 0.00000						
		H, -0.85649, 1.22238, 0.00000						
	CN	N, 0.00000, 0.00000, 0.53434	-243282.319290	1.28E+32	2	1.00E+00	1.06E+02	
	TS	C, 0.00000, 0.00000, -0.62339	-542054.462932	3.95E+32	1	1.67E+02	7.95E+04	
		C, 1.92935, 0.44928, -0.00000						
		O, 2.65542, -0.45810, 0.00000						
		H, 2.21156, 1.53080, 0.00000						
		C, -2.07362, -0.09641, -0.00000						
		N, -3.22704, 0.00240, 0.00000						
53	HCO	C, 0.06118, 0.57927, 0.00000	-298768.200141	1.51E+32	2	1.00E+00	7.26E+02	
		O, 0.06118, -0.58725, 0.00000						
		H, -0.85649, 1.22238, 0.00000						
	OH	O, 0.00000, 0.00000, 0.10734	-198772.724511	6.78E+31	2	1.00E+00	1.09E+01	
	TS	H, 0.00000, 0.00000, -0.85876	-497546.364688	3.02E+32	1	3.64E+01	3.32E+04	
		C, -0.92930, 0.41679, -0.00001						
		O, -1.76441, -0.39597, 0.00000						
		H, -1.08742, 1.52276, 0.00000						
		O, 2.36403, -0.00313, 0.00000						
		H, 1.86621, -0.83067, -0.00003						
54	HCO	C, 0.06118, 0.57927, 0.00000	-298768.200141	1.51E+32	2	1.00E+00	7.26E+02	
		O, 0.06118, -0.58725, 0.00000						
		H, -0.85649, 1.22238, 0.00000						
	³ O	O, 0.00000, 0.00000, 0.00000	-197065.919094	6.19E+31	3	1.00E+00	1.00E+00	
	TS	C, -0.91822, 0.43888, 0.00063	-495836.418546	2.92E+32	2	8.51E+00	3.46E+04	
		O, -1.68693, -0.43685, -0.00021						
		H, -1.17411, 1.52862, -0.00159						
		O, 2.52236, -0.08339, -0.00006						
55	HCO	C, 0.06118, 0.57927, 0.00000	-298768.200141	1.51E+32	2	1.00E+00	7.26E+02	
		O, 0.06118, -0.58725, 0.00000						
		H, -0.85649, 1.22238, 0.00000						
	³ O	O, 0.00000, 0.00000, 0.00000	-197065.919094	6.19E+31	3	1.00E+00	1.00E+00	
	TS	C, 1.11161, 0.61321, -0.00001	-495837.193069	2.92E+32	2	1.17E+01	3.30E+04	
		O, 1.49004, -0.48723, 0.00000						
		H, 0.03627, 0.94174, 0.00005						
		O, -2.32828, -0.09040, -0.00000						
56	HCO	C, 0.06118, 0.57927, 0.00000	-298768.200141	1.51E+32	2	1.00E+00	7.26E+02	
		O, 0.06118, -0.58725, 0.00000						
		H, -0.85649, 1.22238, 0.00000						
	¹ O	O, 0.00000, 0.00000, 0.00000	-196788.921964	6.19E+31	1	1.00E+00	1.00E+00	
	TS	C, -1.12673, 0.41429, -0.00003	-495559.276017	2.92E+32	2	1.22E+01	4.52E+04	
		O, -1.93331, -0.42516, 0.00001						
		H, -1.32485, 1.51568, 0.00006						
		O, 2.94396, -0.07502, 0.00000						
57	HCO	C, 0.06118, 0.57927, 0.00000	-298768.200141	1.51E+32	2	1.00E+00	7.26E+02	
		O, 0.06118, -0.58725, 0.00000						
		H, -0.85649, 1.22238, 0.00000						
		O, 0.00000, 0.00000, 0.00000						
		H, -1.12673, 0.41429, -0.00003						
		O, -1.93331, -0.42516, 0.00001						
		H, -1.32485, 1.51568, 0.00006						
		O, 2.94396, -0.07502, 0.00000						
		C, 0.06118, 0.57927, 0.00000						
		O, 0.06118, -0.58725, 0.00000						
		H, -0.85649, 1.22238, 0.00000						
	NH	N, 0.00000, 0.00000, -0.00325	-144933.050538	5.63E+31	3	1.00E+00	1.24E+01	
	TS	H, 0.00000, 0.00000, 1.03180	-443659.565616	2.83E+32	4	2.37E+00	2.00E+04	
		C, -0.54840, 0.43585, 0.00000						
		O, -1.36093, -0.41218, 0.00000						
		H, -0.77366, 1.52479, 0.00000						
		N, 2.02120, -0.14040, 0.00000						
		H, 0.80313, 0.14032, 0.00000						
58	HCO	C, 0.06118, 0.57927, 0.00000	-298768.200141	1.51E+32	2	1.00E+00	7.26E+02	

		O, 0.06118, -0.58725, 0.00000						
		H, -0.85649, 1.22238, 0.00000						
	NH	N, 0.00000, 0.00000, -0.00325	-144933.050538	5.63E+31	3	1.00E+00	1.24E+01	
		H, 0.00000, 0.00000, 1.03180						
	TS(CO + NH ₂)	C, 1.00716, -0.60363, 0.00000	-443708.520689	2.83E+32	2	2.37E+01	3.02E+04	
		O, 1.51647, 0.44434, 0.00000						
		H, -0.10268, -0.79887, -0.00000						
		N, -2.27732, -0.01975, 0.00000						
		H, -2.13079, 1.00422, 0.00000						
	TS(HNHCO)	C, 0.79683, 0.38808, -0.00001	-443705.666770	2.83E+32	2	3.91E+01	2.95E+04	
		O, 1.68245, -0.37024, 0.00001						
		H, 0.88661, 1.50171, 0.00001						
		N, -2.43159, 0.01415, 0.00001						
		H, -2.10606, -0.96738, -0.00005						
59	HCO	C, 0.06118, 0.57927, 0.00000	-298768.200141	1.51E+32	2	1.00E+00	7.26E+02	
		O, 0.06118, -0.58725, 0.00000						
		H, -0.85649, 1.22238, 0.00000						
	⁴ N	N, 0.00000, 0.00000, 0.00000	-143303.088167	5.07E+31	4	1.00E+00	1.00E+00	
	TS	C, -0.72905, 0.41600, 0.00000	-442073.879138	2.73E+32	3	8.67E+00	2.84E+04	
		O, -1.55200, -0.40943, -0.00000						
		H, -0.91590, 1.51955, -0.00001						
		N, 2.52945, -0.10573, 0.00000						
60	HCO	C, 0.06118, 0.57927, 0.00000	-298768.200141	1.51E+32	2	1.00E+00	7.26E+02	
		O, 0.06118, -0.58725, 0.00000						
		H, -0.85649, 1.22238, 0.00000						
	⁴ N	N, 0.00000, 0.00000, 0.00000	-143303.088167	5.07E+31	4	1.00E+00	1.00E+00	
	TS	C, -0.96022, 0.53343, -0.00000	-442073.275273	2.73E+32	3	6.16E+00	3.08E+04	
		O, -1.70117, -0.36597, 0.00000						
		H, 0.16249, 0.44888, 0.00001						
		N, 2.74403, -0.10310, -0.00000						
61	HCO	C, 0.06118, 0.57927, 0.00000	-298768.200141	1.51E+32	2	1.00E+00	7.26E+02	
		O, 0.06118, -0.58725, 0.00000						
		H, -0.85649, 1.22238, 0.00000						
	² N	N, 0.00000, 0.00000, 0.00000	-143024.189856	5.07E+31	2	1.00E+00	1.00E+00	
	TS	C, -0.78848, 0.42135, 0.00001	-441966.299275	2.73E+32	3	9.33E+00	3.12E+04	
		O, -1.59612, -0.41902, -0.00000						
		H, -0.99546, 1.52140, -0.00001						
		N, 2.64219, -0.09962, -0.00000						
62	HCO	C, 0.06118, 0.57927, 0.00000	-298768.200141	1.51E+32	2	1.00E+00	7.26E+02	
		O, 0.06118, -0.58725, 0.00000						
		H, -0.85649, 1.22238, 0.00000						
	² N	N, 0.00000, 0.00000, 0.00000	-143024.189856	5.07E+31	2	1.00E+00	1.00E+00	
	TS	C, -1.02091, 0.53057, 0.00000	-441965.902825	2.73E+32	3	6.31E+00	3.35E+04	
		O, -1.76359, -0.36744, 0.00000						
		H, 0.10155, 0.44424, 0.00000						
		N, 2.87609, -0.09831, 0.00000						
63	HCO	C, 0.06118, 0.57927, 0.00000	-298768.200141	1.51E+32	2	1.00E+00	7.26E+02	
		O, 0.06118, -0.58725, 0.00000						
		H, -0.85649, 1.22238, 0.00000						
	CH ₃	C, 0.00000, -0.00018, 0.00042	-104455.380974	5.63E+31	2	1.08E+00	2.53E+02	
		H, -0.93570, -0.53955, -0.00085						
		H, 0.93580, -0.53939, -0.00085						
		H, -0.00010, 1.08002, -0.00085						
	TS	C, -1.18076, 0.58286, 0.00000	-403229.239068	2.83E+32	1	1.63E+02	3.94E+04	
		O, -1.80285, -0.40268, 0.00000						
		H, -0.05231, 0.63844, 0.00000						
		C, 2.37921, -0.09594, 0.00000						
		H, 2.60699, 0.39621, -0.93455						
		H, 2.07031, -1.13118, 0.00011						
		H, 2.60705, 0.39639, 0.93444						
64	HCO	C, 0.06118, 0.57927, 0.00000	-298768.200141	1.51E+32	2	1.00E+00	7.26E+02	
		O, 0.06118, -0.58725, 0.00000						
		H, -0.85649, 1.22238, 0.00000						

	³ CH ₂	C, 0.00000, 0.00000, 0.10395 H, 0.00000, -0.99689, -0.31186 H, 0.00000, 0.99689, -0.31186	-102701.224038	5.08E+31	3	1.01E+00	8.96E+01
	TS(CH ₃ + CO)	C, 1.18089, -0.58830, 0.00001 O, 1.76377, 0.42079, -0.00000 H, 0.06058, -0.69428, -0.00001 C, -2.55962, 0.07216, 0.00000 H, -3.28708, -0.72572, -0.00001 H, -2.61129, 1.15053, 0.00001	-401475.384064	2.73E+32	2	1.46E+02	3.90E+04
	TS(CH ₂ HCO)	C, 0.88495, 0.42556, -0.00000 O, 1.70057, -0.40713, 0.00000 H, 1.07614, 1.52704, -0.00000 C, -2.39692, -0.07616, 0.00000 H, -2.55118, -1.14473, -0.00000 H, -3.05762, 0.77835, 0.00001	-401473.748377	2.73E+32	2	1.12E+02	3.36E+04
65	HCO	C, 0.06118, 0.57927, 0.00000 O, 0.06118, -0.58725, 0.00000 H, -0.85649, 1.22238, 0.00000	-298768.200141	1.51E+32	2	1.00E+00	7.26E+02
	¹ CH ₂	C, 0.00000, 0.17399, 0.00000 H, 0.86403, -0.52196, 0.00000 H, -0.86403, -0.52196, 0.00000	-102649.483309	5.08E+31	1	1.00E+00	1.31E+02
	TS	C, -0.82757, 0.32128, 0.00001 O, -1.79760, -0.32405, 0.00001 H, -0.77593, 1.43708, -0.00008 C, 2.51354, 0.07736, -0.00003 H, 2.52039, -0.61837, -0.86354 H, 2.52045, -0.61811, 0.86370	-401422.503868	2.73E+32	2	8.57E+01	3.13E+04
66	HCO	C, 0.06118, 0.57927, 0.00000 O, 0.06118, -0.58725, 0.00000 H, -0.85649, 1.22238, 0.00000	-298768.200141	1.51E+32	2	1.00E+00	7.26E+02
	CH	C, 0.00000, 0.00000, 0.16040 H, 0.00000, 0.00000, -0.96239	-100985.100094	4.54E+31	2	1.00E+00	1.44E+01
	TS	C, -1.00243, 0.52281, 0.00000 O, -1.75206, -0.37324, 0.00000 H, 0.11410, 0.43659, -0.00002 C, 2.70696, -0.00384, -0.00000 H, 3.67526, -0.56446, 0.00001	-399758.934558	2.63E+32	3	2.76E+01	3.09E+04
67	HCO	C, 0.06118, 0.57927, 0.00000 O, 0.06118, -0.58725, 0.00000 H, -0.85649, 1.22238, 0.00000	-298768.200141	1.51E+32	2	1.00E+00	7.26E+02
	CH	C, 0.00000, 0.00000, 0.16040 H, 0.00000, 0.00000, -0.96239	-100985.100094	4.54E+31	2	1.00E+00	1.44E+01
	TS	C, 0.95316, -0.57236, -0.06467 O, 1.55803, 0.41893, 0.04383 H, -0.17127, -0.65680, -0.06725 C, -2.54630, -0.03468, 0.08692 H, -2.73409, 0.94753, -0.41695	-399761.111098	2.63E+32	1	2.66E+01	3.08E+04
68/69	HCO	C, 0.06118, 0.57927, 0.00000 O, 0.06118, -0.58725, 0.00000 H, -0.85649, 1.22238, 0.00000	-298768.200141	1.51E+32	2	1.00E+00	7.26E+02
	H	H, 0.00000, 0.00000, 0.00000	-1307.704984	9.79E+29	2	1.00E+00	1.00E+00
	TS(CO + H ₂)	C, 0.10339, -0.52516, -0.00001 O, -0.66721, 0.34873, 0.00000 H, 1.22122, -0.40653, 0.00005 H, 3.49608, 0.76762, -0.00001	-300077.962322	1.59E+32	1	4.64E+00	4.25E+03
	TS(H ₂ CO)	C, -0.28186, 0.33762, 0.00000 O, 0.67158, -0.33299, -0.00000 H, -0.28760, 1.45702, -0.00001 H, -3.39393, -0.81883, -0.00000	-300077.773286	1.59E+32	1	5.26E+00	4.04E+03
71	CO	C, 0.00000, 0.00000, -0.64038 O, 0.00000, 0.00000, 0.48029	-297385.023729	1.43E+32	1	1.00E+00	1.06E+02
	OH	O, 0.00000, 0.00000, 0.10734 H, 0.00000, 0.00000, -0.85876	-198772.724511	6.78E+31	2	1.00E+00	1.09E+01
	TS	O, 0.00000, 0.00000, 2.70789	-496160.381617	2.92E+32	2	2.35E+01	2.55E+03

			H, 0.00000, 0.00000, 1.73998					
			C, 0.00000, 0.00000, -1.03211					
			O, 0.00000, 0.00000, -2.15130					
72	H ₂ O		O, 0.00000, 0.00000, 0.11552	-200534.424509	7.40E+31	1	1.00E+00	8.42E+01
			H, 0.00000, 0.75819, -0.46207					
			H, 0.00000, -0.75819, -0.46207					
	¹ O		O, 0.00000, 0.00000, 0.00000	-196788.921964	6.19E+31	1	1.00E+00	1.00E+00
	TS		H, -1.88062, 0.75858, 0.39238	-397326.729119	1.92E+32	1	6.89E+00	1.12E+04
			O, -1.58903, -0.00000, -0.10594					
			H, -1.88068, -0.75855, 0.39240					
			O, 2.05919, -0.00000, 0.00784					
73	H ₂ O		O, 0.00000, 0.00000, 0.11552	-200534.424509	7.40E+31	1	1.00E+00	8.42E+01
			H, 0.00000, 0.75819, -0.46207					
			H, 0.00000, -0.75819, -0.46207					
	CN		N, 0.00000, 0.00000, 0.53434	-243282.319290	1.28E+32	2	1.00E+00	1.06E+02
	TS(H ₂ OCN)		C, 0.00000, 0.00000, -0.62339					
			O, 2.08577, 0.00000, -0.06154	-443824.893350	2.83E+32	2	9.43E+01	1.73E+04
			H, 2.49878, -0.75915, 0.34133					
			H, 2.49878, 0.75915, 0.34133					
			C, -1.06261, 0.00000, -0.16237					
			N, -2.18687, 0.00000, 0.11198					
	H ₂ OCN		O, 1.54613, 0.01966, 0.06013	-443834.360904	2.83E+32	2	2.57E+01	1.35E+04
			H, 1.66854, 0.07098, -0.88769					
			H, 1.48124, -0.91327, 0.26476					
			C, -0.65504, 0.35401, 0.09666					
			N, -1.65551, -0.20558, -0.06257					
	TS(OH + HCN)		N, 1.75725, 0.08450, -0.04306	-443802.027871	2.83E+32	2	6.63E+00	9.16E+03
			C, 0.62537, -0.11926, 0.05446					
			H, -0.82101, -0.40068, 0.33516					
			O, -1.68801, -0.04415, -0.06984					
			H, -1.72792, 0.87798, 0.19825					
74	H ₂ O		O, 0.00000, 0.00000, 0.11552	-200534.424509	7.40E+31	1	1.00E+00	8.42E+01
			H, 0.00000, 0.75819, -0.46207					
			H, 0.00000, -0.75819, -0.46207					
	² N		N, 0.00000, 0.00000, 0.00000	-143024.189856	5.07E+31	2	1.00E+00	1.00E+00
	TS		O, 1.09981, 0.00000, -0.11558	-343579.105176	1.75E+32	2	4.61E+00	6.00E+03
			H, 1.26171, 0.76121, 0.43633					
			H, 1.26170, -0.76122, 0.43633					
			N, -1.61741, 0.00000, 0.00743					
75	H ₂ O		O, 0.00000, 0.00000, 0.11552	-200534.424509	7.40E+31	1	1.00E+00	8.42E+01
			H, 0.00000, 0.75819, -0.46207					
			H, 0.00000, -0.75819, -0.46207					
	CH		C, 0.00000, 0.00000, 0.16040	-100985.100094	4.54E+31	2	1.00E+00	1.44E+01
	TS		H, 0.00000, 0.00000, -0.96239					
			O, -0.00000, -1.50496, 0.00000	-301522.701458	1.67E+32	2	3.93E+01	9.93E+03
			H, -0.00001, -2.08192, -0.75874					
			H, -0.00001, -2.08192, 0.75874					
			C, -0.00000, 2.47505, 0.00000					
			H, 0.00006, 1.35321, 0.00000					
76/92	H ₂ O		O, 0.00000, 0.00000, 0.11552	-200534.424509	7.40E+31	1	1.00E+00	8.42E+01
			H, 0.00000, 0.75819, -0.46207					
			H, 0.00000, -0.75819, -0.46207					
	CH		C, 0.00000, 0.00000, 0.16040	-100985.100094	4.54E+31	2	1.00E+00	1.44E+01
	TS		H, 0.00000, 0.00000, -0.96239					
			O, -0.71798, 0.12903, -0.06268	-301498.502225	1.67E+32	2	1.32E+00	2.82E+03
			H, -0.02388, -0.65891, -0.55561					
			H, -1.11251, -0.35890, 0.66244					
			C, 0.92714, -0.14736, 0.06666					
			H, 1.31739, 0.86979, -0.00541					
	OH		O, 0.00000, 0.00000, 0.10734	-198772.724511	6.78E+31	2	1.00E+00	1.09E+01
			H, 0.00000, 0.00000, -0.85876					
	³ CH ₂		C, 0.00000, 0.00000, 0.10395	-102701.224038	5.08E+31	3	1.01E+00	8.96E+01
			H, 0.00000, -0.99689, -0.31186					

			H, 0.00000, 0.99689, -0.31186					
77	OH		O, 0.00000, 0.00000, 0.10734	-198772.724511	6.78E+31	2	1.00E+00	1.09E+01
			H, 0.00000, 0.00000, -0.85876					
	HCN		N, 0.00000, 0.00000, 0.64811	-245122.398339	1.36E+32	1	1.05E+00	1.38E+02
			C, 0.00000, 0.00000, -0.49567					
	TS		H, 0.00000, 0.00000, -1.56273					
			N, 1.18289, -0.45813, 0.00000	-443875.717780	2.83E+32	2	1.87E+00	1.34E+04
			C, 0.53038, 0.50741, 0.00000					
			H, 0.29374, 1.55076, 0.00000					
			O, -1.31803, -0.04783, 0.00000					
			H, -1.21204, -1.00567, -0.00000					
78	OH		O, 0.00000, 0.00000, 0.10734	-198772.724511	6.78E+31	2	1.00E+00	1.09E+01
			H, 0.00000, 0.00000, -0.85876					
	CN		N, 0.00000, 0.00000, 0.53434	-243282.319290	1.28E+32	2	1.00E+00	1.06E+02
			C, 0.00000, 0.00000, -0.62339					
	TS(HO···CN)		C, -2.32702, -0.06687, 0.00000	-442060.005996	2.73E+32	3	5.33E+01	1.75E+04
			N, -2.73556, 0.80898, -0.00001					
			O, 1.05860, -0.23905, -0.00000					
			H, 2.14288, 0.16576, 0.00000					
	HO···CN		C, -0.57866, -0.37506, 0.00000	-442071.736730	2.73E+32	3	1.19E+01	1.16E+04
			N, -1.57329, 0.21644, 0.00000					
			O, 1.62266, -0.02542, 0.00000					
			H, 1.50373, 0.93862, 0.00000					
	TS(³ HO ₁ CN ₁)		O, 1.31726, -0.06057, -0.11557	-442065.795223	-4.42E+05	3	1.87E+00	1.06E+04
			H, 1.41697, -0.47382, 0.75883					
			C, -0.47337, 0.51436, 0.07208					
			N, -1.30212, -0.30396, -0.03811					
	³ HO ₁ CN ₁		O, 1.00788, -0.18867, -0.07300	-442201.236892	2.73E+32	3	1.38E+00	6.50E+03
			H, 1.59896, 0.17125, 0.59267					
			C, -0.15259, 0.44358, -0.05620					
			N, -1.24949, -0.18905, 0.04693					
	TS(³ HO ₁ CN ₂)		O, 1.07076, -0.23701, 0.00000	-442054.894147	2.73E+32	3	1.47E+00	6.08E+03
			H, 1.04987, 0.95445, -0.00000					
			C, -0.10294, 0.31551, 0.00000					
			N, -1.28547, -0.13592, 0.00000					
79	OH		O, 0.00000, 0.00000, 0.10734	-198772.724511	6.78E+31	2	1.00E+00	1.09E+01
			H, 0.00000, 0.00000, -0.85876					
	CN		N, 0.00000, 0.00000, 0.53434	-243282.319290	1.28E+32	2	1.00E+00	1.06E+02
			C, 0.00000, 0.00000, -0.62339					
	TS		O, 1.77507, -0.07477, 0.00000	-442050.029096	2.73E+32	3	4.92E+00	5.45E+03
			H, 0.93798, 0.53268, 0.00000					
			C, -0.54988, 0.09824, 0.00000					
			N, -1.69132, -0.07485, 0.00000					
80	OH		O, 0.00000, 0.00000, 0.10734	-198772.724511	6.78E+31	2	1.00E+00	1.09E+01
			H, 0.00000, 0.00000, -0.85876					
	CN		N, 0.00000, 0.00000, 0.53434	-243282.319290	1.28E+32	2	1.00E+00	1.06E+02
			C, 0.00000, 0.00000, -0.62339					
	TS		O, -1.47228, -0.16710, 0.00000	-442023.178107	2.73E+32	3	5.20E+00	1.32E+04
			H, -0.76057, 0.60968, 0.00000					
			N, 0.63490, 0.49714, 0.00000					
			C, 1.34908, -0.45881, 0.00000					
81	OH		O, 0.00000, 0.00000, 0.10734	-198772.724511	6.78E+31	2	1.00E+00	1.09E+01
			H, 0.00000, 0.00000, -0.85876					
	TS		H, 1.14564, -0.83725, -0.00002	-397324.930652	1.92E+32	3	2.29E+00	6.78E+03
			O, 1.44781, 0.08292, 0.00000					
			O, -1.44744, -0.08304, 0.00000					
			H, -1.14860, 0.83818, -0.00002					
85	OH		O, 0.00000, 0.00000, 0.10734	-198772.724511	6.78E+31	2	1.00E+00	1.09E+01
			H, 0.00000, 0.00000, -0.85876					
	NH		N, 0.00000, 0.00000, -0.00325	-144933.050538	5.63E+31	3	1.00E+00	1.24E+01
			H, 0.00000, 0.00000, 1.03180					
	TS		O, 0.05070, -1.15122, 0.00000	-343699.917559	1.75E+32	4	1.36E+00	3.77E+03
			H, -0.90707, -1.27429, 0.00000					

			N, 0.05070, 1.44403, 0.00000					
86	OH		H, 0.14658, 0.37578, 0.00000					
		O, 0.00000, 0.00000, 0.10734	-198772.724511	6.78E+31	2	1.00E+00	1.09E+01	
		H, 0.00000, 0.00000, -0.85876						
	⁴ N	N, 0.00000, 0.00000, 0.00000	-143303.088167	5.07E+31	4	1.00E+00	1.00E+00	
	TS	N, 0.00000, 0.00000, 2.12773	-342075.455071	1.67E+32	3	7.93E+00	1.40E+03	
		O, 0.00000, 0.00000, -1.76227						
		H, 0.00000, 0.00000, -0.79594						
87	OH	O, 0.00000, 0.00000, 0.10734	-198772.724511	6.78E+31	2	1.00E+00	1.09E+01	
		H, 0.00000, 0.00000, -0.85876						
	² N	N, 0.00000, 0.00000, 0.00000	-143024.189856	5.07E+31	2	1.00E+00	1.00E+00	
	TS	N, 0.00000, 0.00000, 2.47080	-341799.071312	1.67E+32	3	3.84E+00	1.87E+03	
		O, 0.00000, 0.00000, -2.02920						
		H, 0.00000, 0.00000, -1.06200						
88	OH	O, 0.00000, 0.00000, 0.10734	-198772.724511	6.78E+31	2	1.00E+00	1.09E+01	
		H, 0.00000, 0.00000, -0.85876						
	CH ₄	C, 0.00006, -0.00000, -0.00001	-106174.920693	6.21E+31	1	1.01E+00	4.36E+02	
		H, -1.07741, 0.05086, 0.15637						
		H, 0.23679, -0.86565, -0.61803						
		H, 0.33754, 0.90709, -0.50065						
		H, 0.50273, -0.09229, 0.96235						
	TS	C, -1.21215, -0.01020, 0.00000	-304916.333491	1.84E+32	2	5.67E+00	8.57E+03	
		H, -1.46698, -0.54700, 0.90908						
		H, -1.46698, -0.54699, -0.90909						
		H, -1.55136, 1.02213, 0.00001						
		H, 0.02596, 0.10426, 0.00000						
		O, 1.28596, 0.10848, 0.00000						
		H, 1.44458, -0.83906, 0.00000						
89/108	OH	O, 0.00000, 0.00000, 0.10734	-198772.724511	6.78E+31	2	1.00E+00	1.09E+01	
		H, 0.00000, 0.00000, -0.85876						
	CH ₃	C, 0.00000, -0.00018, 0.00042	-104455.380974	5.63E+31	2	1.08E+00	2.53E+02	
		H, -0.93570, -0.53955, -0.00085						
		H, 0.93580, -0.53939, -0.00085						
		H, -0.00010, 1.08002, -0.00085						
	TS	O, -0.00007, -0.00013, -0.00044	-303192.942164	1.75E+32	3	1.47E+00	7.34E+03	
		C, -0.00002, -0.00004, 2.50190						
		H, 1.05722, -0.00003, 2.74763						
		H, -0.53051, -0.90983, 2.76246						
		H, -0.52076, 0.92007, 2.74764						
		H, -0.00299, -0.00512, 1.18955						
	³ O	O, 0.00000, 0.00000, 0.00000	-197065.919094	6.19E+31	3	1.00E+00	1.00E+00	
	CH ₄	C, 0.00006, -0.00000, -0.00001	-106174.920693	6.21E+31	1	1.01E+00	4.36E+02	
		H, -1.07741, 0.05086, 0.15637						
		H, 0.23679, -0.86565, -0.61803						
		H, 0.33754, 0.90709, -0.50065						
		H, 0.50273, -0.09229, 0.96235						
90	OH	O, 0.00000, 0.00000, 0.10734	-198772.724511	6.78E+31	2	1.00E+00	1.09E+01	
		H, 0.00000, 0.00000, -0.85876						
	CH ₃	C, 0.00000, -0.00018, 0.00042	-104455.380974	5.63E+31	2	1.08E+00	2.53E+02	
		H, -0.93570, -0.53955, -0.00085						
		H, 0.93580, -0.53939, -0.00085						
		H, -0.00010, 1.08002, -0.00085						
	TS	O, 1.20499, 0.00000, -0.10296	-303191.306477	1.75E+32	3	3.53E+00	6.49E+03	
		H, 1.34393, -0.00000, 0.84773						
		H, -0.00448, 0.00000, -0.13864						
		C, -1.25104, 0.00000, 0.01772						
		H, -1.73656, 0.96513, 0.00413						
		H, -1.73656, -0.96513, 0.00413						
91	OH	O, 0.00000, 0.00000, 0.10734	-198772.724511	6.78E+31	2	1.00E+00	1.09E+01	
		H, 0.00000, 0.00000, -0.85876						
	³ CH ₂	C, 0.00000, 0.00000, 0.10395	-102701.224038	5.08E+31	3	1.01E+00	8.96E+01	
		H, 0.00000, -0.99689, -0.31186						
		H, 0.00000, 0.99689, -0.31186						

	TS	C, -1.96653, -0.00000, -0.07282 H, -2.26898, 0.99852, 0.20670 H, -2.26889, -0.99855, 0.20669 O, 1.92265, -0.00000, 0.00728 H, 0.95586, 0.00006, -0.03469	-301475.536976	1.67E+32	2	1.71E+01	1.32E+04
93	OH	O, 0.00000, 0.00000, 0.10734 H, 0.00000, 0.00000, -0.85876	-198772.724511	6.78E+31	2	1.00E+00	1.09E+01
	¹ CH ₂	C, 0.00000, 0.17399, 0.00000 H, 0.86403, -0.52196, 0.00000 H, -0.86403, -0.52196, 0.00000	-102649.483309	5.08E+31	1	1.00E+00	1.31E+02
	TS	C, -2.44506, 0.00000, 0.00000 H, -3.13818, -0.86525, -0.00001 H, -3.13818, 0.86525, -0.00001 O, 2.43494, 0.00000, -0.00000 H, 1.46726, -0.00000, 0.00001	-301424.906834	1.67E+32	2	1.24E+01	1.77E+04
94	OH	O, 0.00000, 0.00000, 0.10734 H, 0.00000, 0.00000, -0.85876	-198772.724511	6.78E+31	2	1.00E+00	1.09E+01
	CH	C, 0.00000, 0.00000, 0.16040 H, 0.00000, 0.00000, -0.96239	-100985.100094	4.54E+31	2	1.00E+00	1.44E+01
	TS	C, 0.00000, 0.00000, 2.37260 H, 0.00000, 0.00000, 3.49322 O, 0.00000, 0.00000, -2.07740 H, 0.00000, 0.00000, -1.10959	-299760.379217	1.59E+32	3	1.14E+01	1.84E+03
95/96	OH	O, 0.00000, 0.00000, 0.10734 H, 0.00000, 0.00000, -0.85876	-198772.724511	6.78E+31	2	1.00E+00	1.09E+01
	CH	C, 0.00000, 0.00000, 0.16040 H, 0.00000, 0.00000, -0.96239	-100985.100094	4.54E+31	2	1.00E+00	1.44E+01
	TS	O, 1.29353, 0.10161, -0.00059 H, 1.07320, -0.83833, 0.00525 C, -1.61513, -0.15543, -0.00081 H, -1.73068, 0.95803, 0.00430	-299772.178214	1.59E+32	1	3.59E+00	6.81E+03
97	OH	O, 0.00000, 0.00000, 0.10734 H, 0.00000, 0.00000, -0.85876	-198772.724511	6.78E+31	2	1.00E+00	1.09E+01
	H ₂	H, 0.00000, 0.00000, 0.37683 H, 0.00000, 0.00000, -0.37683	-3031.139750	2.77E+30	1	1.00E+00	3.52E+00
	TS	O, 0.30315, -0.10744, 0.00000 H, 0.44412, 0.84567, 0.00000 H, -1.03684, -0.11258, 0.00000 H, -1.83251, 0.12645, 0.00000	-201777.115667	8.02E+31	2	1.16E+00	4.52E+02
98/115	OH	O, 0.00000, 0.00000, 0.10734 H, 0.00000, 0.00000, -0.85876	-198772.724511	6.78E+31	2	1.00E+00	1.09E+01
	H	H, 0.00000, 0.00000, 0.00000	-1307.704984	9.79E+29	2	1.00E+00	1.00E+00
	TS	O, -0.00007, 0.00000, 0.00695 H, 0.00016, 0.00000, 1.21695 H, 0.00032, 0.00000, 2.11574	-200053.453913	7.40E+31	3	1.10E+00	6.56E+01
	³ O	O, 0.00000, 0.00000, 0.00000	-197065.919094	6.19E+31	3	1.00E+00	1.00E+00
	H ₂	H, 0.00000, 0.00000, 0.37683 H, 0.00000, 0.00000, -0.37683	-3031.139750	2.77E+30	1	1.00E+00	3.52E+00
99/100/ 101	³ O	O, 0.00000, 0.00000, 0.00000	-197065.919094	6.19E+31	3	1.00E+00	1.00E+00
	H ₂ CN	C, -0.50346, 0.00000, 0.00005 N, 0.73653, 0.00000, -0.00006 H, -1.06749, 0.93849, 0.00008 H, -1.06748, -0.93850, 0.00008	-246571.579821	1.43E+32	2	1.02E+00	1.39E+03
	TS(CH ₂ NO)	C, -1.17076, 0.51441, 0.00000 N, -1.43659, -0.69718, 0.00000 H, -1.96887, 1.26430, -0.00004 H, -0.13238, 0.86080, 0.00004 O, 2.39774, -0.04141, -0.00000	-443639.120847	2.83E+32	2	8.34E+00	3.93E+04
	CH ₂ NO	C, -1.10868, 0.12008, 0.00000 N, 0.06743, -0.35642, 0.00000 H, -1.92868, -0.58030, 0.00000 H, -1.27043, 1.19243, 0.00000 O, 1.17239, 0.14529, 0.00000	-443897.716844	2.83E+32	2	1.18E+00	6.75E+03

	TS(HCNO + H)	C, -1.01152, 0.43493, 0.00000 N, 0.00000, -0.12833, 0.00000 H, -2.06888, 0.55214, 0.00000 H, -0.60205, 2.58631, 0.00000 O, 1.09251, -0.60621, 0.00000 HCNO N, 0.02185, -0.00027, 0.00000 C, 1.16967, -0.00244, 0.00000 H, 2.23036, 0.01076, 0.00000 O, -1.17517, 0.00072, 0.00000 H, 0.00000, 0.00000, 0.00000 TS(HCNOH) C, 0.01434, -0.00045, 0.00190 N, 0.00003, 0.00007, 1.24192 H, 1.35095, 0.00005, 0.03246 H, -0.76839, -0.00108, -0.74539 O, 1.46065, 0.00063, 1.28767 HCNOH C, 1.13711, 0.29236, 0.00000 N, 0.15491, -0.44299, 0.00000 H, 2.17692, -0.01488, 0.00000 H, -1.07487, 1.00421, -0.00000 O, -1.12614, 0.04468, 0.00000 TS(HCN + OH) C, 0.03328, 0.00008, 0.03546 N, 0.00597, 0.00012, 1.22817 H, 0.70873, -0.00010, -0.80034 O, -1.48608, 0.00048, 1.88445 H, -2.05048, 0.00059, 1.10631	-443628.579465 2.83E+32 2 1.99E+00 7.86E+03 -442327.940896 2.73E+32 1 1.36E+00 4.47E+01 -1307.704984 9.79E+29 2 1.00E+00 1.00E+00 -443625.880451 2.83E+32 2 1.16E+00 8.32E+03
102/103	³ O HCN	O, 0.00000, 0.00000, 0.00000 N, 0.00000, 0.00000, 0.64811 C, 0.00000, 0.00000, -0.49567 H, 0.00000, 0.00000, -1.56273 TS(³ NCOH) N, -1.13197, 0.37849, 0.00000 C, 0.00000, 0.67094, 0.00000 H, 0.85045, 1.32090, 0.00000 O, 0.88417, -0.99949, 0.00000 ³ NCOH N, -1.20011, -0.25305, 0.00000 C, 0.00408, 0.38112, 0.00000 H, -0.02616, 1.48060, 0.00000 O, 1.05030, -0.24950, 0.00000 TS(NCO + H) N, -1.26179, -0.12562, 0.00000 C, -0.05403, 0.06003, -0.00000 H, 0.18851, 1.79314, 0.00000 O, 1.12103, -0.15925, 0.00000	-197065.919094 6.19E+31 3 1.00E+00 1.00E+00 -245122.398339 1.36E+32 1 1.05E+00 1.38E+02 -442153.408158 2.73E+32 3 1.36E+00 1.17E+04 -442333.955917 2.73E+32 3 1.10E+00 7.47E+03 -442173.054775 2.73E+32 3 1.15E+00 6.63E+03
104	NCO H ³ O CN TS	N, 0.00000, 0.00000, -1.25802 C, 0.00000, 0.00000, -0.03723 O, 0.00000, 0.00000, 1.12869 H, 0.00000, 0.00000, 0.00000 O, 0.00000, 0.00000, 0.00000 N, 0.00000, 0.00000, 0.53434 C, 0.00000, 0.00000, -0.62339 C, 0.00000, 0.63892, 0.00000 O, -1.01780, -1.05945, 0.00000 N, 1.16321, 0.66316, 0.00000 O, 0.00000, 0.00000, 0.00000 N, 0.00000, 0.00000, -0.00325 H, 0.00000, 0.00000, 1.03180 TS N, 0.06397, 1.48451, 0.00000 H, -0.95957, 1.33241, 0.00000 O, 0.06397, -1.46549, 0.00000 O, 0.00000, 0.00000, 0.00000 N, 0.00000, 0.00000, -0.00325 H, 0.00000, 0.00000, 1.03180 TS N, -0.00010, 0.00000, 0.00292 H, 0.00018, 0.00000, 1.13190 O, 0.00052, 0.00000, 2.48190	-440893.44121 2.63E+32 2 1.14E+00 5.23E+02 -1307.704984 9.79E+29 2 1.00E+00 1.00E+00 -197065.919094 6.19E+31 3 1.00E+00 1.00E+00 -243282.319290 1.28E+32 2 1.00E+00 1.06E+02 -440356.875652 2.63E+32 4 1.25E+00 9.58E+03 -197065.919094 6.19E+31 3 1.00E+00 1.00E+00 -144933.050538 5.63E+31 3 1.00E+00 1.24E+01 -342002.972893 1.67E+32 1 2.29E+00 5.13E+03 -197065.919094 6.19E+31 3 1.00E+00 1.00E+00 -144933.050538 5.63E+31 3 1.00E+00 1.24E+01 -342002.972893 1.67E+32 1 2.29E+00 5.13E+03 -341984.221572 1.67E+32 5 1.12E+00 5.64E+02
106	³ O NH TS		
107	³ O NH TS		

109	³ O CH ₃	O, 0.00000, 0.00000, 0.00000 C, 0.00000, -0.00018, 0.00042 H, -0.93570, -0.53955, -0.00085 H, 0.93580, -0.53939, -0.00085 H, -0.00010, 1.08002, -0.00085 C, -1.66894, -0.00071, 0.00146 H, -1.70398, -0.20404, -1.05871 O, 1.88105, 0.00081, -0.00165 H, -1.64859, -0.81774, 0.70751 H, -1.68219, 1.01954, 0.35561	-197065.919094 -104455.380974 -301523.504861	6.19E+31 5.63E+31 1.67E+32	3 1.00E+00 1.00E+00 2 1.08E+00 2.53E+02 2 9.00E+00 1.43E+04	
112	³ O ¹ CH ₂	O, 0.00000, 0.00000, 0.00000 C, 0.00000, 0.17399, 0.00000 H, 0.86403, -0.52196, 0.00000 H, -0.86403, -0.52196, 0.00000 C, 1.72138, 0.00000, -0.16790 H, 1.61465, 0.86374, 0.51996 H, 1.61465, -0.86374, 0.51996 O, -1.69470, 0.00000, -0.00406	-197065.919094 -102649.483309	6.19E+31 5.08E+31	3 1.00E+00 1.00E+00 1 1.00E+00 1.31E+02	
114	³ O CH	TS	C, 0.03805, 0.00000, 0.00739 H, -0.08343, 0.00000, 1.12287 O, 3.25815, 0.00000, 1.32701	-299717.767352	1.59E+32	3 4.38E+00 1.02E+04
116/117/ 118	¹ O H ₂ CN	TS	O, 0.00000, 0.00000, 0.00000 C, -0.50346, 0.00000, 0.00005 N, 0.73653, 0.00000, -0.00006 H, -1.06749, 0.93849, 0.00008 H, -1.06748, -0.93850, 0.00008 C, -0.00026, -2.06042, 0.00000 N, 0.00000, -0.82063, 0.00000 H, -0.00039, -2.62401, -0.93865 H, -0.00039, -2.62401, 0.93865 O, 0.00030, 2.91937, 0.00000	-196788.921964 -246571.579821	6.19E+31 1.43E+32	1 1.00E+00 1.00E+00 2 1.02E+00 1.39E+03
	TS(CH ₂ NO)		C, -1.10868, 0.12008, 0.00000 N, 0.06743, -0.35642, 0.00000 H, -1.92868, -0.58030, 0.00000 H, -1.27043, 1.19243, 0.00000 O, 1.17239, 0.14529, 0.00000	-443364.228372	2.83E+32	2 7.58E+01 2.15E+04
	CH ₂ NO		C, -1.17076, 0.51441, 0.00000 N, -1.43659, -0.69718, 0.00000 H, -1.96887, 1.26430, -0.00004 H, -0.13238, 0.86080, 0.00004 O, 2.39774, -0.04141, -0.00000	-443897.716844	2.83E+32	2 1.18E+00 6.75E+03
	TS(³ O + H ₂ CN)		C, -1.01152, 0.43493, 0.00000 N, 0.00000, -0.12833, 0.00000 H, -2.06888, 0.55214, 0.00000 H, -0.60205, 2.58631, 0.00000 O, 1.09251, -0.60621, 0.00000	-443639.120847	2.83E+32	2 8.34E+00 3.93E+04
	TS(HCNO + H)		C, 0.01434, -0.00045, 0.00190 N, 0.00003, 0.00007, 1.24192 H, 1.35095, 0.00005, 0.03246 H, -0.76839, -0.00108, -0.74539 O, 1.46065, 0.00063, 1.28767	-443628.579465	2.83E+32	2 1.99E+00 7.86E+03
	TS(HCNOH)		C, 1.13711, 0.29236, 0.00000 N, 0.15491, -0.44299, 0.00000 H, 2.17692, -0.01488, 0.00000 H, -1.07487, 1.00421, -0.00000 O, -1.12614, 0.04468, 0.00000	-443625.880451	2.83E+32	2 1.16E+00 8.32E+03
	HCNOH		C, 1.13711, 0.29236, 0.00000 N, 0.15491, -0.44299, 0.00000 H, 2.17692, -0.01488, 0.00000 H, -1.07487, 1.00421, -0.00000 O, -1.12614, 0.04468, 0.00000	-443791.239692	2.83E+32	2 1.32E+00 7.41E+03
	TS(HCN + OH)		C, 0.03328, 0.00008, 0.03546 N, 0.00597, 0.00012, 1.22817 H, 0.70873, -0.00010, -0.80034 O, -1.48608, 0.00048, 1.88445	-443764.756273	2.83E+32	2 1.82E+00 9.57E+03

121	¹ O	H, -2.05048, 0.00059, 1.10631 O, 0.00000, 0.00000, 0.00000 C, 0.00000, -0.00018, 0.00042 H, -0.93570, -0.53955, -0.00085 H, 0.93580, -0.53939, -0.00085 H, -0.00010, 1.08002, -0.00085					
	CH ₃		C, -1.93246, -0.00001, 0.00003 H, -1.94189, -0.95530, -0.50390 O, 2.17754, 0.00002, -0.00003 H, -1.94115, 0.04121, 1.07930 H, -1.94251, 0.91405, -0.57530	-301245.952754	1.67E+32	2	1.03E+01 1.90E+04
122	¹ O	O, 0.00000, 0.00000, 0.00000 C, 0.00000, 0.00000, 0.10395 H, 0.00000, -0.99689, -0.31186 H, 0.00000, 0.99689, -0.31186	-196788.921964	6.19E+31	1	1.00E+00 1.00E+00	
	³ CH ₂		C, -2.00426, -0.00000, -0.10318 H, -2.08479, 0.99757, 0.30347 H, -2.08468, -0.99758, 0.30347 O, 2.02438, 0.00000, 0.00152	-102701.224038	5.08E+31	3	1.01E+00 8.96E+01
	TS		C, -299491.422997	1.59E+32	3	7.05E+00 1.42E+04	